Journal of Archaeological Science: Reports 52 (2023) 104224

Contents lists available at ScienceDirect

Journal of Archaeological Science: Reports

journal homepage: www.elsevier.com/locate/jasrep

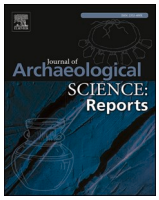

Obsidian sources from the Aegean to central Turkey: Geochemistry, geology, and geochronology

Ellery Frahm

Council on Archaeological Studies and Department of Anthropology, Yale University, New Haven, Connecticut, United States
Anthropology Division, Yale Peabody Museum of Natural History, New Haven, Connecticut, United States

ARTICLE INFO

Keywords:
Southwest Asia
Greece
Turkey
Cappadocia
Galatia
Anatolia
Obsidian sourcing

ABSTRACT

The monograph *L'obsidienne au Proche et Moyen Orient: Du volcan à l'outil* (Cauvin et al., 1998) was first published 25 years ago, and between its covers, Poidevn's (1998) chapter summarized the geochemical and geochronological data for obsidian sources that lie within what is now western, central, and eastern Turkey and the Caucasus. That chapter was a highly valuable resource at the time. A revision, though, is long overdue, and this is the second of two articles (see Frahm, 2023) in which I endeavor to provide an update. Here I focus on the obsidian sources from the Greek islands in the South Aegean Volcanic Arc to the Central Anatolian Volcanic Province in central Turkey. Many more elemental data are available for these sources today than during the 1990s. For example, Poidevin (1998) listed 17 analyses of Nenezi Dağ obsidian from seven different facilities. In contrast, here I summarize 359 measurements of Nenezi Dağ obsidian from 26 different laboratories using a variety of analytical techniques. Consequently, there is an opportunity to derive robust elemental consensus values for such well-characterized obsidian sources. Of the 24 obsidian sources that I summarize in this article, however, not all have been so well studied, and there remains important work to be done, especially in western Turkey.

Preface

Author's note: The work I share here is a culmination of research that I undertook with the support of George R. Rapp, Jr., known to everyone as "Rip," who passed away in March 2023 at the age of 92. His nickname came from his reputation as a hard skater and hockey player on the ice rinks of Duluth, where he lived most of his life. He was a geologist by training (B.A. in geology and mineralogy, University of Minnesota, 1952; Ph.D. in geochemistry, Penn State, 1960), yet he is best known for his contributions to archaeological research. He was a professor at the South Dakota School of Mines & Technology (1957), University of Minnesota-Twin Cities (UMN, 1965), and University of Minnesota-Duluth (UMD, 1975). From 1975 until he retired in 2003, Rip was the Director of the UMD Archaeometry Laboratory and Professor of Interdisciplinary Archaeological Studies (IAS) at UMN and UMD. He was an advisor for my Master's degree in IAS and set me on the obsidian sourcing path for my doctoral studies. I am briefly mentioned in his 2011 autobiography (titled, of course, *Rip: An Autobiography*) as the graduate student who had taken up the mantle of his unfinished obsidian sourcing project in Turkey from 1990 to 1991. When I decided to take on this project in 2003, my aim was to complete it to the standards that Rip had originally envisioned in 1990. When Rip handed the remaining obsidian specimens and project materials over to me in 2004, he told me, "Do something great with them." This article, together with my previous one (Frahm, 2023), includes all of the data that I was able to collect from those obsidian specimens so that others may also benefit from the work that Rip started. Publishing the data took a lot longer than Rip had hoped (it has been 33 years since 1990), but finally seeing this project through to its full publication is my way of honoring Rip and recognizing his immeasurable influence on my life. RIP, Rip.

1. Introduction

This is the second of two papers (see Frahm, 2023) in which I endeavor to update and augment a chapter from the monograph *L'obsidienne au Proche et Moyen Orient: Du volcan à l'outil* (*Obsidian in the Near and Middle East: From Volcano to Tool*; edited by Cauvin et al., 1998) by Jean-Louis Poidevin, titled "Les gisements d'obsidienne de Turquie et de

E-mail address: ellery.frahm@yale.edu.

https://doi.org/10.1016/j.jasrep.2023.104224
Received 19 July 2023; Received in revised form 19 September 2023; Accepted 24 September 2023
Available online 5 October 2023

Transcaucasie: géologie, géochimie et chronométrie" ("The obsidian deposits of Turkey and Transcaucasia: geology, geochemistry, and chronometry"). At the time, this book collected state-of-the-art information involving obsidian across the ancient Near East, from its geological origin to its cultural significance, and Poidevin's (1998) chapter assembled almost all that was known about the obsidian sources of Southwest Asia. It included published and unpublished elemental data, including his own, for known sources in a 36-page appendix, which was an invaluable resource for those of us interested in this topic during the early 2000s. While most earlier publications presented elemental values for obsidian sources and/or artifacts from only one analytical technique (e.g., Cauvin et al., 1986; Gratuze et al., 1993; Pernicka et al., 1997), Poidevin (1998) listed data from X-ray fluorescence (XRF), neutron activation analysis (NAA), and inductively coupled plasma (ICP) spectrometry from various analytical facilities side-by-side. This approach enabled more inter-laboratory comparisons, an important step in evaluating measurement accuracy and arriving at consensus values.

Given that 2023 marks the 25th anniversary of Poidevin's (1998) chapter, I have sought to update his database to reflect current knowledge regarding the region's obsidian sources. The field has grown so much, though, that two articles are needed to achieve this goal. In the previous article (Frahm, 2023), I focused on the obsidian sources within the Caucasian segment of the Alpine–Himalayan collisional belt, which corresponds to eastern Turkey and southwestern Russia as well as the former Soviet republics of Armenia, Azerbaijan, and Georgia. That area, where the Arabian and Eurasian tectonic plates collide, has been given various names, including the Armenian Highlands, Southern Caucasus, and Caucasian-Arabian Syntaxis. In contrast, this paper focuses on obsidian sources to the west, spanning from the Greek islands in the South Aegean Volcanic Arc to the Central Anatolian Volcanic Province in central Turkey (Figs. 1 and 2). Although obsidian from Aegean obsidian sources has since been identified at archaeological sites in western Turkey (Perlès et al., 2011: Fig. 1, Milić, 2014: Fig. 2, Gemici et al., 2022: Figs. 1–2), Poidevin (1998) did not include those sources in his chapter. He listed the most data for those sources in central Turkey, also known as Cappadocia; however, many more data are available today than in the 1990s. Consider, for example, one of the most prominent obsidian sources within the region: Nenezi Dağ (e.g., Gratuze et al., 1993; Pernicka et al., 1997; Carter and Shackley, 2007; Carter et al., 2020). Poidevin (1998) listed 17 analyses of Nenezi Dağ obsidian from seven laboratories, whereas here I summarize 359 measurements of Nenezi Dağ obsidian, both published and previously unpublished, from 26 analytical techniques and laboratories. As pointed out by Hancock and Carter (2010: 245), "although analytical chemistry is not a democratic process, the agreement of specific elemental concentration data between (among) independent analytical techniques adds credibility" to datasets that, in turn, enable us to derive accurate consensus values for elements at the core of obsidian artifact sourcing.

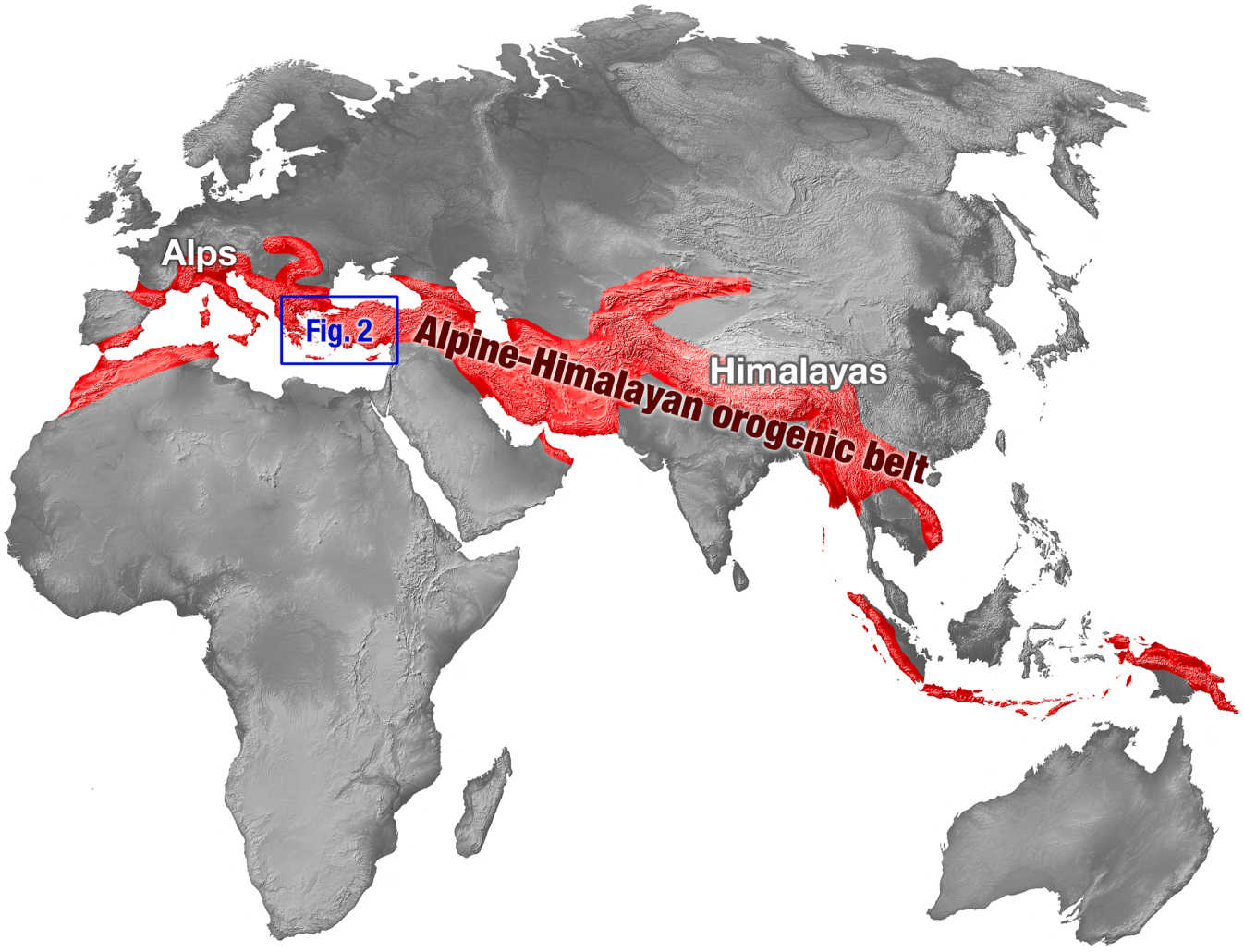

Fig. 1. Topographic map of the eastern hemisphere, highlighting the Alpine-Himalayan orogenic belt (highlighted in red) and the region of interest in the current paper (blue box, which corresponds to the area shown in Fig. 2). (For interpretation of the references to color in this figure legend, the reader is referred to the web version of this article.)

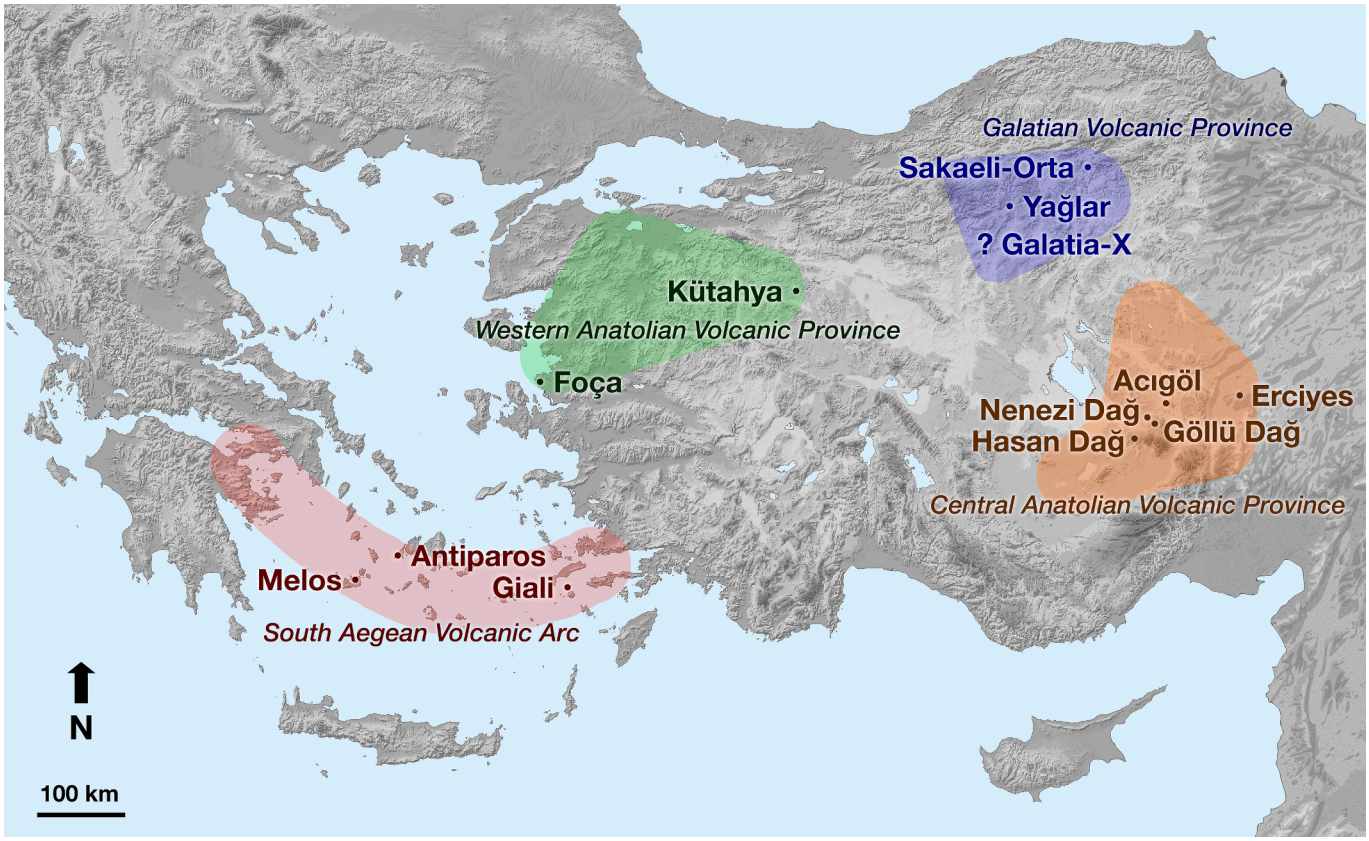

Fig. 2. Topographic map of the relevant area, highlighting the four major obsidian-producing volcanic regions along this segment of the Alpine-Himalayan belt. Background map based on the ASTER Global Digital Elevation Map Version 3 (GDEM V3), NASA (USA) and METI (Japan).

Like my previous article, my goal in this endeavor is to be comprehensive but not authoritative, to facilitate but not to prescribe. In creating such a database as this, choices must be made. I expect that friends and colleagues in this field may disagree with some choices that are based on my own experience and interpretations. Consequently, I have documented these choices (Section 2) for transparency, and it should be stressed that this endeavor is possible only through the transparency of others. That is, such a project cannot happen without the researchers who report their elemental data. For example, Orange et al. (2016), Carter (2016), and Moutsiou (2019) include their measurements using laser-ablation ICP mass spectrometry (LA-ICP-MS), energy-dispersive XRF (EDXRF), and portable XRF (pXRF), respectively. Each of these individual datasets is referenced here in the supplementary tables, much like how Poidevin (1998) reported the available data at that time in an appendix at the end of his chapter.

Poidevin (1998) emphasized the importance of analytical data collected from independent labs and techniques; however, he was frustrated that the few data available confounded efforts to distinguish real differences in obsidian composition from simple variability among different laboratories. Today, the amount of data available can advance this field closer to what Poidevin (1998) envisioned. In his chapter, Poidevin (1998) compiled 258 analyses for the obsidian sources in western and central Turkey and none from the Aegean area. Here, 25 years after Poidevin (1998), I have summarized more than 2100 obsidian analyses from the Aegean and more than 2400 from western and central Turkey. That is, there has been a 1600% increase in the amount of obsidian elemental data available for this area. At the time of writing his chapter, Poidevin (1998: 152) bemoaned that, with the limited data then available, he had to list "the very good alongside the more mediocre, if not useless" [translated from French]. With larger datasets, as demonstrated here, it is now possible distinguish those very good measurements from the useless ones and, as a result, statistically determine consensus ranges for important elements. Assembling data from independent techniques and laboratories permits better recognition of outliers and, in turn, confidence in the accuracy of averaged elemental concentrations. A lab-by-lab breakdown of the data used here to calculate consensus ranges and the corresponding references enables a reader to find additional details, such as calibration methods and accuracy assessments, for each analytical technique and facility. It is my sincere hope that this database will be as useful to current and future archaeologists as Poidevin's (1998) chapter was to me and other researchers in this field over the last three decades.

2. Methods

My methods for this article are very much the same as those in my prior one. Hence, while I still summarize them here, more nuanced discussions can be found in Frahm (2023). In this section, I describe my organizing principles for gathering more than 4500 published and unpublished obsidian analyses and using them to calculate consensus concentration ranges for a set of 22 elements. Like others who have sought to document, describe, and summarize the obsidian sources in this region (e.g., Blackman, 1984; Keller and Seifried, 1990; Chataigner et al., 1998; Poidevin, 1998), I have endeavored to capture the state-of-the-field for the benefit of current researchers as well as future scholars.

One of the few differences from Frahm (2023) is a cut-off date of 1990 for the included element values. Some of the obsidian sources covered in this paper have been geochemically studied for several decades longer than those sources farther to the east, as far back as the earliest obsidian sourcing work by Renfrew and colleagues (e.g., Cann and Renfrew, 1964; Renfrew et al., 1965, 1966). As a result, older element measurements are available for the region, and I chose 1990 as a cut-off for including values in a table for each obsidian source. This protocol was adopted due to frequent accuracy issues noted in data from

the 1980s and before (e.g., NAA datasets in Blackman, 1984; Bigazzi et al., 1986; XRF values in Francaviglia, 1984). Such accuracy issues might have been due to unrecognized spectral interferences at the time. For example, in NAA, the presence of ^{235}U in many geological materials (and the resulting fission products) necessitates correction factors for elements of interest in obsidian artifact sourcing, including Ce, Ba, La, Nd, and Zr (Landsberger, 1986). Today, these data corrections are considered so routine that they are rarely mentioned in publications; however, a failure to account for such interferences will lead to errors. Similarly, the means of measuring XRF spectra and quantifying their signals has improved since the 1980s, meaning more recent measurements tend to be more accurate.

It is important to clarify the term "source" as it is used here. Two distinct uses of "source" can be found in the obsidian literature: (1) the geographic use (i.e., a given location in space where a deposit of obsidian occurs) and (2) the geochemical use (i.e., a cluster in elemental data, also known as a "chemical group"). Simply put, the first definition means that an obsidian source can be placed on a map, whereas the second one means that a source can be placed on a compositional scatterplot. While some scholars prefer the former definition (e.g. Hughes, 1998; Wilson and Pollard, 2001), others prefer the latter (e.g., Harbottle, 1982; Neff, 1998). Following Hughes (1998: 104), who maintained that obsidian "sources are defined, geochemically speaking, on the basis of chemical composition – not spatial distribution," here I use the geochemical definition of a "source," synonymous with what some authors (i.e., those who prefer the geographic use) might call an obsidian "chemical group" or "chemical type.".

For each obsidian source, the elemental values reflect (1) the data previously published by other scholars and (2) published and unpublished data for obsidian specimens that I either measured myself or sent to another lab for measurement. Data for both geological specimens and artifacts were culled from the archaeological, geological, and analytical literature. In their publications, some researchers reported summary statistics (i.e., means and standard deviations) in tables within the manuscript, whereas other authors listed all of the individual analyses in the supplementary materials. For each obsidian source, the supplementary tables include citations for all of the contributing publications.

My previously published and unpublished data have been organized (and, in some instances, re-organized) so that they can be shared in a coherent fashion. That is, data as I have organized here should be considered to supersede past work, including my thesis (Frahm, 2010). I conducted two types of X-ray spectrometry myself: (1) electron microprobe analysis (EMPA) with wavelength-dispersive spectrometry (WDS) in the Department of Earth and Environmental Sciences, University of Minnesota-Twin Cities (see protocols in Frahm, 2020: 6–8, 2010: 302–364) and (2) portable XRF analysis (pXRF), which is essentially EDXRF housed with a small form factor. Most of the pXRF data were collected using an Olympus Vanta VMR instrument in the Yale University Archaeological Laboratories (e.g., Frahm and Brody, 2019; Frahm and Tryon, 2019) based on the Peabody-Yale Reference Obsidians (PYRO) calibration (Frahm, 2019a). The Aegean obsidian specimens, however, were mostly analyzed at the University of Sheffield using Thermo Niton XL3t instruments (see Frahm et al., 2014a). I sent a fraction of the geological specimen to be tested in other laboratories using three different techniques: (1) NAA and (2) EDXRF at the University of Missouri Research Reactor's (MURR) Archaeometry Laboratory and (3) wavelength-dispersive XRF (WDXRF) in the University of Wisconsin-Eau Claire's (UWEC) Materials Science Center. These datasets are marked in the supplementary files as having been collected either by myself or at my behest.

The same 22 elements (Na, Mg, Al, Si, K, Ca, Ti, Mn, Fe, Zn, Rb, Sr, Y, Zr, Nb, Ba, La, Ce, Nd, Pb, Th, U) are reported here as in Frahm (2023). Also, as in that article, values were converted from oxides to elements (e.g., TiO_2 to Ti) and from weight percent to parts per million (ppm) (e.g., 0.075% to 750 ppm), as needed. The list of elements reflects those most frequently detected and reported among published and unpublished obsidian data for the region, although there is likely a skew towards the elements best measured in obsidian with various types of X-ray spectrometry – EDXRF, WDXRF, pXRF, EMPA-WDS, PIXE, etc. – due to the prevalence of such techniques relative to NAA or LA-ICP-MS.

During data processing, no analytical technique was favored or given preference over any other one. That is, NAA data were not assumed to be more or less accurate than LA-ICP-MS data, EDXRF data were not assumed to be more or less accurate than EMPA data, etc. Given that accuracy depends on data correction and calibration, the procedures for which often differ across analytical laboratories, it is simply not true that a particular technique (e.g., NAA, ICP-MS) inherently yields better accuracy than any other does (e.g., EDXRF, EMPA). Furthermore, when deriving consensus values for each obsidian source, I calculated one table entry per analytical laboratory and technique. For instance, the 323 measurements of Kömürcü (East Göllü Dağ) obsidian using LA-ICP-MS at the Université d'Orléans have been combined here in a single table entry, despite those data originally having been dispersed in five articles. This way, no one research group or analytical lab can unduly influence the consensus values simply because they publish more. Therefore, it does not matter if a particular laboratory published five analyses in only one article or five hundred analyses in a dozen articles – the influence is the same. In cases when a research group used two different analytical techniques (e.g., NAA and EDXRF at MURR), there are two entries in the resulting table, given that those two sets of measurements are, at least in theory, independent (but see Latour and Woolgar, 1986). The benefits of this approach, I propose, outweigh potential weaknesses (e.g., protocols can and, in fact, often do change through time in laboratories).

Given the different ways in which elemental data are reported for obsidian, I chose an approach able to accommodate both summary statistics (i.e., means, standard deviations, number of observations) alone and long lists of specimen-by-specimen measurements. Following the procedures in Frahm (2023), the mathematical result approximates the mean and standard deviation that could be calculated if all of the individual measurements had been listed by all authors. As an example, let us imagine that an EDXRF lab has published three different means and standard deviations for Sr in Nenezi Dağ obsidian: (1) 100 ± 10 ppm, $n = 10$; (2) 95 ± 5 ppm, $n = 20$; and (3) 90 ± 15 ppm, $n = 5$. These data can be used to calculate a combined mean and standard deviation for Sr based on all 35 observations: 95.7 ± 8.8 ppm, which can be rounded to 96 ± 9 ppm. It should be noted that, in the supplementary tables, the listed "n" is the number of analytical observations, not necessarily the number of specimens and/or artifacts. For EDXRF, the "n" might include replicate measurements after a specimen or artifact was reoriented, and in EMPA, the "n" might reflect the total measured spots. For this database, I chose to list the author-reported numbers of observations without additional scrutiny to determine how they were counted.

As in Frahm (2023), outlier values were identified and removed. There are many factors that can yield outliers, from errors (e.g., mistakes during specimen handling or preparation, incorrect calibration, uncorrected interferences, human transcription error) and malfunctions (e.g., electronic noise) to actual elemental variation (e.g., heterogeneity due to differences in mineral inclusions, a zoned obsidian flow) within a specimen or its source. There can also be technique-specific differences. EMPA, for example, can be used (as I did) to measure only the glassy component and avoid microscopic mineral inclusions, such as miniscule magnetite (Fe_3O_4) grains. As a result, my EMPA measurements commonly exhibit lower Fe values than those from bulk analytical techniques (e.g., EDXRF, NAA) that measure both the glass and the mineral inclusions together and report average element concentrations.

Outliers were identified using a standard interquartile range method (for most obsidian sources, there were too few data to apply more sophisticated methods for outlier detection; e.g., the two-sided double Grubbs test, Cochran's C test). First, the compiled data were used to calculate the quartiles (Q1 and Q3) and interquartile range (IQR: Q3

– Q1) for each element of interest. Second, outliers were found according to these ranges (i.e., outliers fell below Q1 – 1.5 IQR or above Q3 + 1.5 IQR). Third, any outliers were removed. The three steps repeated until there were no longer any outliers remaining. Finally, the newly calculated medians and quartiles, along with the other summary statistics (i.e., mean and standard deviation), are reported in the supplementary tables as the proposed ranges.

Many analytical techniques treat each element as a measurement that is (largely) independent of other elements, and the element sum is not normalized (e.g., EMPA in Frahm, 2012). Nevertheless, one can envision a critique of eliminating an outlier value for only one element because compositional data necessitate a sum of 100%, at least in theory. The question might be asked, if a certain Rb measurement is too high, would not elements like Zr or Sr be lower? Consider a case in which a Rb measurement is too high by 20% relative, increasing it from, for example, 100 ppm to 120 ppm. If the data are normalized, the other elements must all add up to 99.988%, instead of 99.990%, a relative decrease of only 0.002%. That is the (immeasurably small) magnitude of error that would be introduced through normalization in such a case. Consequently, trace elements like Zr or Rb essentially function as independent variables. It is true that researchers did once use ternary diagrams in which three elements summed to a constant (e.g., Sr, Zr, and Rb and Nb, Zr, and Rb in Shackley, 1988; see also Fornaseri et al., 1975 and Cauvin et al., 1986), whereby a high value for one element would yield low values for the other two. Such a protocol, though, fell out of favor in the 1990s. It is worth acknowledging, however, that I did not conduct the calculations needed to find out whether any covariance existed between elements from a given laboratory, although I suspect that there were insufficient data to do a rigorous statistical assessment.

Variations in the amounts, sizes, or compositions of mineral inclusions can also affect the overall elemental measurements of obsidian specimens. Previously I discussed the influences of magnetite and titanomagnetite ($Fe^{2+}(Fe^{3+},Ti)_2O_4$), ilmenite ($FeTiO_3$), zircon ($ZrSiO_4$), and monazite (Ce, La, Nd, and/or Th phosphate) on elements commonly used in obsidian sourcing (Frahm, 2023). In the case, for example, of Ce-rich monazite grains, an obsidian specimen containing two such grains would have a greater amount of Ce than a specimen containing only one, leading to a perceived difference in otherwise homogeneous obsidian from the same volcanic source. For the obsidian sources covered in this paper, the presence of spherulites are repeatedly mentioned, so their potential effects on composition should be considered as well. Spherulites, like that in Fig. 3, are small, round mineral clusters that grew around an initial crystal that served as a nucleation point. Many spherulites have millimeter-scale diameters, although there are occasional instances of spherulites on the scale of centimeters and, especially rarely, meters. In fact, the largest known spherulites occur in a rhyolitic vitrophyre layer near Silver Cliff, Colorado (USA) and have diameters as large as 4.3 m (Fig. 4). The minerals in spherulites have often been

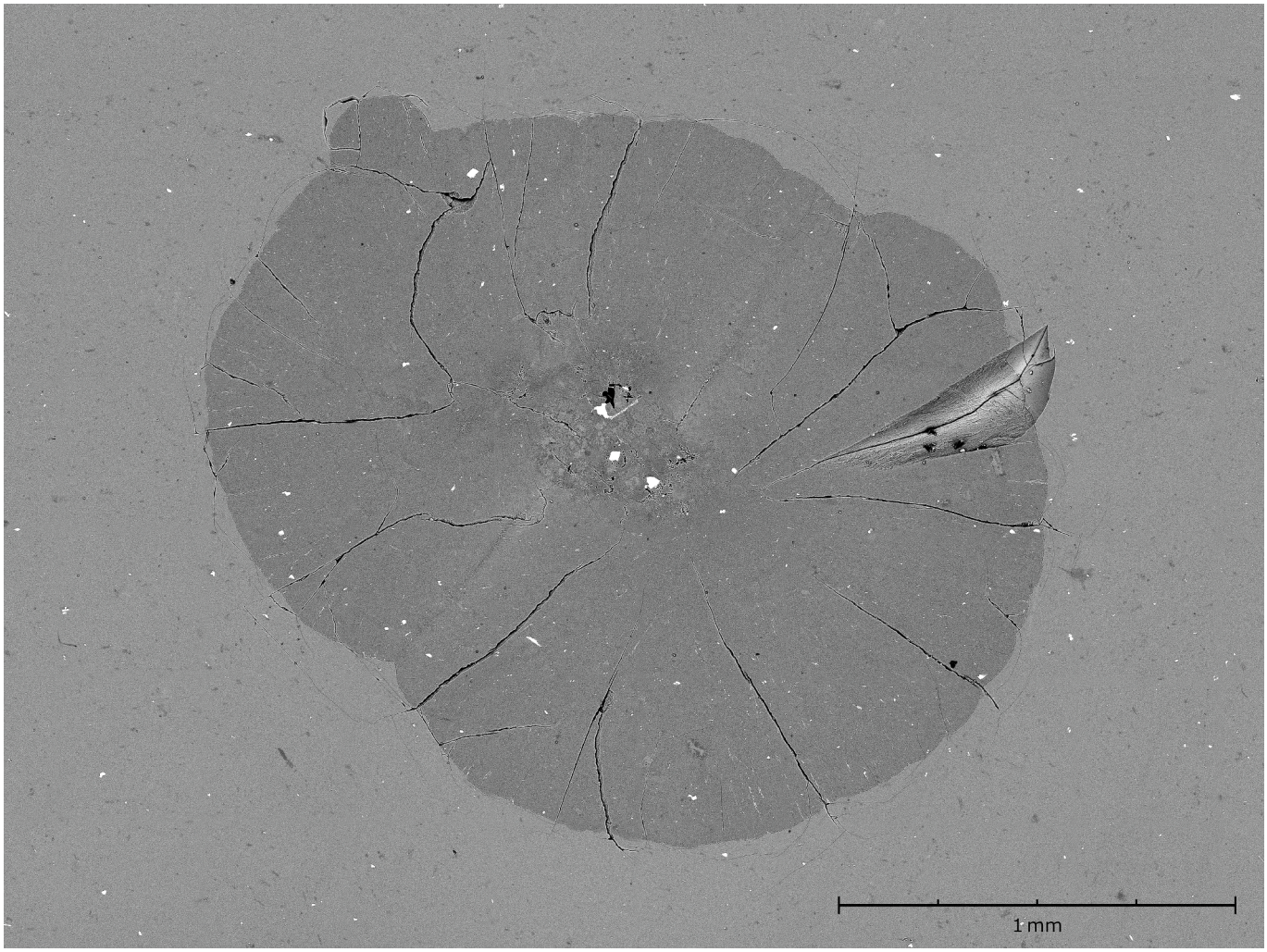

Fig. 3. Backscattered-electron (BSE) image of a spherulite, ca. 2 mm in diameter, within an obsidian specimen from the Sırça Deresi outcrops at the Göllü Dağ complex. BSE images show compositional contrast: brighter areas have a higher mean atomic number, while darker areas have a lower mean atomic number. Image acquired using a Thermo Scientific Phenom XL G2 Desktop scanning electron microscope (SEM) housed in the Yale University Archaeological Laboratories.

Fig. 4. Immense spherulites – sometimes called "megaspherulites" (Breitkreuz et al., 2021) – in volcanic glass (pitchstone rather than true obsidian) near Silver Cliff, Colorado, USA. The author (1.8 m) is shown for scale. Photograph taken in October 2010; these particular spherulites have since been destroyed by renewed activities at this quarry.

assumed to be a high-temperature silica (SiO_2) mineral named cristobalite (a polymorph of quartz which forms under volcanic conditions); however, spherulites in obsidian are often composed of alkali (K–Na) feldspars (such as the high-temperature mineral sanidine) ingrown with cristobalite and/or other minerals (Fig. 5) (e.g., Tuffen and Castro, 2009; Watkins et al., 2009; Gardner et al., 2012; Clay et al., 2013; Arzilli et al., 2015; Befus et al., 2015; Bustos et al., 2020). Research has established that, in obsidian, Ba and Sr can be concentrated within alkali feldspars (Berlin and Henderson, 1969). Specifically, Ba and Sr can be as much as three and nine times higher, respectively, in alkali feldspars relative to the glass matrix. Analyzing the glass using a small-spot analytical technique, such as EMPA or LA-ICP-MS, would consequently yield measurements that reflect Ba- and Sr-depleted concentrations. The implication, therefore, is that caution is warranted for certain elements, measured by spot techniques, for spherulite-rich obsidian.

The potential effects of water on obsidian composition must also be recognized. Water becomes incorporated into obsidian in two ways: (1) during its eruption and emplacement as previously dissolved gases, including water, are released under less intense pressure at/near the Earth's surface and (2) after emplacement as water from the environment slowly infiltrates, hydrates, and alters the glass. In the first scenario, degassing lava is similar to opening a carbonated beer bottle. Under pressure while inside the bottle, carbon dioxide is dissolved within the liquid; however, with that pressure is removed, the carbon dioxide comes out of the liquid and forms bubbles. The same thing happens with obsidian and water. In this comparison, the beer is analogous to the smooth obsidian, whereas the foam (or head) on top of the beer is a frothy pumiceous–perlitic layer atop the glassy obsidian. This is the reason that pumice–perlite deposits often co-occur with obsidian. Obsidian that forms near the boundary between these layers can contain abundant microscopic bubbles, giving the resulting obsidian a grey appearance and/or a metallic sheen. Such obsidian is generally less suitable for knapping, as it is no longer isotropic and thus tends to preferentially fracture along any planes of bubbles. In the second scenario, water from the environment infiltrates and diffuses into the glass, potentially dissolving and forming new compounds in the resulting perlite. This is important because Zielinski et al. (1977) found, after studying perlite and obsidian in the American West, marked elemental differences between them. Although there was "little mobilization of most trace elements" (436), a few elements, including Sr and Ba, were elevated in the perlite relative to the obsidian. Thus, Zielinski et al. (1977: 426) asserted that "significant errors can be made in estimating the original composition of rhyolitic obsidian simply by relying on abundances of elements in associated perlite." Issues of water content will occasionally reemerge in the sections below.

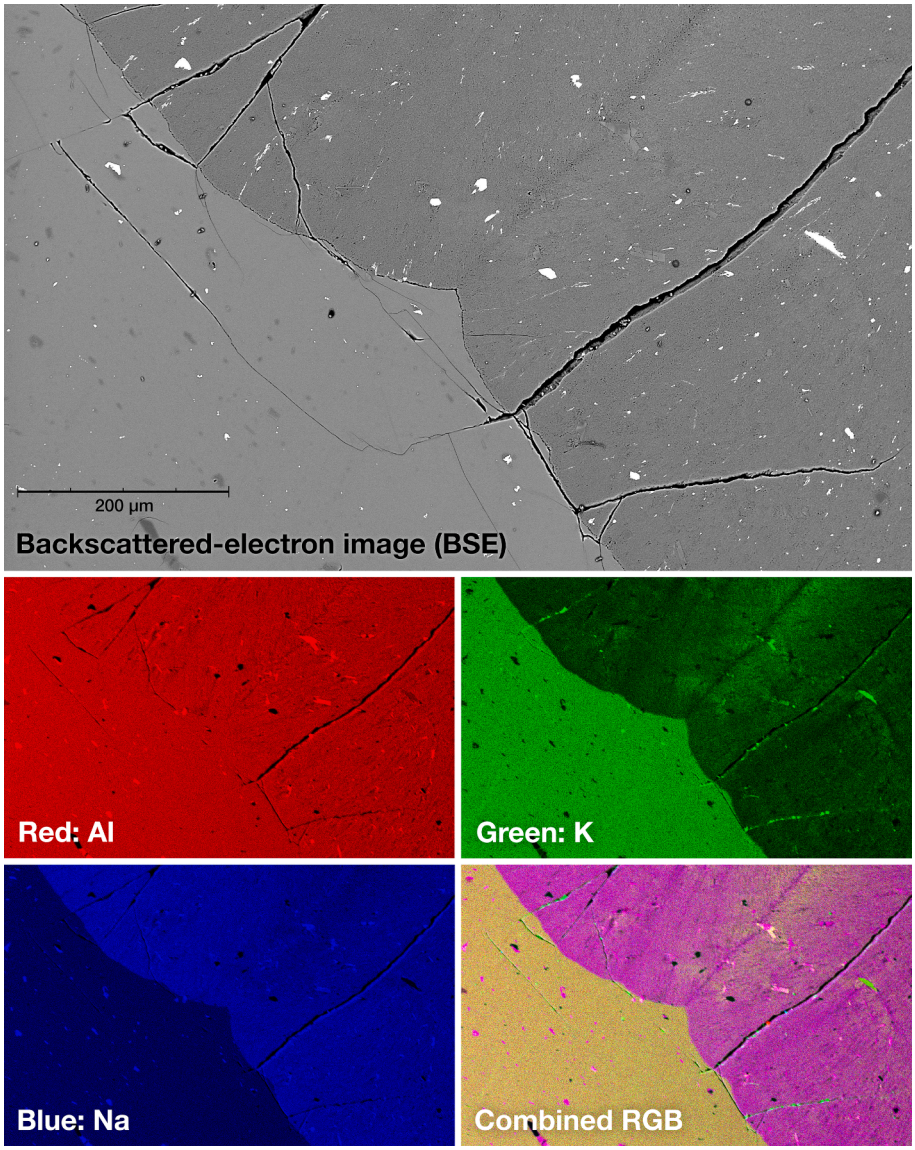

Fig. 5. BSE image and element maps of a spherulite within an obsidian specimen from the Sırça Deresi outcrops at Göllü Dağ. These element maps demonstrate that the spherulite is largely composed of feldspar and silica polymorphs. Image and maps acquired using a Thermo Scientific Phenom XL G2 Desktop scanning electron microscope (SEM) housed in the Yale University Archaeological Laboratories.

3. Obsidian sources

Poidevin's (1998) chapter examined obsidian sources in a roughly west-to-east order, beginning along Turkey's western coast and ending in the Caucasus. I follow this practice here, as shown in Table 1 (which includes alternative source names as well as commonly used outcrop names). Ideally, each of the sources could be discussed here with the same level of detail; however, as the reader will notice, not all of these sources are understood equally well, thereby necessitating additional work in both the field and the lab. Table 2 lists the available geochronological data for the sources. When relevant, I include scans of the original field maps used in 1991 by George "Rip" Rapp (one of my graduate advisors), Tuncay Ercan (Directorate of Mineral Research and Exploration, Turkey), and their colleagues.

3.1. South Aegean volcanic Arc

The Aegean obsidian sources had a key role in the development of obsidian sourcing during the 1960s (Cann and Renfrew, 1964; Renfrew et al., 1965). In 1962, Colin Renfrew and Johnson "Joe" Cann considered the potential to analyze Aegean obsidian artifacts chemically as a means to determine their geological origins. Prior to their technique, it was widely thought that Aegean islands were the sources of obsidian artifacts found throughout the Near East and Mediterranean due to erroneous identifications based on wet chemical methods (i.e., gravimetry, titration) or visual traits (Georgiades, 1956; Cornaggia-Castiglioni et al., 1962). Renfrew and Cann's use of optical emission spectroscopy (OES) established that Aegean obsidian instead largely remained within that region, whereas obsidian sources in the Near East and Mediterranean supplied the areas around them. In Aegean obsidian studies, OES was soon replaced with NAA (Aspinall et al. 1972) and WDXRF (Shelford et al. 1982). Decades later, non-destructive EDXRF and pXRF (e.g., Frahm et al., 2014a; Milić, 2014) helped to bring about a resurgence in obsidian sourcing in Aegean archaeology (e.g., Carter, 2016; Carter et al., 2018, 2023).

3.1.1. Melos: Sta Nychia and Dhemenegaki

The island of Melos (Fig. 6) has two well-known obsidian sources: (1) Sta Nychia (also known as Adhamas; 36.724° N, 24.432° E, sea level to ca. 100 m asl) and (2) Dhemenegaki (36.706° N, 24.543° E, sea level to

Table 1
Index of **o**bsidian sources (listed West to East) with their supplementary tables and manuscript sections. Associated terms (i.e., alternative or earlier names, common transliterations, named geological outcrops or facies) are listed for the convenience of readers.

Table	Section	Source name (this publication)	Associated terms (e.g., outcrops, alt spellings)
Southern Aegean Volcanic Arc			
S1	3.1.1	Melos – Sta Nychia	Adhamas, Adamas, Aghia Nychia, Nihia, Bombarda
S2	3.1.1	Melos – Dhemenegaki	Demenegaki, Dhemenegakion
S3	3.1.2	Antiparos	Soros Hill
S4	3.1.3	Giali A	Yali, Gyali
S5	3.1.3	Giali B	
Western Anatolian Volcanic Province			
S6	3.2.1	Foça	İzmir
S7, S8, S9	3.2.2	Kütahya A, B, C	Kalabak Valley, Alayunt
Galatian Volcanic Province			
S10	3.3.1	Yağlar	Gerede
S11	3.3.2	Sakaeli-Orta	Orta-Sakaeli
S12	3.3.3	Galatia-X	Güdül
Central Anatolian Volcanic Province			
S13	3.4.1	Hasan Dağ	Karakapu, Karakapı, Taşpınar, Helvadere
S14	3.4.2	Nenezi Dağ	Bekarlar
S15	3.4.3	West Göllü Dağ – North Bozköy	Göllü Dağ 1 (Binder et al. 2011), Bozköy Ibiz/Muneninyeri
S16	3.4.3	West Göllü Dağ – Kayırlı Village	Göllü Dağ 2 (Binder et al. 2011)
S17	3.4.3	East Göllü Dağ (nonspecific)	Göllü Dağ East
S18	3.4.3	East Göllü Dağ - Kömürcü	Göllü Dağ 5 (Binder et al. 2011), Kaletepe, Korukuyu
S19	3.4.3	East Göllü Dağ - East Kayırlı	Göllü Dağ 4a/b (Binder et al. 2011), Bitlikeler, Ekinlik
S20	3.4.3	East Göllü Dağ - Bozköy-Boztepe/Sırça Deresi	Göllü Dağ 3/6/7 (Binder et al. 2011), Bozköy East, Hamidin Yeri
S21	3.4.4	West Acıgöl	Güneydağ, Korudağ, Acıgöl Crater, Acıgöl-maar, Kalecitepe
S22	3.4.4	East Acıgöl – White Tuffs Hotamış Dağ (WTHD)	East Acıgöl ante-caldera
S23	3.4.4	East Acıgöl – Boğazköy	East Acıgöl ante-caldera, Kartal Tepe, Tuluce Tepe
S24	3.4.4	East Acıgöl – Hotamış Dağ	East Acıgöl post-caldera, Koca Dağ
S25	3.4.4	East Acıgöl – Taşkesiktepe	East Acıgöl ante-caldera
S26	3.4.5	Erciyes Dağ (rhyolitic tephras)	Kayseri, Dikkartın, Perikartın, Karagüllü

ca. 100 m asl). Occasionally other purported obsidian sources or deposits have been mentioned in the literature (e.g., the Mandrakia outcrop in Shelford et al., 1982). Arias et al. (2006) reported a new obsidian source, which they termed Agios Ioannes, based on two obsidian specimens recovered near a hydrothermal vent. When Agios Ioannes was revisited by Sterba et al. (2018), the researchers could not identify any specific outcrop, and 16 obsidian specimens collected from the surface chemically matched either Sta Nychia (n = 6) or Dhemenegaki (n = 10). Thus, Agios Ioannes is either a secondary deposit or an archaeological site, and the obsidian specimens measured by Arias et al. (2006) could have been altered by hydrothermal activity (Section 2) or perhaps differed for some other reason.

Fytikas et al. (1986) still, after publishing their work four decades ago, provide the best overview of volcanism on Melos, and the geological history of the Sta Nychia obsidian source in particular, created during an eruption of the Bombarda volcano, is discussed in detail by Rinaldi and Campos Venuti (2003). Fission-track ages from Arias et al. (2006) yielded dates of 1.57 ± 0.12 Ma for Sta Nychia obsidian and 1.60 ± 0.06 Ma for Dhemenegaki obsidian, suggesting that the two Melos obsidian sources had closely timed emplacements during the Early Pleistocene. Similarly, Yeğingil et al. (2020) measured fission-track

Table 2
Summary of the available geochronological data for the obsidian sources of interest.

Source name	Fission tracks	K-Ar or Ar-Ar	Sr isotopes	(U–Th)/He zicron
Southern Aegean Volcanic Arc				
Melos – Sta Nychia	1.57 ± 0.12 Ma	1.47 ± 0.05 Ma		
Melos – Dhemenegaki	1.60 ± 0.06 Ma			
Antiparos	4.9–5.2 Ma	4.0–5.4 Ma		
Giali A	31.4 ± 4.7 ka			
Giali B	ca. 150 ka			
Western Anatolian Volcanic Province				
Foça	4–9 Ma			
Kütahya A, B, C				
Galatian Volcanic Province				
Yağlar		20.7 Ma		
Sakaeli-Orta	21.3–23.7 Ma			
Galatia-X	21.2–23.8 Ma			
Central Anatolian Volcanic Province				
Hasan Dağ	390 ± 50 ka			
Nenezi Dağ	1.14–1.20 Ma	0.91 ± 0.13 Ma	0.98 ± 0.6 Ma	
West Göllü Dağ – North Bozköy	1.15 ± 0.07 Ma			
West Göllü Dağ – Kayırlı Village				
East Göllü Dağ - Kömürcü	1.33 ± 0.08 Ma			
East Göllü Dağ - East Kayırlı	1.48 ± 0.09 Ma			
East Göllü Dağ - Bozköy-Boztepe/ Sırça Deresi	0.98 ± 0.06 Ma			
West Acıgöl	19–20 ka			23.3–24.9 ka
East Acıgöl – White Tuffs Hotamış Dağ	> 112 ka			
East Acıgöl – Boğazköy	150–182 ka			190 ± 11 ka
East Acıgöl – Hotamış Dağ	> 77 ka			190 ± 9 ka
East Acıgöl – Taşkesiktepe				147 ± 8 ka
Erciyes Dağ (rhyolitic tephras)		110–140 ka		

dates between 1.48 and 1.80 Ma and a mean age of 1.65 Ma. K-Ar dating reported by Fytikas et al. (1976) yielded an age of 1.47 ± 0.05 Ma for Sta Nychia, consistent with the fission-track ages, whereas their K-Ar date for Dhemenagaki (0.88 ± 0.18 Ma) appears to be erroneous for whatever reason. Bigazzi et al. (1986) also determined fission-track dates highly consistent with those above: 1.57 ± 0.15 Ma for Dhemenagaki and 1.54 ± 0.18 Ma for Sta Nychia, further supporting their approximate ages.

The supply of Sta Nychia and Dhemenegaki obsidian, just 10 km apart and similar in workability, throughout the Aegean seems to have been largely influenced by the collection preferences of different peoples who landed on the island of Melos. In general, obsidian from Sta Nychia, which lies on the shore of the island's natural harbor, can be collected as large pebbles within volcaniclastic deposits along the coastline, whereas Dhemenegaki obsidian occurs high atop a cliff and was often accessed via quarries or small mines (Shelford et al., 1982). Torrence (1986) argued that, contrary to one widely held notion, neither of the two obsidian sources were overseen by a centralized commercial industry.

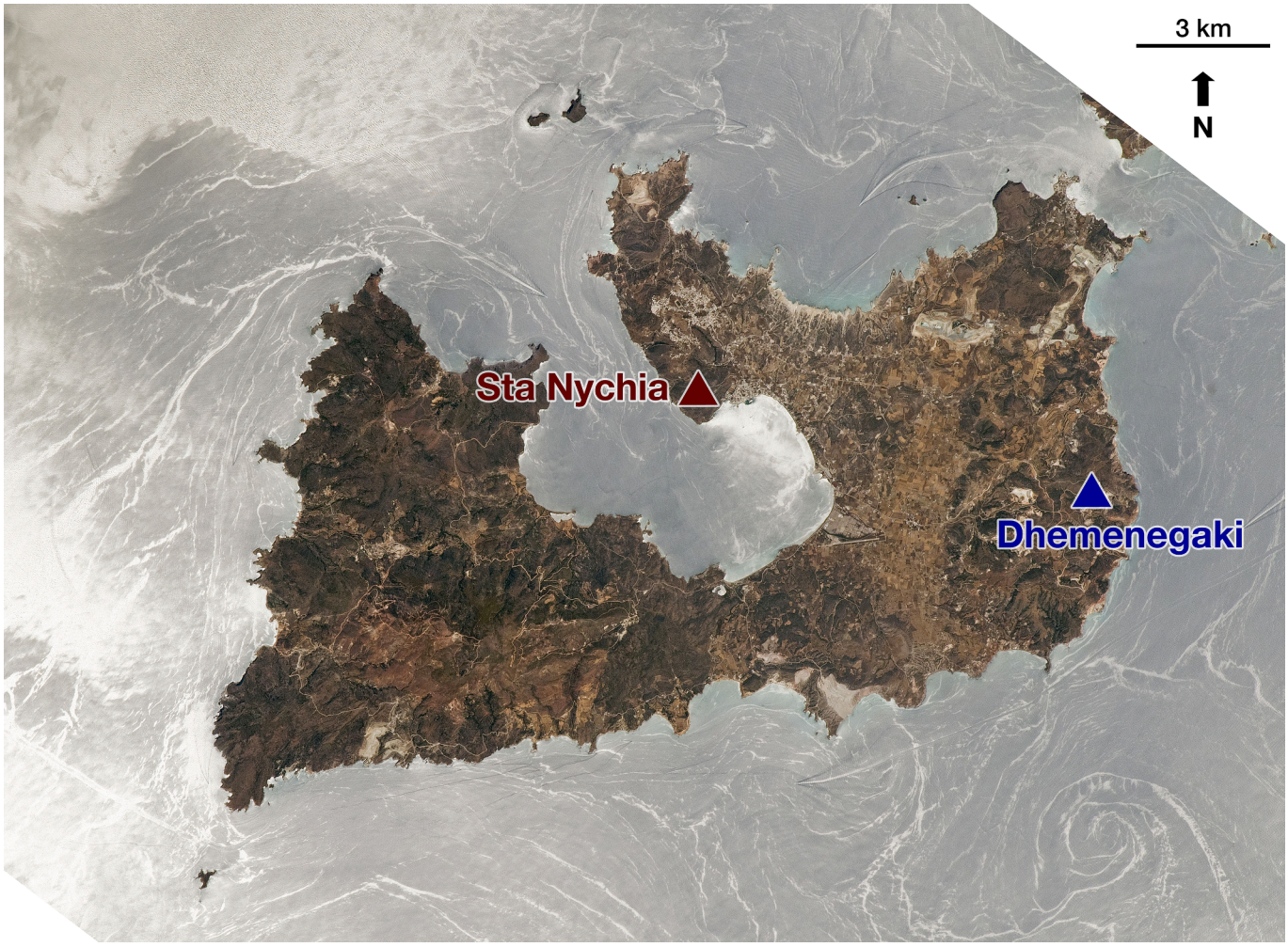

Fig. 6. The island of Melos with the location of its two obsidian sources – Sta Nychia (red triangle) and Dhemenegaki (blue triangle) – highlighted in this photograph taken by an astronaut onboard the International Space Station. Credit: Astronaut photograph ISS067-E-153817 acquired on 25 June 2022 and freely provided to the public by the ISS Crew Earth Observations Facility and the Earth Science and Remote Sensing Unit, Johnson Space Center via the NASA/JSC Gateway to Astronaut Photography of Earth. (For interpretation of the references to color in this figure legend, the reader is referred to the web version of this article.)

Instead, Melos obsidian had been distributed throughout the Aegean region by a variety of noncommercial means, from, for example, procurement embedded in mobile forager-fisher subsistence activities during the Neolithic Period to special-purpose collection expeditions during the Bronze Age.

Diachronic shifts in the use of Sta Nychia versus Dhemenegaki obsidian have been recognized in the lithic assemblages of Aegean sites (e.g., Carter et al., 2023), especially at Neolithic settlements on the island of Crete (e.g., Carter and Kilikoglou, 2007, 2022). These studies indicate that there were changing social factors tied to the procurement and/or distribution of obsidian from the two Melian sources. For example, Pappalardo et al. (2003) report notable changes through time at the Cretan archaeological sites of Phaistos and Haghia Triada based on their XRF analyses of a series of 26 obsidian artifacts. All of the Final Neolithic artifacts originated from the Dhemenegaki source, whereas most of the Early Minoan I and all of the Early Minoan II artifacts originated instead from Sta Nychia. During the Middle Minoan I phase, obsidian artifacts from both Sta Nychia and Dhemenegaki are found at these sites. At the Cretan site of Malia, for comparison, the Middle Minoan II assemblage included obsidian from both Melian sources but strongly skewed toward Sta Nychia (ca. 95–97%; Carter and Kilikoglou, 2007).

Obsidian from Sta Nychia and Dhemenegaki are sufficiently similar in chemical composition that differentiating them has been used a benchmark to test the potential effectiveness of various scientific techniques for obsidian sourcing. In general, elemental techniques – for example, ICP-AES (Kilikoglou et al., 1997), NAA (Aspinall et al. 1972), and WDXRF (Shelford et al. 1982) – were successful, whereas other techniques (e.g., fission-track dating, Durrani et al., 1971; Sr isotopes, Gale, 1981; electrical conductivity, Kotsakis, 1982; mineral inclusions, Acquafredda and Paglionico, 2004; Raman spectroscopy, Arias et al. 2006; luminescence dating, Polymeris et al., 2010) were not. These successful techniques (e.g., XRF, NAA, ICP-AES/MS) have been applied in obsidian sourcing studies worldwide, but the unsuccessful ones have seen limited, if any, subsequent use. Consequently, Melos has often been used as a "proving ground" for sourcing techniques, given the compositional similarity of its obsidian sources.

It should not be surprising, therefore, that Melos obsidian was used to test the performance of pXRF instruments as the technology has advanced (Fig. 7). An early "portable" EDXRF system (ca. 1992) – a multi-component Spectrace 9000 TN instrument – was tested by Liritzis (2008) for analyzing Aegean obsidian. Its 2-kg handheld probe, which connected to a 7-kg electronics unit via a long cable, contained a HgI_2 X-ray detector (ca. 260 eV spectral resolution) and three radioactive isotopes (^{55}Fe, ^{109}Cd, ^{241}Am) as X-ray sources (Fig. 7a). Thus it should be noted that, when Liritzis and Zacharias (2011) discuss "current" work on obsidian sourcing by pXRF in Shackley (2011), the instrument was already two decades old and, in turn, reflected outdated technology.

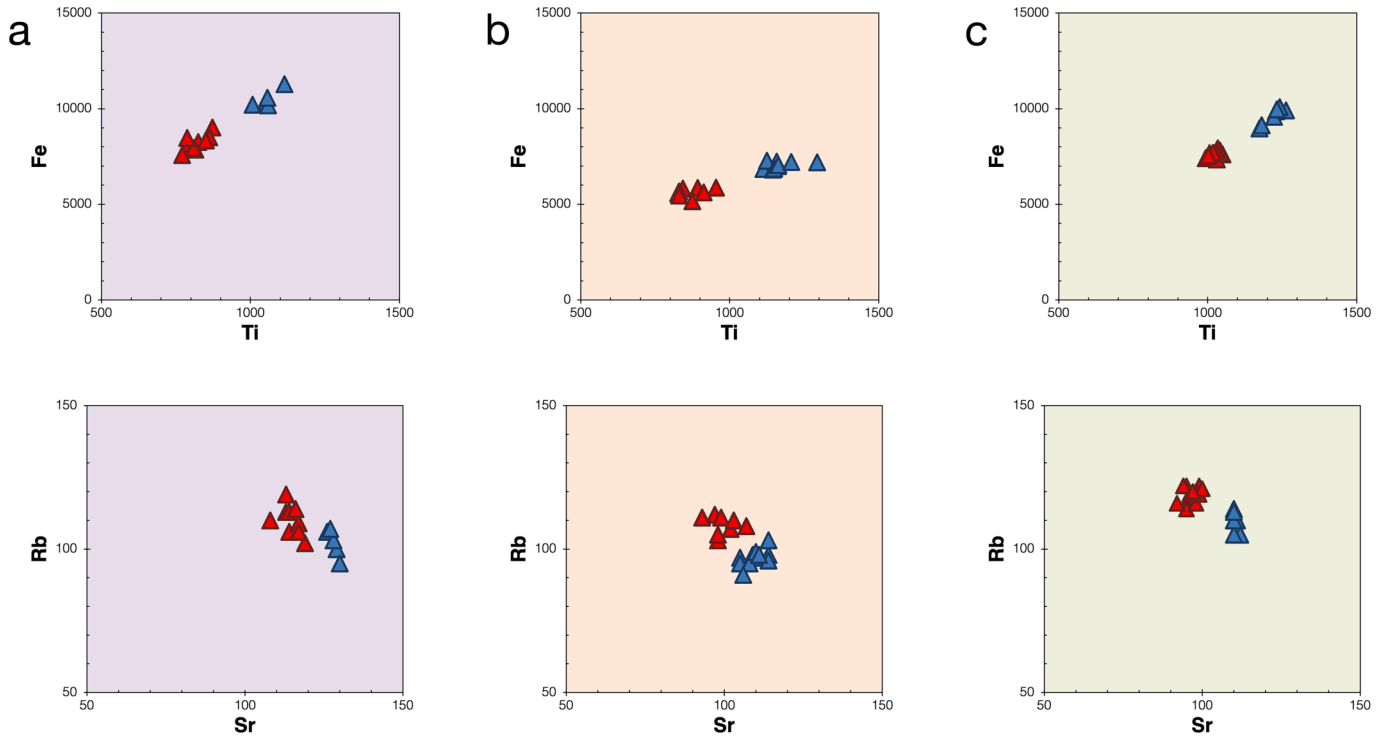

Fig. 7. Elemental differences (Ti vs. Fe and Sr vs. Rb) in Sta Nychia (red triangles) and Dhemenegaki (blue triangles) obsidian as measured using increasingly portable and sophisticated EDXRF instruments. These scatterplots show measurements from (a) a Spectrace 9000 TN instrument with a HgI_2 detector (ca. 260 eV resolution), radioactive isotopes as X-ray sources, and a weight of 9 kg (20 lbs) (Liritzis, 2008); (b) an Innov-X Delta instrument with a Si drift detector (SDD), a miniature Rh-anode X-ray tube, and Compton normalization correction (Milić, 2014); and (c) a Thermo Scientific XL3t GOLDD + instrument with a SDD (ca. 155 eV resolution), an Ag-anode tube, and fundamental parameters (FP) correction with standards (Frahm et al., 2014a). (For interpretation of the references to color in this figure legend, the reader is referred to the web version of this article.)

Milić (2014) and I (Frahm et al., 2014a) instead used newer and more sophisticated pXRF instruments in our tests (Fig. 7b and 7c), and our results illustrate increasingly clear distinctions made on the basis of elemental differences (Ti vs. Fe, Sr vs. Rb) as the hardware (e.g., newer detectors) and software (e.g., better quantification algorithms) both improved.

The compiled elemental data and consensus ranges for Sta Nychia and Dhemenegaki obsidian are available in Supplementary Table S1 and S2, respectively.

3.1.2. *Antiparos*

Obsidian on the island of Antiparos occurs in an area known as Soros Hill (36.967° N, 25.050° E, ca. 0–110 m asl; Carter and Contreras, 2012; see also Nikolakopoulos et al., 2018: Fig. 12 for an updated geological map of the island). Fission-track dating of Antiparos obsidian has yielded ages of 4.9 to 5.2 Ma (Arias et al., 1986), while K-Ar dating of associated vitrophyre resulted in an age between 4.0 and 5.4 Ma (Innocenti et al., 1982). Hence, Antiparos obsidian is about three times older than that from Melos. This obsidian principally occurs as lenses and nodules within perlitic-tuffaceous deposits surrounding the lava dome and in secondary colluvial deposits between the dome and the shore (Carter and Contreras, 2012; Acquafredda et al., 2019). Although the obsidian can be high-quality (i.e., predictable conchoidal fracture, translucency indicative of few phenocrysts within the glass), it saw little use in the past due to its small size. Renfrew et al. (1965: 232) report that Antiparos obsidian occurs as "small lumps… up to 5 cm" in diameter. Similarly, during a survey by Carter and Contreras (2012: 590), "rarely were nodules larger than 4 cm in their long dimension observed." Consequently, this issue of size is commonly presumed to be the reason that so little Antiparos obsidian has been identified archaeologically.

Even on the island of Antiparos, its obsidian has rarely been found. During their obsidian-focused survey of Soros Hill area, Carter and Contreras (2012: 599) "saw precious little evidence for the material having been knapped at the source, with the exception of one blade-like piece." Renfrew et al. (1965: 239) thought there to be "no artifacts of obsidian from Antiparos." They knew only of a "pebble" (Bent, 1884: 51) or "small natural lump of Antiparos obsidian, obviously buried as an attractive curiosity," found in an Early Bronze Age cemetery (Apantima/Agios Sostis) on the island. This attribution, however, is based only on its visual traits, and the cemetery lies less than 2 km from the source. Other rare, visually identified obsidian pieces (e.g., a small, unworked nodule from an Early Bronze Age cemetery on the island of Ano Kouphonisi; Zapheiropoulou, 2008) have since been determined to be Giali obsidian (T. Carter, personal communication). There is, to my knowledge, only one earlier instance of obsidian chemically sourced to Antiparos: just off the coast of Antiparos, on the tiny island of Saliagos, Antiparos obsidian nodules and flakes were recovered from a Late Neolithic settlement (Cann et al., 1968).

Here I can add a previously unpublished instance of chemically identified Antiparos obsidian. In 2012, I visited the Bronze Age (Early Helladic I and II, 2650 to 2000 BCE) site of Keryneia Achaea in the northern Peloponnese of Greece (Fig. 8; 38.212° N, 22.124° E), which was excavated from 2009 to 2013 ahead of the Olympia Motorway construction (Kolia, 2012, 2013; Kolia and Spiroulias, 2017). Kolia (2013) proposed that the site, which spans 5 ha, was an early proto-urban center that served an administrative function for the surrounding area in the third millennium BCE. Using pXRF, I tested 333 obsidian artifacts that were housed at the 6th Ephoria of Prehistoric and Classical Antiquities in Patras. The Keryneia-Achaea obsidian assemblage, which consisted of many hundreds of artifacts, is dominated by prismatic blades and their associated cores, rejuvenation flakes, and so forth, so my sampling approach focused on the blades and cores. Of these artifacts, 328 originated from the Melos–Sta Nychia source, and three derived from Melos–Dhemenegaki. The remaining two obsidian pieces

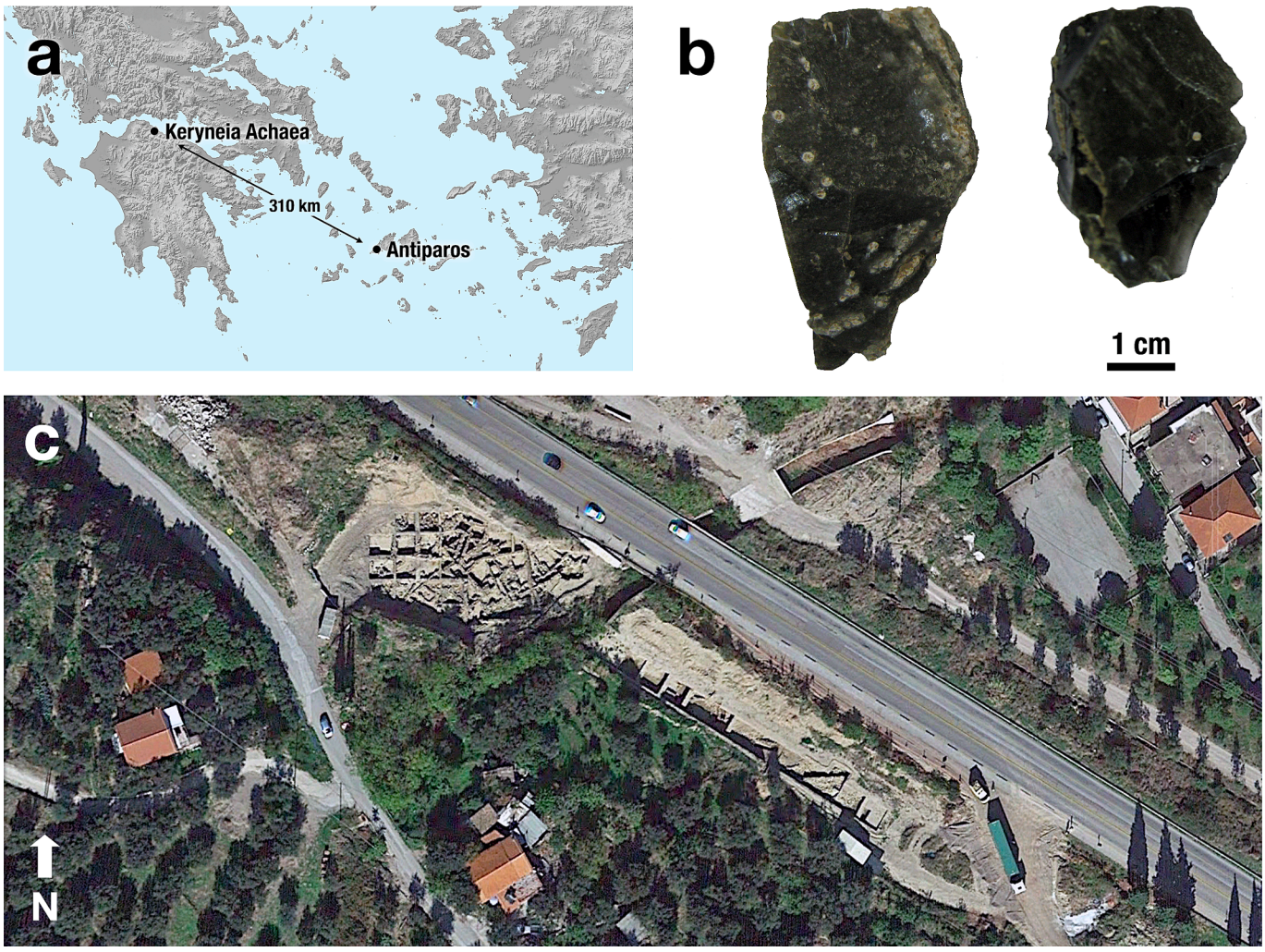

Fig. 8. (a) The Bronze Age archaeological site of Keryneia Achaea lies in the northern Peloponnese of Greece, ca. 310 km over sea and land, from the island of Antiparos. (b) The two pieces of Antiparos obsidian (note the presence of light-grey spherulites in both) identified at Keryneia Achaea. (c) Satellite image of the Keryneia Achaea excavations (dated 24 October 2013) from Google Earth, reproduced here in accordance with Google's Terms of Service and General Guidelines regarding fair use in publications.

match Antiparos (Fig. 9), ca. 310 km away over both land and sea, and they fit the description of Antiparos obsidian found at other sites: largely unworked nodules with some weathered surfaces, about 4 cm in maximum dimension. Thus, these two pieces from Keryneia Achaea are the farthest-travelled instances of Antiparos obsidian currently known, and it seems that there is more to its distribution and use than is presently clear to us. Given the size of Keryneia-Achaea's obsidian assemblage, the use of pXRF was crucial in conclusively identifying these two Antiparos obsidian pieces, which constituted less than 1% of the lithic artifacts.

The compiled elemental data and their consensus ranges for Antiparos obsidian are available in Supplementary Table S3.

3.1.3. *Giali A and B*

Giali ("glass" in Greek; also transliterated as Gyali or Yali) is one of the Dodecanese islands in the southeastern Aegean, just off the southwestern coast of Turkey (36.664° N, 27.119°E). As shown in Fig. 10, this small island (4.6 km^2) consists of two volcanic domes – a northeastern one and a southwestern one – connected via a narrow isthmus of reef sediments. Indeed, Giali was, until recently (in a geological sense), two separate islands. Fission-track dating by Bigazzi and Radi (1981) resulted in an age of ca. 24–30 ka for the northeastern eruptive center and ca. 150 ka for the southwestern one. Bigazzi et al. (1986) updated the former age to 31.4 ± 4.7 ka, but these authors entirely ignored the latter age. The term "Giali obsidian" is almost always used in the literature in a singular sense, so Bigazzi and colleagues might have felt a need to report only a single age. Furthermore, Giali obsidian is widely considered to be unsuitable for knapping due to its large mineral inclusions, principally plagioclase feldspars and iron-rich pyroxenes, leading to unpredictable flaking (Kayani and McDonnell, 1996). Such inclusions can account for as much as 5% of the obsidian by volume and be as large as 1–2 mm. Carter et al. (2016), though, explored the use of Giali obsidian through time, from its earliest use by local Dodecanesian people to make flaked tools to its later exploitation by lapidarists in Cretian palaces to create prestige items. As an example of the latter, in their *Scientific American* article, Dixon et al. (1968) included a photograph of a sculpted seashell, found in a Minoan context on Crete and carved from inclusion-rich Giali obsidian.

The possibility of two Giali distinct obsidian sources was suggested by McDougall et al. (1983) in a pioneering study on obsidian's magnetic properties and the potential for sourcing artifacts throughout the Mediterranean region. All obsidian, even when it is completely transparent, contains sub-millimeter minerals, albeit comprising a tiny fraction of the rock's volume. Indeed, the black color of most obsidian is a result of microscopic magnetite (Fe_3O_4) grains suspended within the glass. McDougall et al. (1983) hoped that variation in such magnetite grains –

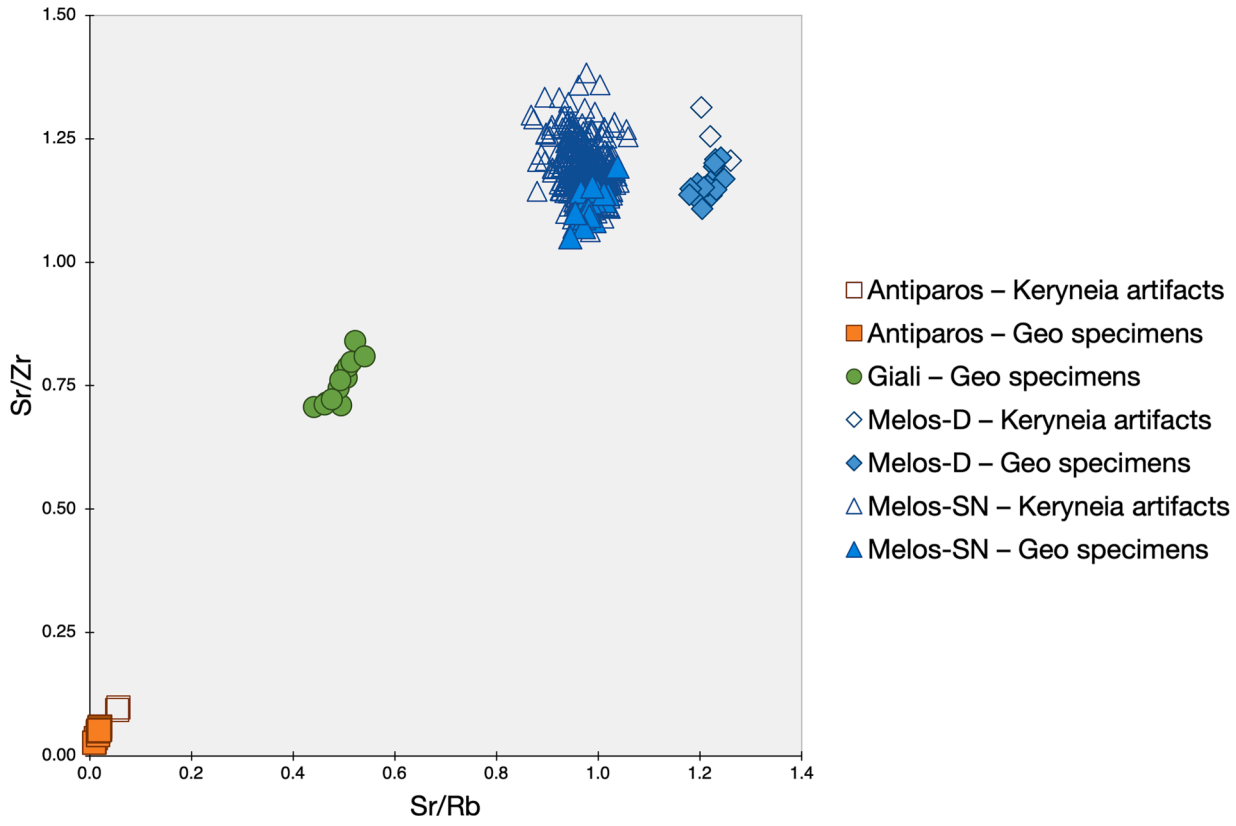

Fig. 9. Elemental data for 333 obsidian artifacts from the Bronze Age archaeological site of Keryneia Achaea in the northern Peloponnese of Greece. Two obsidian artifacts match Antiparos, three match Melos–Dhemenegaki, and the remainder match Melos–Sta Nychia. All analyses were conducted by pXRF in December 2012 at the 6th Ephoria of Prehistoric and Classical Antiquities in Patras, Greece.

modal (i.e., concentration); morphological (e.g., grain sizes, shapes), and mineralogical (e.g., Ti-free magnetite vs. high-Ti titanomagnetite) – might prove useful for sourcing obsidian artifacts. Their work resulted in mixed success. For example, the two Melos obsidian sources – Dhemenegaki and Sta Nychia – were differentiated magnetically, but Dhemenegaki obsidian overlapped with that from Giali, as shown in Fig. 11a. McDougall et al. (1983) concluded that obsidian from a Giali beach, collected by John Cherry and Robin Torrence in 1976, differed in magnetic parameters from the specimens collected elsewhere on the island. They proposed, therefore, that the "Giali Beach" obsidian differed origin from the rest of the Giali specimens. Additional context, though, is required to understand why the beach specimens do not *necessarily* reflect a distinct source.

McDougall et al. (1983) measured three magnetic parameters: natural remanent magnetization (NRM), low-field susceptibility (χ), and saturation magnetization (M_s). NRM is the magnetization acquired by a specimen through natural processes, primarily the magnetization acquired from Earth's geomagnetic field as the obsidian cooled after its eruption but potentially altered by other processes (e.g., reheating, lightning strikes, secondary mineralization). It is a vector sum with both a direction and a magnitude, but McDougall et al. (1983) apparently relied only on the NRM magnitude (presumably because Cherry and Torrence did not collect oriented specimens). While NRM is largely considered a record of Earth's field at the time of a specimen's last heating, its magnitude also reflects the amount of magnetic material within that specimen. Low-field χ measures the magnetization of a specimen temporarily induced when a weak magnetic field is applied, and it primarily serves as a proxy for the amount of magnetic material within a specimen (although χ data are more complicated in the presence of multiple minerals or widely varying grain sizes). M_s, in comparison, is the maximum possible magnetization of a specimen in the presence of a strong magnetic field (much stronger than that in χ measurements and sufficiently powerful to reset a specimen's NRM), and it is also principally a measure of the concentration of magnetic material within a specimen. Therefore, McDougall et al. (1983) measured three parameters that, in large part, reflect the amounts of magnetic material, principally magnetite, within Aegean obsidian.

The issue is that, as I have previously shown (e.g., Frahm and Feinberg, 2013; Frahm et al., 2014b; Frahm et al., 2016), magnetic properties can vary throughout an obsidian flow. The magnetic properties of obsidian are a net product of the concentrations, compositions, morphologies, grain sizes, and spatial arrangements of magnetite grains and other magnetic minerals. Local conditions within an obsidian flow, such as the cooling rate, viscosity, oxygen and water availability, and post-emplacement forces, influence the final magnetic mineral assemblage and its magnetic recording. Thus, magnetic minerals can be highly sensitive recorders of conditions that varied within a certain obsidian flow, meaning that their magnetic properties can also vary within that flow. This is best demonstrated using an example from my research involving perhaps the most magnetically studied obsidian source: Gutansar volcano in Armenia. McDougall et al. (1983) tested 22 obsidian specimens from Giali, whereas I have analyzed more than 600 geo-referenced obsidian specimens from Gutansar and almost 400 Palaeolithic artifacts from this obsidian source. All of these specimens and artifacts were characterized with magnetic hysteresis loops (Fig. 11b), which plot a material's magnetization (M) in response to an applied magnetic field of varying strength (B). M_s as well as saturation remanence (M_r), coercivity (B_c), and coercivity of remanence (B_{cr}) are collectively known as hysteresis parameters and have been described in detail by Harrison and Feinberg (2009), Tauxe (2010), and others. I took these measurements with a Princeton Measurements vibrating sample magnetometer (VSM) at the University of Minnesota's Institute for Rock Magnetism (IRM).

Note that the M_s measurements by McDougall et al. (1983) of Giali

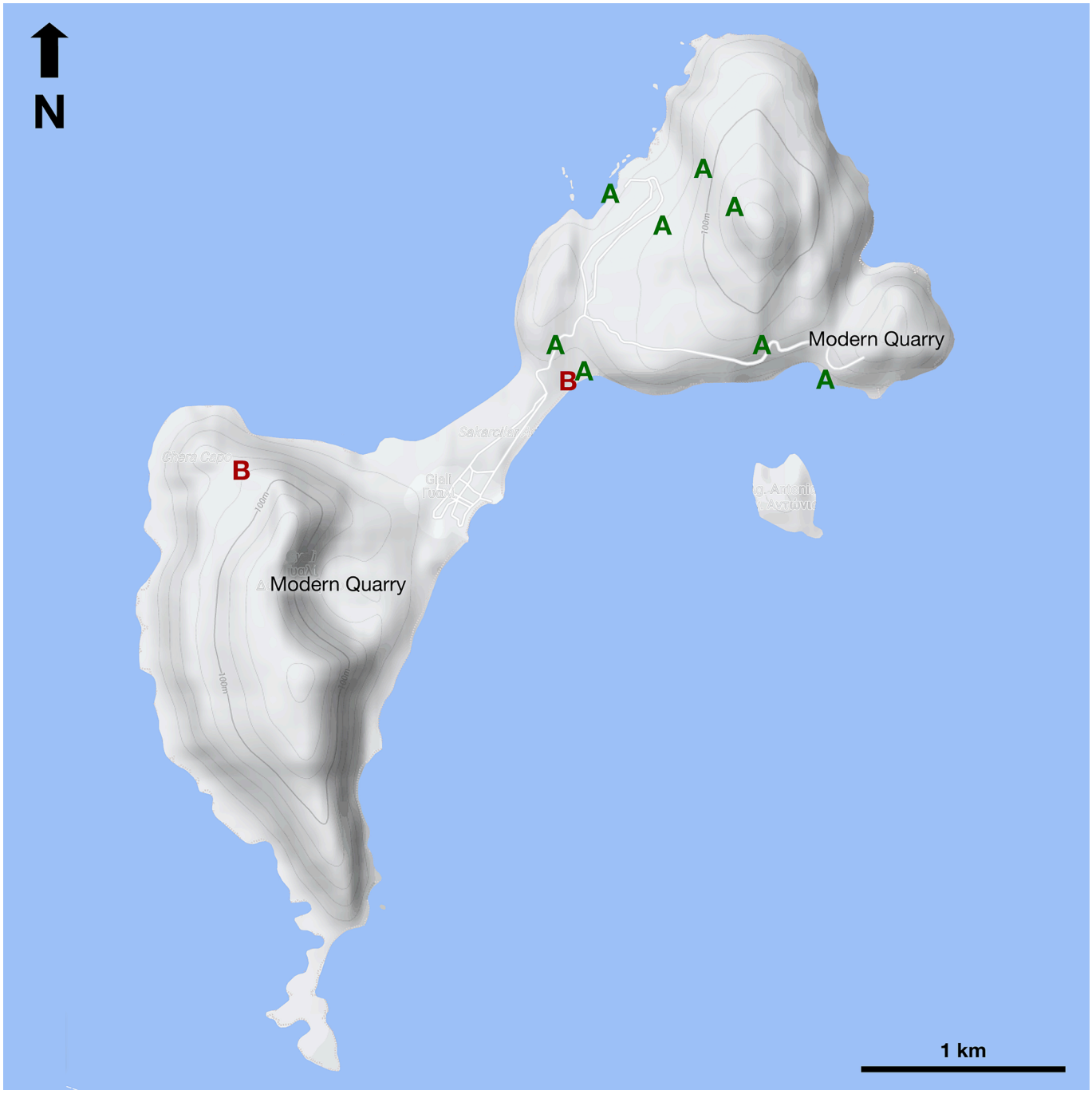

Fig. 10. The island of Giali and the sampling locations of Carter et al. (2016: Fig. 2) for Giali A and B obsidian (marked as such). The vast pumice deposits of these two rhyolitic domes have been intensively quarried as an economic resource. Background map from Google Earth, reproduced here in accordance with Google's Terms of Service and General Guidelines regarding fair use in publications.

and "Giali Beach" specimens vary over three orders of magnitude (Fig. 11a). Fig. 12a is a scatterplot of M_r versus M_s for 618 Gutansar obsidian specimens, and these M_r and M_s data also vary over three orders of magnitude. M_r reflects the maximum permanent magnetization possible for a specimen, and much like M_s, it is primarily a proxy for the magnetic mineral concentration and, to a lesser extent, grain size. Thus, Fig. 11a and 12a reflect the same degree of magnetic variation and, in turn, abundance of magnetic material (i.e., concentrations of magnetite grains). Such multi-order variation, however, is not observed in hysteresis parameters that do not principally reflect the amount of magnetic material. B_c (the applied field strength when a specimen's induced magnetization reaches zero) is, in general, inversely related to grain size (until size decreases to a diameter of ca. 50 nm, below which B_c values drop exponentially), and B_{cr} (the field strength needed to remagnetize half of a specimen's magnetic minerals so that M_r equals zero) is interpreted with the same conventions as B_c, whereby values are inversely related to grain size. Fig. 12b illustrates the much lower variation in the B_c and B_{cr} values of Gutansar obsidian, indicating that the magnetic grain sizes are more consistent than their abundances. Examining fewer obsidian specimens from two outcrops (n = 52 from one outcrop, 39 from the other), located less than 3 km apart at Gutansar, reveals a separation in the M_r and M_s data (Fig. 12c) but an overlap in the B_c and B_{cr} data (Fig. 12d). That is, the two different outcrops of Gutansar obsidian exhibit a greater difference in M_s values than Giali and "Giali

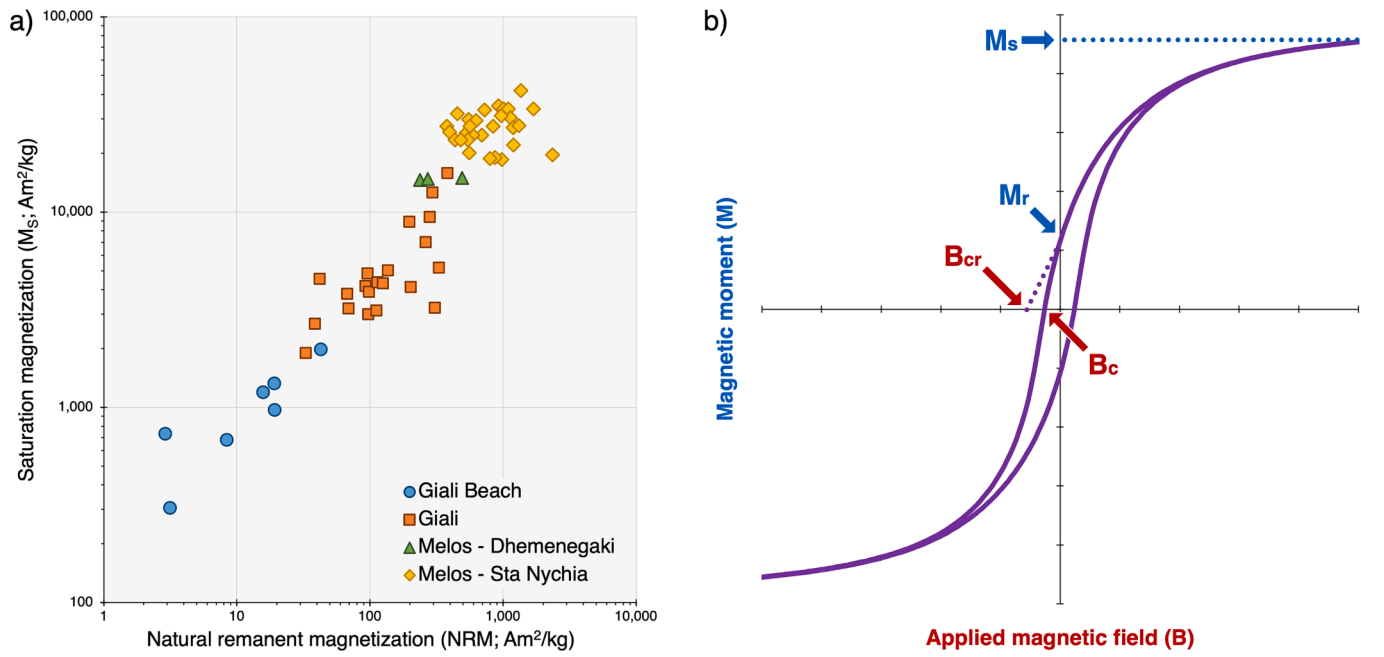

Fig. 11. (a) Magnetic measurements (NRM vs. M_s) extracted from McDougall et al. (1983: Fig. 3) using WebPlotDigitizer v4.6 for Aegean obsidian sources, showing the basis for McDougall et al. (1983) to differentiate "Giali" and "Giali Beach" obsidian. (b) An example of a magnetic hysteresis loop for a magnetite-bearing obsidian specimen illustrates how the saturation remanence (M_r), saturation magnetization (M_s), coercivity (B_c), and coercivity of remanence (B_{cr}) are measured.

Beach" obsidian in the measurements of McDougall et al. (1983); however, B_c and B_{cr}, if measured instead, might have yielded a different outcome. McDougall et al. (1983) mention differences in the "visual characteristics" of Giali and "Giali Beach" obsidian and, ultimately, that it what their magnetic data reflect: differences in the amount of magnetic minerals. Their observed magnetic differences, though, are insufficient to define a separate obsidian source, given that such variation can occur within a single source.

Carter et al. (2016) found better evidence for two distinct compositions of Giali obsidian, which they termed Giali A and Giali B. Their elemental compositions are extremely similar, but Rb is one of the key trace elements for distinguishing them: 143 ± 8 ppm in Giali A and 132 ± 4 ppm in Giali B. The spatial distributions also differ: Giali A corresponds to the 31.4 ± 4.7 ka obsidian in the northeastern part of the island, and Giali B corresponds to the obsidian ca. 150 ka in age in the southwestern part (Fig. 10). Their morphologies and mineralogies also differ. Based on the surveys of Carter et al. (2016), Giali B obsidian occurs as small pebbles and appears homogeneous and glassy to the naked eye, whereas Giali A obsidian exists as boulders and exhibits the millimeter-scale mineral inclusions discussed above. These differences explain the distinct magnetic properties measured by McDougall et al. (1983).

The elemental data and their consensus ranges for Giali A obsidian can be found in Supplementary Table S4. Supplementary Table S5 compares the elemental measurements for Giali A and Giali B obsidian from Carter et al. (2016), and it demonstrates that the inter-laboratory error for Giali A obsidian equals or exceeds the measurement difference between Giali A and Giali B from Carter et al. (2016) using the same instrument. Hence, attributing artifacts to either Giali A or Giali B might involve considerable uncertainty, especially if one is unable to use the same analytical instrument, protocols, etc. in order to measure both the geological specimens from Giali and the archaeological artifacts of interest.

3.2. *Western Anatolian volcanic province*

Obsidian and associated volcanics (i.e., perlite, vitrophyre) in far western Turkey occur within an area known as the Western Anatolian Volcanic Province (Fig. 2). Chataigner et al. (1998: 523) note that, within this region, "small deposits… are not well known, and samples collected today from these deposits appear unsuitable for tool-making," making it unlikely that these materials were exploited for knapping tools in antiquity. Özdoğan (1994: 426) claimed that "it seems highly possible that there are many more small but significant sources all around Western Anatolia," whereas Pernicka et al. (1996) asserted that, "although claims have occasionally been made that obsidian occurs in western Anatolia, no sources of workable obsidian have yet been found." In the sections below, I include new data about the formation of Foça perlite, and I provide the first elemental analyses of Kütahya obsidian.

3.2.1. *Foça*

Poidevin (1998: Fig. 1) – like Chataigner et al. (1998: Fig. 1), Carter et al. (2011: Fig. 1), and others – included a source on the Foça Peninsula near İzmir along Turkey's Aegean coast (ca. 38.67° N, 26.77° E, 130 m asl). This peninsula has at least four rhyolitic lava flows and domes (Akay, 2000; Akay and Erdogan, 2001), suggesting that favorable conditions might have existed for the formation of obsidian. Akay (2000: 24) describes the Foça rhyolites as having porphyritic textures (i.e., distinct crystals embedded in either a fine-grained or glassy matrix). Specifically, the rhyolites contain ca. 20% feldspar and quartz phenocrysts, some as large as 2 mm across, within a devitrified glassy groundmass. Akay (2000: 25) also mentions their concurrence with perlite. This is consistent with Ercan et al. (1996: 506), who reported the presence of "thin obsidian beds intercalated with perlites [which] are not suitable for use… and, therefore, have no archaeological value." My own observations of the Foça material agrees with the descriptions from Akay (2000) and Ercan et al. (1996). Fig. 13 shows a backscattered electron image and EMPA element maps for a Foça specimen, revealing porphyritic texture as described by Akay (2000). In addition, my EMPA data for a set of Foça specimens indicated a high degree of hydration (5.1–5.6% H_2O; Frahm, 2010), compared to < 2% for obsidian specimens from central Turkey. This large amount of water interfered with efforts to fission-track date of this material. Bigazzi et al. (1997) measured an *apparent* fission-track age of 3.94 ± 0.30 Ma; however, this is an underestimate compared to what would be the correct plateau age. Storzer and Wagner (1969) estimated an age of 9 Ma, despite the

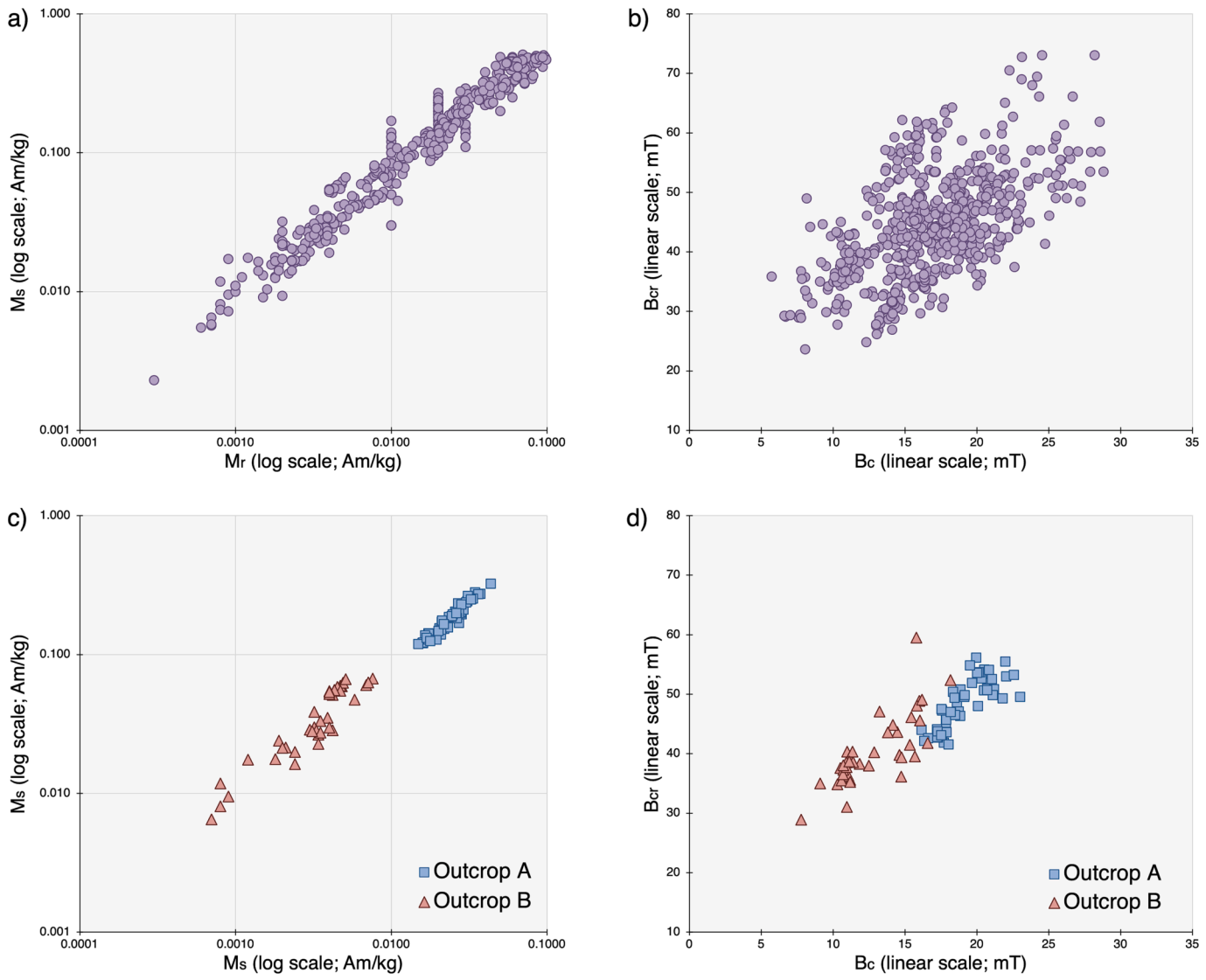

Fig. 12. Magnetic data for, to my knowledge, the most magnetically studied obsidian source in the world: Gutansar in Armenia (Frahm et al., 2014b, 2016). (a) The scatterplot of M_r vs. M_s shows that these variables, both of which principally reflect the amount of magnetic material within a material, span three orders of magnitude, like the data of McDougall et al. (1983) do. (b) The scatterplot of B_c vs. B_{cr}, two variables which primarily reflect magnetic grain morphology, shows greater consistency in the values for Gutansar obsidian. (c) Two specific outcrops of Gutansar obsidian exhibit a clear separation in a M_r vs. M_s plot, despite being geochemically indistinguishable. (d) Obsidian from the two outcrops are more consistent in their B_c vs. B_{cr} values. All measurements taken using a Princeton Measurements vibrating sample magnetometer (VSM) at the University of Minnesota's Institute for Rock Magnetism.

challenge posed by hydration. The mechanism behind this degree of hydration, though, had not been hitherto investigated.

There are two primary mechanisms by which such hydration can occur: (1) during eruption and emplacement, water dissolved within the magma, originating from deep underground, can create perlitic and/or devitrified fabrics while still at high temperatures; and (2) obsidian gradually converts into perlite via hydration, diffusion, and alteration over long timespans (i.e., millions of years) at lower temperatures. How the hydration of the Foça specimens compared to those from central Turkey was a core question of an undergraduate student research project at the University of Wisconsin-Eau Claire, co-overseen by me, that has never been fully published and was only presented at conferences (Conde et al., 2009a, 2009b, 2010, 2011). Water content was measured by Fourier-transform infrared spectroscopy (FTIR) microscopy, sometimes called micro-FTIR or μFTIR. Specimens were cut and polished into small discs with a thickness of ca. 0.5–1.5 mm, and these discs were measured using a DigiLab Excalibur series FTS 700 bench (liquid N_2-cooled MCT detector and tungsten-halogen source) linked to a UMA 600 microscope. Focusing on the Near IR (NIR) spectra enabled quantitative peak-fitting of the Si-OH (hydroxyl) and HOH (molecular water) absorbance bands using the Win-IR software from Bio-Rad Laboratories, Inc.

Fig. 14 shows the results of our FTIR microscopy measurements for the hydrous content of two Foça specimens as well as obsidian specimens from Nenezi Dağ, Acıgöl, and Göllü Dağ in central Turkey. In Fig. 14a, two measures of the water content – 7100 cm^{-1} band vs. 5200 and 4500 cm^{-1} bands – reveal that the water content of the Foça specimens is considerably higher ($\geq$5% H_2O) than it is in the obsidian specimens from central Turkey ($\leq$2% H_2O). In Fig. 14b, equilibration of the two water species – hydroxyl (Si–OH) and molecular water (HOH) – is strongly dependent on temperature, so the proportion between these water species can serve as an indicator of the temperature at which hydration occurred. Our data suggest that the Foça specimens were hydrated at low temperatures (ca. 200° C; i.e., by surface water after their eruption) while the obsidian from central Turkey experienced hydration at high temperatures (ca. 400–800° C; i.e., by magmatic water

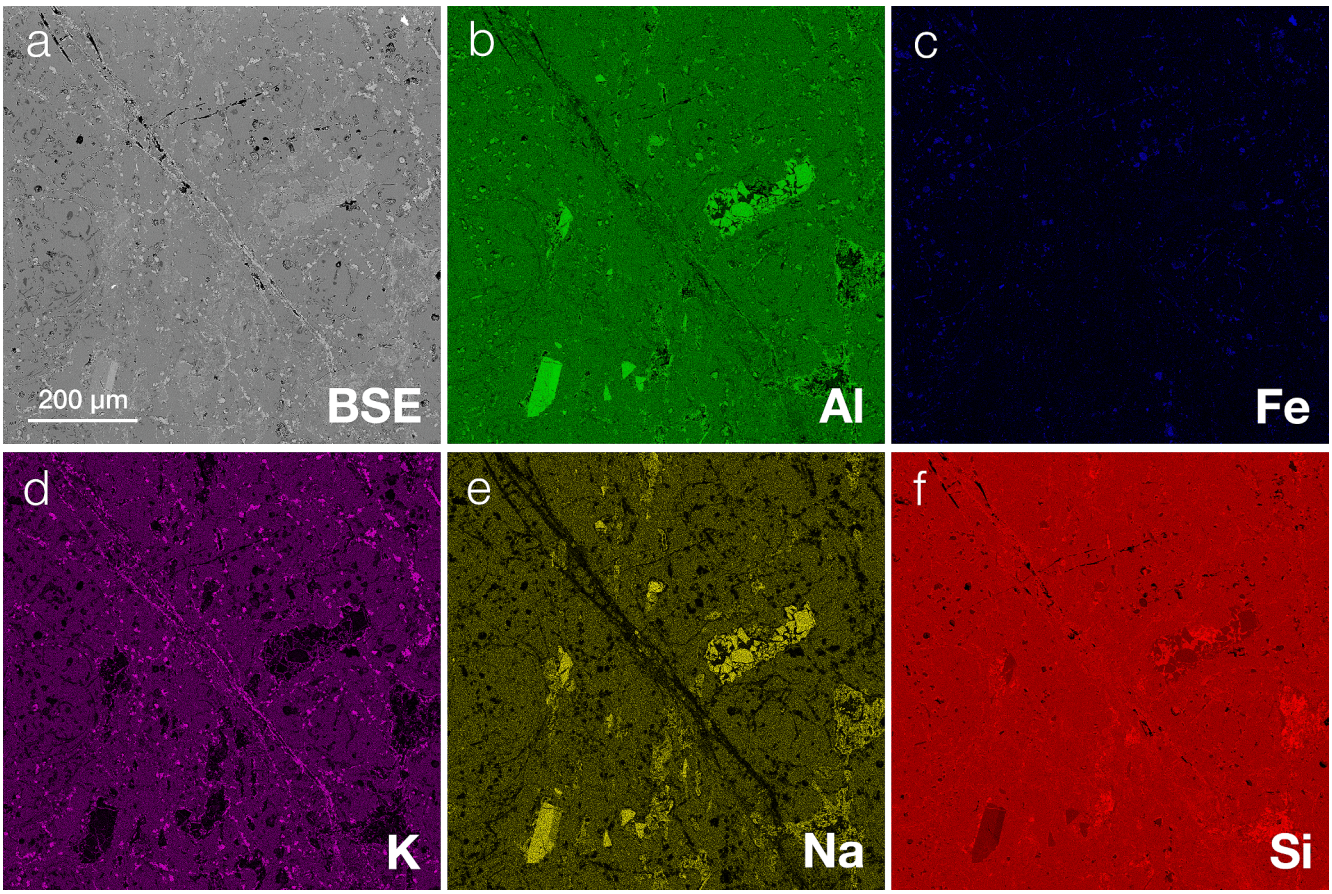

Fig. 13. BSE image and element maps for a Foça specimen show a porphyritic texture consistent with the observations of Akay (2000), who described the presence of ca. 20% feldspar and quartz phenocrysts in a devitrified glassy groundmass. The brightest minerals in both the Al and Na maps reveal the presence of Na-feldspars, whereas the brightest minerals in the K map indicate the presence of K-feldspars. The brightest red in the Si map also shows the presence of quartz. Images collected by the author in the Electron Microprobe Laboratory in the Department of Earth and Environmental Sciences, University of Minnesota-Twin Cities. (For interpretation of the references to color in this figure legend, the reader is referred to the web version of this article.)

during eruption). Consequently, our data demonstrate that (1) the Foça specimens contain sufficient water to be classified as perlite and that (2) the perlite is a product of gradual, post-eruption hydration, not an initially high water content.

For the sake of completeness here, the compiled elemental data for Foça perlite are available in Supplementary Table S6. It should be noted, though, that Ercan et al. (1996: 506) regarded this material as having "no archaeological value" due to its unsuitability for knapping.

3.2.2. *Kütahya A, B, and C*

Kütahya (or Kalabak Valley) obsidian is rarely mentioned in the literature and, when it is, there is usually only a passing reference and a citation to Ercan et al. (1996). Ercan et al. (1996: 506) report little about Kütahya obsidian: "In Western Anatolia, 7 km east of Kütahya, obsidian beds of 10–15 cm thickness were discovered. These obsidians, which crop out in close vicinity to Alanyurt [sic] train station, are found together with Neogene deposits. The obsidians observed in Kütahya… are not suitable for use as tools and therefore have no archaeological value." This description, though, seems to be based not on their own observations but on a geological study of the Kütahya area by Akkuş (1962).

Akkuş (1962) described outcrops about 1–1.5 km to the east and the north of the Alayunt station (ca. 39.40° N, 30.11° E). In these outcrops, he reported that obsidian intercalates with Neogene (23–2.58 Ma) lacustrine deposits of diatomite, and other Neogene deposits in the area consist of lacustrine, marly, soft limestone and clays, principally montmorillonite. Akkuş (1962) did not explicitly state whether the obsidian occurs in a primary volcanic deposit or a secondary lacustrine deposit, but the implication is that he favored the former scenario. For example, Akkuş (1962: 27) wrote that intercalation of this obsidian "with Neogene layers indicates that the volcanism must have occurred during that time." For a secondary deposit, eruption and emplacement of the obsidian would not be contemporaneous to deposition of the diatomaceous sediments, while Akkuş (1962) favored a degree of synchronicity. In a geological map for the region, however, Alan et al. (2018) document Miocene (23–5.3 Ma) rhyolitic lava flows, which appear to be the appropriate age and, in turn, the most likely origins of this obsidian.

I was sent a series of small, subangular obsidian nodules, most less than a centimeter in diameter, from the Porsuk basin near Kütahya via an Istanbul-based stone supplier. Alayunt lies upstream from the collection area ca. 20 km to the north, so any obsidian that erodes out from between the soft diatomite could easily be transported northward by the Porsuk River. As shown in Supplementary Tables S7, S8, and S9, three obsidian compositions were present among these nodules, suggesting that this collection area is an alluvial secondary deposit that contains obsidian from different sources within the catchment zone of the Porsuk. It remains possible that (1) the obsidian deposits observed near Alayunt train station are secondary deposits, perhaps lacustrine in origin, that contain nodules from various volcanic sources, (2) the various deposits near Alayunt station (e.g., to the east, to the north) reflect distinct sources (e.g., different lava domes) and, therefore, have obsidian with different compositions, or (3) the deposits near Alayunt station reflect one of the three obsidian compositions while (at least) two other obsidian sources lie elsewhere within the Porsuk basin and

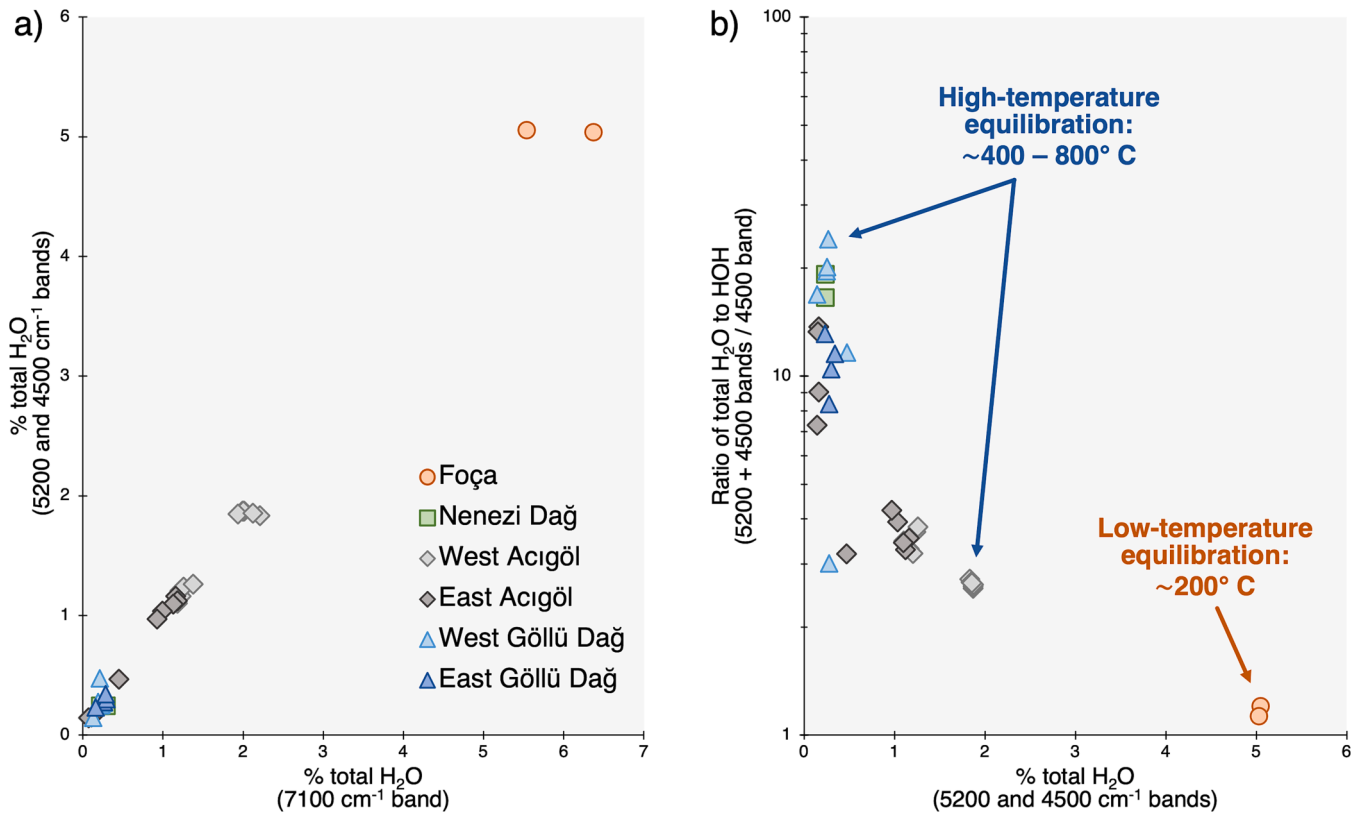

Fig. 14. FTIR measurements of the water content in two Foça specimens. (a) Two metrics of the water content – 7100 cm^{-1} band vs. 5200 and 4500 cm^{-1} bands – in Foça, Nenezi Dağ, Acıgöl, and Göllü Dağ specimens, demonstrating that the water content of the Foça specimens is notably higher (≥5% H_2O) than in the other specimens (≤2% H_2O). (b) The proportion between the two water species – hydroxyl (Si–OH) and molecular water (HOH) – can reflect the temperature at which hydration occurred. This permits us determine that the Foça specimens were hydrated at low temperatures (i.e., after their eruption by surface water) while the others occurred at high temperatures (i.e., during eruption by magmatic water). The FTIR microscopy was conducted at the University of Wisconsin–Eau Claire.

contributed nodules to the secondary deposit. Testing any of these three hypotheses will necessitate additional field surveys and sampling.

3.3. Galatian volcanic province

The Galatian Volcanic Province (Fig. 2) and the Western Anatolian Volcanic Province are typically lumped together within the obsidian literature (e.g., Chataigner et al., 1998; Varoutsikos and Chataigner, 2012), despite reflecting different regions of Miocene, Pliocene, and Quaternary (i.e., from 23 Ma to the present) volcanism (Tankut et al., 1998). In contrast to obsidian sources in the Western Anatolian Volcanic Province, those in the Galatian Volcanic Province are known to have been utilized archaeologically, albeit at sites local to the sources (Chataigner et al., 1998: 523). One of the Galatian sources – known as "Galatia X" – is only known archaeologically, and its location remains a mystery.

3.3.1. Yağlar

Information about the Yağlar ("oils") obsidian source (not to be confused with Yağlica in the Kars province of eastern Turkey; Frahm, 2023) is scant, and nearly all of it derives from research conducted by Keller and colleagues (Keller and Seifried, 1990; Keller et al., 1992, 1996). The source is described as ca. 20 km northwest of Kizilçahamam (somewhere around 40.6° N, 32.8° E), and Keller et al. (1992) report a K-Ar date of 20.7 Ma, making it one of the oldest obsidian sources in Turkey. Keller and Seifried (1990: 62) mention that "worked obsidian has been seen" at the source, attesting to its utilization sometime in the past. The elemental data for Yağlar obsidian from Keller and Seifried (1990) and Keller et al. (1996) are available in Supplementary Table S10.

3.3.2. Sakaeli-Orta

Bigazzi et al. (1993: 590) refers to Sakaeli-Orta as a "hitherto unknown" obsidian source "recently discovered in an older (Oligocene–Miocene) volcanic region, located to the north of Ankara," and their geological map shows the locations sampled by Ercan et al. (1989) for this source (ca. 40.63° N, 33.13° E, 1250 m asl). Like Yağlar obsidian, Sakaeli-Orta obsidian is old. Wagner and Weiner (1987) report fission-track dates of ca. 24–25 Ma, whereas newer fission-track measurements from Bigazzi et al. (1993) yield a somewhat younger age: 21.3–23.7 Ma. Descriptions of this source vary slightly, from "obsidian pebbles (diameter up to 10 cm)" in perlite deposits (Bigazzi et al., 1993: 591) to "small lithoclasts in ignimbrites" (Chataigner et al., 1998: 520) and "nodules in tuffs" (Ercan et al. 1996: 506). Artifacts made from Sakaeli-Orta obsidian have been found at Neolithic settlements near the Sea of Marmara (e.g., Fikirtepe, Ilıpınar), establishing that the source was at least locally used (Chataigner et al., 1998). The compiled elemental data and consensus ranges for Sakaeli-Orta obsidian are available in Supplementary Table S11, including a direct comparison between elemental data for the Sakaeli and Orta facies, which demonstrates that the two named obsidian deposits for this source are chemically indistinguishable.

3.3.3. Galatia-X

A third obsidian source in the Galatian Volcanic Province is known as "Galatia-X" since its location remains unclear (Keller et al., 1996). This obsidian has only been identified in a field near Güdül (40.21° N, 32.24° E), ca. 40 km southwest of Kizilçahamam, where a few pieces of obsidian debitage were found on the surface (during a search for a pleasant site for a lunch break) along with chert flakes and blades, all less than 1.5 cm in maximum dimension (Keller et al., 1996). Eight of the obsidian chips

were analyzed and had a consistent composition, but they could not be matched to a known volcanic source (Keller and Seifried, 1990; Keller et al., 1996). Fission-track dating of the artifacts resulted in ages of 21.2–23.8 Ma, nearly identical to the dates for Sakaeli-Orta obsidian (Keller et al., 1996). Keller et al. (1996) suggest, on the basis of fission-track parameters, that one artifact from the Neolithic site of Pendik could also be Galatia-X obsidian, while the other artifacts match Yağlar and Sakaeli-Orta. Elemental data for Galatia-X obsidian from Keller et al. (1996) are available in Supplementary Table S12.

3.4. Central Anatolian volcanic province

Obsidian sources in the Central Anatolian Volcanic Province are also known as the Cappadocian or Central Anatolian sources. This was one of the two main volcanic areas on which Renfrew and colleagues (Renfrew et al., 1966, 1968; Dixon et al., 1968; Cann et al., 1969) first focused their attention – the other was the Lake Van area in eastern Turkey (see Frahm, 2023). As such, the region has received considerable attention over the decades from archaeologists and geologists interested in obsidian sourcing, beginning in the 1960s with source visits by Colin Renfrew, Herb Wright, Ian Todd, Giorgio Pasquaré, and others. In 1973, Sebastian Payne and colleagues conducted extensive surveys and sampling, but most of this work went unpublished (Todd, 1980; Yellen, 1995). This region has also received attention from volcanologists and other geologists focused on earth processes, not archaeology. Perhaps inevitably, more attention also leads to more opportunities for conflicting interpretations. In the following sections, I have attempted to sort through these conflicts and, when appropriate, offer new interpretations.

3.4.1. Hasan Dağ

Hasan Dağ (38.127°N 34.167°E) is a double-peaked stratovolcano with a shorter eastern summit (ca. 3070 m asl) and a taller western summit (ca. 3250 m asl) that rise about 2 km above the surrounding Konya Plain. This volcano is perhaps best known amongst archaeologists as, contentiously, the purported subject of an ochre mural at the Neolithic settlement of Çatalhöyük, ca. 180 km to the southeast (Schmitt et al., 2014). James Mellaart, the controversial archaeologist who first excavated Çatalhöyük during the 1960s, argued that the famous mural in Shrine 14 of Level VII was an illustration of the settlement's structures and, above that, "the strange object in the back which looks at first sight like a leopard's skin becomes… the twin peaks of Hasan Dağ" during an eruption (Mellaart, 1964: 194). Mellaart also linked the mural to the abundance of obsidian artifacts, which, at that point, had yet to be elementally analyzed and matched to their volcanic sources. He wrote: "when we realize that it was from here or nearby that the Neolithic people obtained their obsidian, a volcanic glass which is the most prized and earliest commodity of trade, and perhaps the basis of Chatal Huyuk's wealth, then it is not such a far cry to suggest that what was shown here was an eruption of Hasan Dağ" (Mellaart, 1964: 194). Given his belief in the economic importance of obsidian to the residents of Çatalhöyük, Mellaart thought it only logical that the painting depicted Hasan Dağ whilst erupting. His mural interpretation remains hotly debated (as do other aspects of his work; e.g., mother goddess worship, Indo-European migrations, suspected smuggling and forgeries). From my perspective, Meece (2006) effectively debunked Mellaart's interpretations of the mural, especially when she showed that this "earliest map" is similar to other murals with geometric patterns and that spotted leopards and their skins (not to mention other animals) are common mural motifs throughout the site. Meece (2006) also noted that no Hasan Dağ obsidian has ever been found at Çatalhöyük (see also a discussion in Carter, 2011: 4). Indeed, no artifact from *any* archaeological site, to the best of my knowledge, has been compositionally matched to Hasan Dağ, almost certainly due to its poor knapping qualities (Arslan et al., 1998; Cauvin and Balkan-Atlı, 1996).

Hasan Dağ has been the subject of considerable geological research (e.g., Aydar and Gourgaud, 1998; Deniel et al., 1998; Dogan et al., 2008; Friedrichs et al., 2020; Gall et al., 2022; Köprübaşi et al., 2014; Kuzucuoğlu et al., 2020; Tank and Karaş, 2020; Toprak and Göncöoğlu, 1993), much of it focused on the history of its formation from the Miocene to the Holocene. For most of its history, Hasan Dağ's eruptions have produced andesitic and dacitic lavas, whereas rhyolitic lavas mostly erupted during the most recent volcanic phases. Obsidian was only produced during the later phases as well, and it has been fission-track dated to ca. 0.39 ± 0.5 Ma (Bigazzi et al., 1998). According to field notes and maps from Rapp and Ercan (Fig. 15), small pieces of obsidian occur in ignimbrite deposits on the western and southern flanks. Their presence in this pyroclastic flow appears related to what Arslan et al. (1998) call the Tahtayayla rhyolite-obsidian flow, ca. 3 km to the north of the taller summit at an elevation of ca. 1950 m asl. As described by Arslan et al. (1998), obsidian from these outcrops would be unsuitable for knapping. They report that the rocks continuously grade from rhyolite into obsidian with "a wide range of surface structure and textures that vary in vesicularity, crystallinity, color, and flow layering" (77). The obsidian, they explain, "is mainly dark greenish black and reddish brown," has "horizontal flow layering, and contains lens- and spherical-shaped rhyolite fragments" (77). Furthermore, the obsidian contains up to 5% feldspar phenocrysts, and it "characteristically fractured giving a brecciated appearance" (Arslan et al., 1998: 77). Consequently, it would have been a poor choice for knapping material in an obsidian-rich region.

Despite its low suitability for knapping, the compiled elemental data and consensus ranges for Hasan Dağ obsidian are available in Supplementary Table S13.

3.4.2. Nenezi Dağ

Nenezi Dağ (38.375° N, 34.459° E, ca. 1600 m asl) is one of the most archaeologically significant obsidian sources in this article. It is an isolated lava dome that rises about 500 m above the surrounding plains and lies only a few kilometers northwest of the Göllü Dağ complex. Its formation has been dated by various techniques. Fission-track dating has resulted in ages between 1.14 ± 0.07 and 1.20 ± 0.06 Ma (Bigazzi et al., 1998; Bellot-Gurlet et al., 1999). Ar-Ar dating yielded a slightly younger of age: 0.91 ± 0.13 Ma (Chataigner et al., 1998), as did Sr isotopes: 0.98 ± 0.6 Ma (Olanca, 1994). Together the three dating techniques reveal that the lava dome and its obsidian formed ca. 0.9–1.2 Ma, roughly contemporaneous with the Göllü Dağ complex. Its obsidian occurs on the western slopes, principally exposed by streams cutting into the dome, and knapping workspaces, where cores were shaped, are known on these slopes as well (Cauvin and Balkan-Atlı, 1996).

Nenezi Dağ obsidian has a long history of use. Carter et al. (2011) sourced various artifacts from Öküzini Cave near the Mediterranean coast, including an Early Epi-Palaeolithic core rejuvenation flake in GH VIII, dated by radiocarbon to 16–18 ka, that originated from Nenezi Dağ. As the crow flies (linearly), this corresponds to a distance of 380 km; however, on foot, it would be ca. 470 km along the least-cost path (which, undoubtedly, the flake did not follow). Nenezi Dağ obsidian is found within the assemblage of Aşıklı Höyük, a Pre-Pottery Neolithic B site (Balkan-Atlı, 1994), and that of Domuztepe, a Late Neolithic settlement more than 350 km on foot from the source (Healey, 2000). Carter et al. (2020) also identified Nenezi Dağ obsidian at the Early Chalcolithic site of Ein el-Jarba in the southern Levant, which reflects a distance of ca. 620 km linearly (over the sea) and more than 800 km on foot.

Nenezi Dağ obsidian is likely best known for its use at Çatalhöyük. Poupeau et al. (2010) sourced 100 obsidian artifacts from Çatalhöyük, and almost one third of them (n = 32) originated from Nenezi Dağ (and the rest were East Göllü Dağ obsidian). Carter and Milić (2013) further developed this investigation based on a larger sample size. Importantly, the proportions of Nenezi Dağ and East Göllü Dağ obsidian changed through time. During the Pre-Pottery Neolithic, East Göllü Dağ was the main origin of obsidian used at Çatalhöyük, but midway through the

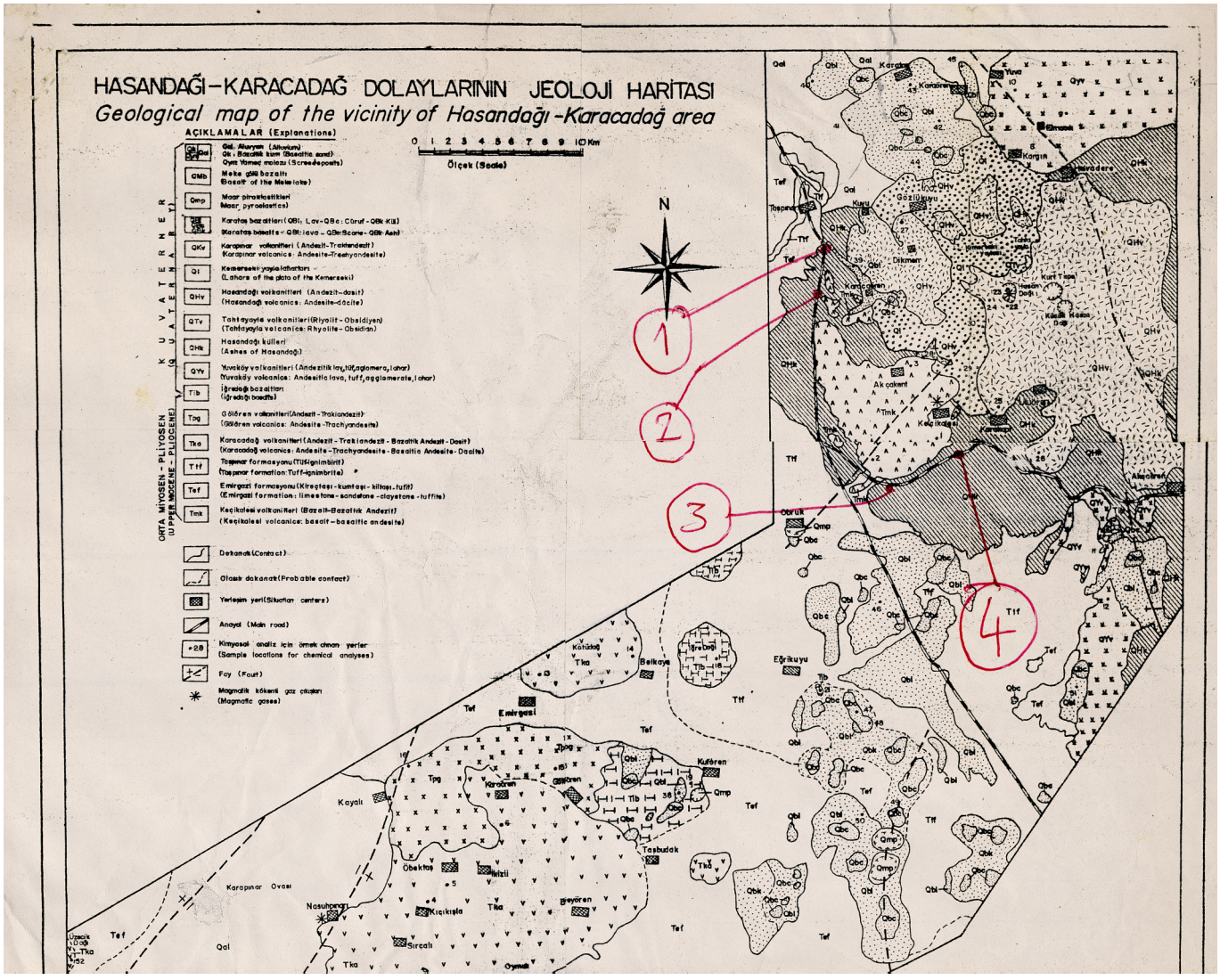

Fig. 15. A scan of the 1991 obsidian sampling map for Hasan Dağ from Rapp and Ercan (the author's personal collection). Their annotations in red pen denote their four sampling loci at the volcano. (For interpretation of the references to color in this figure legend, the reader is referred to the web version of this article.)

Pottery Neolithic, during the seventh millennium BCE, there was a "radical shift" (Carter et al., 2006: 906) towards the use of Nenezi Dağ obsidian together with a technological change (i.e., the rise of unipolar pressure-flaked blades). Various authors have commented on this association – perhaps a logical one given the proximity – between the use of Nenezi Dağ and East Göllü Dağ obsidian, not only at Çatalhöyük but throughout the broader region.

The compiled elemental data and their consensus ranges for Nenezi Dağ obsidian are available in Supplementary Table S14.

3.4.3. Göllü Dağ complex

The Göllü Dağ volcanic complex (38.28° N, 34.57° E, ca. 1500–1800 m asl), also known as Çiftlik in the early literature (e.g., Renfrew et al., 1966, 1968; Dixon et al., 1968; Wright, 1969), includes multiple obsidian sources, although the precise number has been a matter of debate. The entire complex appears to be less than 4 Ma in age, and a series of obsidian-bearing lava flows erupted 0.9–1.3 Ma, according to fission-track dates from Bigazzi et al. (1993, 1998). One portion of the complex, known as East Göllü Dağ, has some of the most archaeologically important obsidian in the ancient Near East, comprising artifacts as diverse as a far-traveled Upper Paleolithic tool found in what is now Lebanon (Frahm and Tryon, 2019) to a carved Babylonian amulet (Frahm et al., 2019). In contrast, as of Chataigner et al. (1998), only one artifact (from Aşıklı Höyük) had been identified as West Göllü Dağ obsidian.

Early sourcing studies often regarded Göllü Dağ as a single obsidian source (e.g., Renfrew et al., 1966; Wright, 1969; Blackman, 1984). In 1973, Sebastian Payne, then a researcher at the British Institute of Archaeology at Ankara, conducted an intensive survey and collection of obsidian from Göllü Dağ (and Acıgöl, as discussed the next section). Fig. 16 is a topographic map that shows where Payne collected his obsidian specimens from varied contexts (i.e., on the surface, in streambeds, from pyroclastic deposits, from outcrops). The obsidian specimens were sent to Hugh McKerrell at Scotland's National Museum of Antiquities for analyses, but McKerrell was fired shortly thereafter. Hence his specimens sat unanalyzed until Yellen (1995) tested about half of them with NAA at the Hebrew University of Jerusalem. The tested specimens included 63 from the Göllü Dağ complex (although none from its westernmost portion), and Yellen (1995) recognized three "subgroups" in the resulting chemical data, primarily based on Ba, Eu, and Cs. One subgroup (Yellin's GLD-A) was largely confined to the southern part of the complex, another (his GLD-C) largely was localized to the northeastern part, and the third (his GLD-B) was more scattered over the complex. The observed mixing of the subgroups across the landscape is consistent with, as shown In Fig. 16, Payne's collection of loose specimens from the surface and streams.

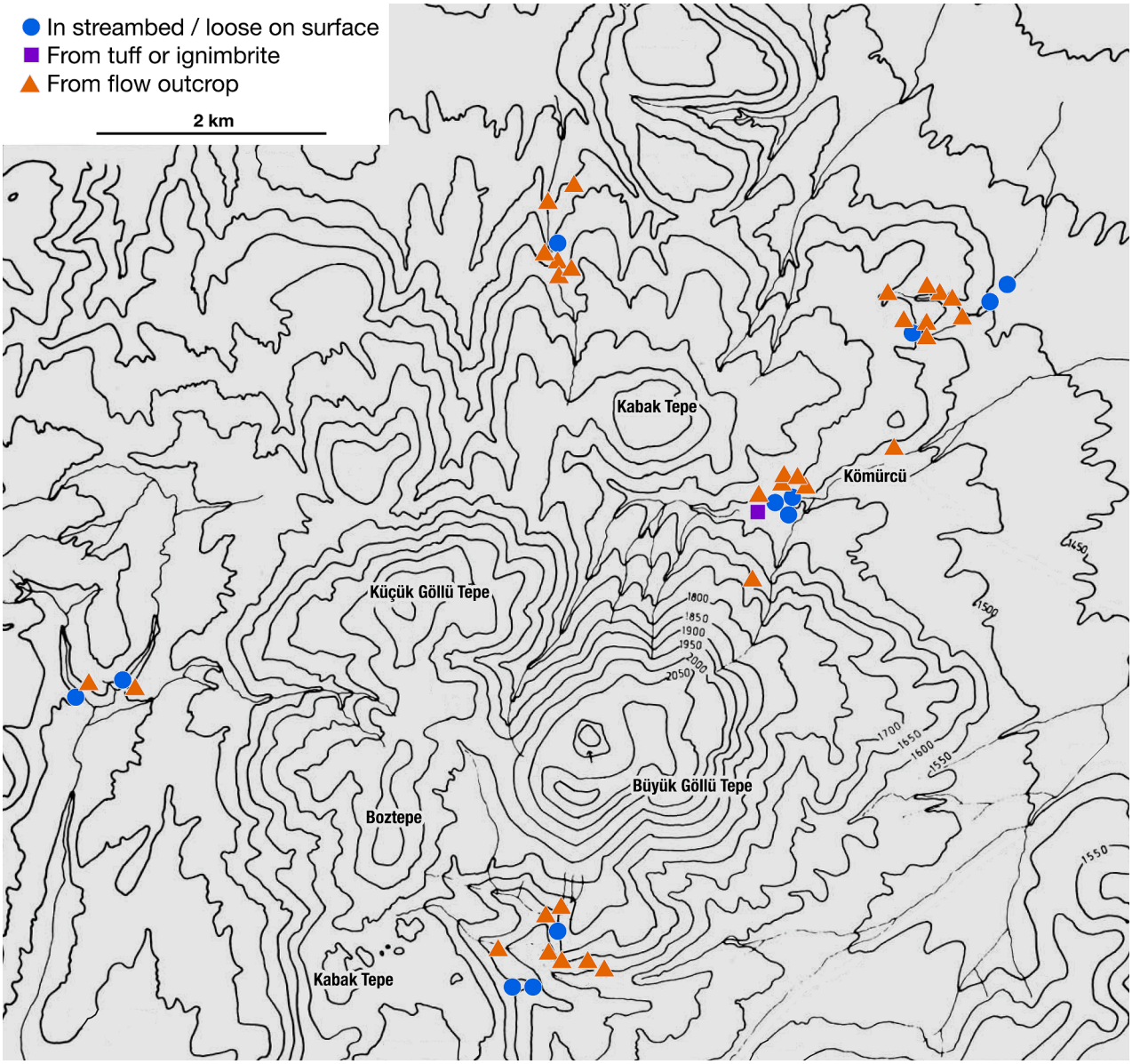

Fig. 16. Topographic map of the Göllü Dağ complex with Payne's 1973 collection locations, redrawn from Todd (1980: Fig. 8), which was, in turn, modified from Payne's original map. The symbols denote if the specimens were collected loose on the surface or in streambeds (blue circles), from pyroclastic deposits including volcanic tuff and ignimbrite (purple squares), or from the outcrops of an obsidian flow (orange triangles). (For interpretation of the references to color in this figure legend, the reader is referred to the web version of this article.)

Rapp and Ercan visited the Göllü Dağ complex in 1991 and sampled obsidian from eleven loci, as illustrated in Fig. 17. Fig. 18 shows the Göllü Dağ interpretation from Poidevin (1998) and, subsequently, Varoutsikos and Chataigner (2012), in which there are mixed descriptions of any chemical differentiation beyond the level of western vs. eastern deposits (e.g., "The three deposits of the Göllü Dağ East group cannot be distinguished geochemically" in Varoutsikos and Chataigner, 2012; obsidian from Kayırlı Village and North Bozköy "are virtually indistinguishable" [translated] and, therefore, grouped together under the label of West Göllü Dağ in Poidevin, 1998: 118). Similarly, Chataigner et al. (1998) group the eastern obsidian outcrops (i.e., Kömürcü, East Kayırlı, Sırça Deresi) together as a single chemical source, and they do the same for the western occurrences (Kayırlı Village, North Bozköy). After more and more Göllü Dağ obsidian specimens and artifacts had been analyzed using modern instruments (e.g., Carter et al., 2006; Carter and Shackley, 2007), Hancock and Carter (2010) considered the issue of whether intra-laboratory repeatability and inter-laboratory reproducibility allowed for finer distinctions, such as reliably assigning artifacts to either the Kömürcü obsidian outcrops or the East Kayırlı ones.

Binder et al. (2011) published a new interpretation of the Göllü Dağ complex that included seven or eight distinct sources (depending on how one counted their 4a and 4b chemical groups). A key aspect of their model, as redrawn in Fig. 19, is the interpretation of the obsidian outcrops as ring-dike intrusions that surround the lava domes (see Binder et al., 2011: Fig. 2), following their preferred interpretation for steeply dipped flow bands within rhyolites (Mouralis et al., 2002; Türkecan et al., 2004). The actual distribution, though, of obsidian outcrops across the dome surfaces, as illustrated in Fig. 20, instead suggests to me the more traditional model of rhyolitic lava domes with an inner shell of glassy obsidian (e.g., Fink, 1987; Fink and Manley, 1987; Hughes and Smith, 1993). In this model, the places where obsidian outcrops are exposed largely reflect post-emplacement forces, especially erosion and slope failure where gullies and streams have cut into the dome and, consequently, revealed its glassy inner shell.

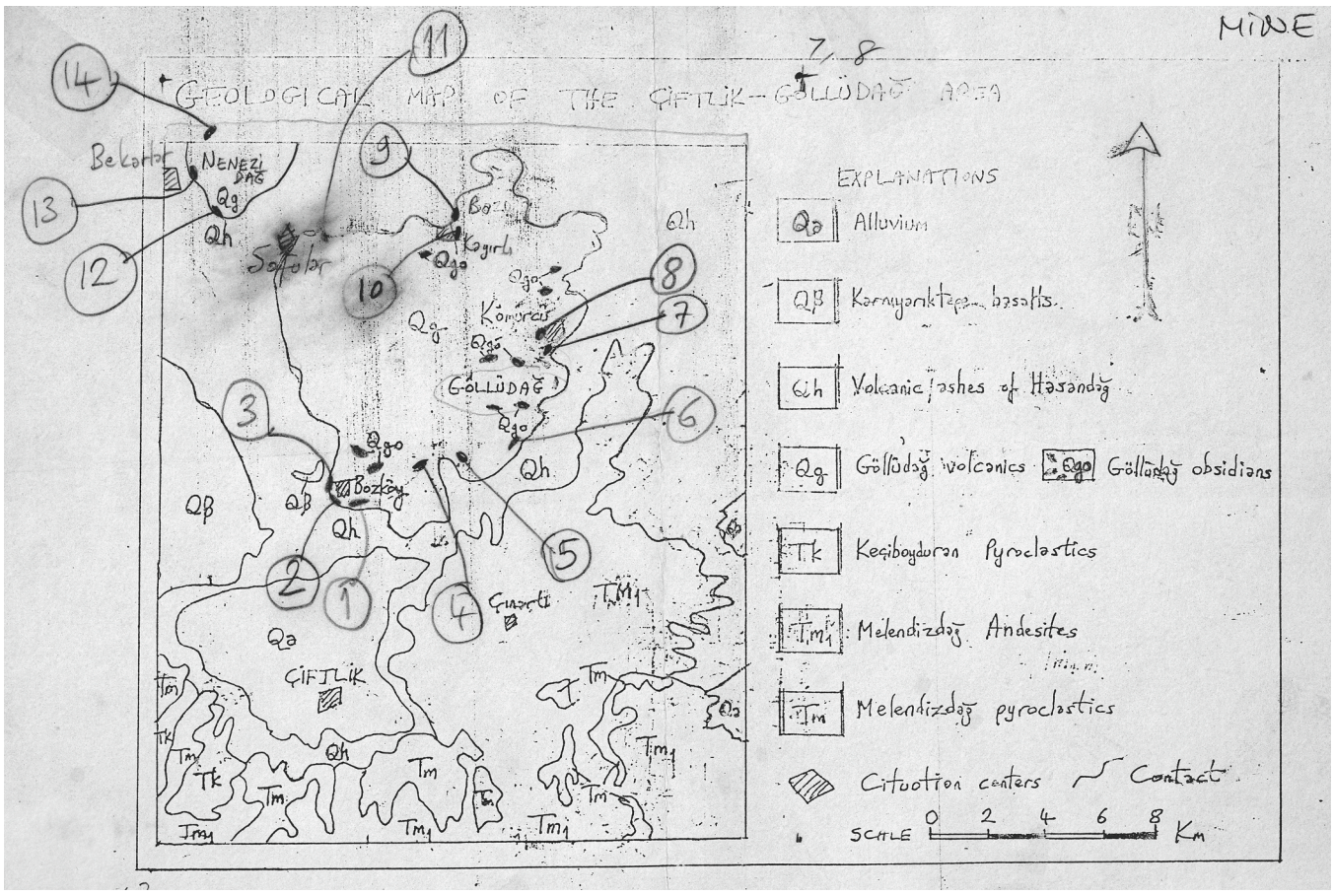

Fig. 17. A scan of the 1991 obsidian sampling map for Göllü Dağ and Nenezi Dağ from Rapp and Ercan (the author's personal collection). Their annotations in pencil denote their fourteen sampling loci.

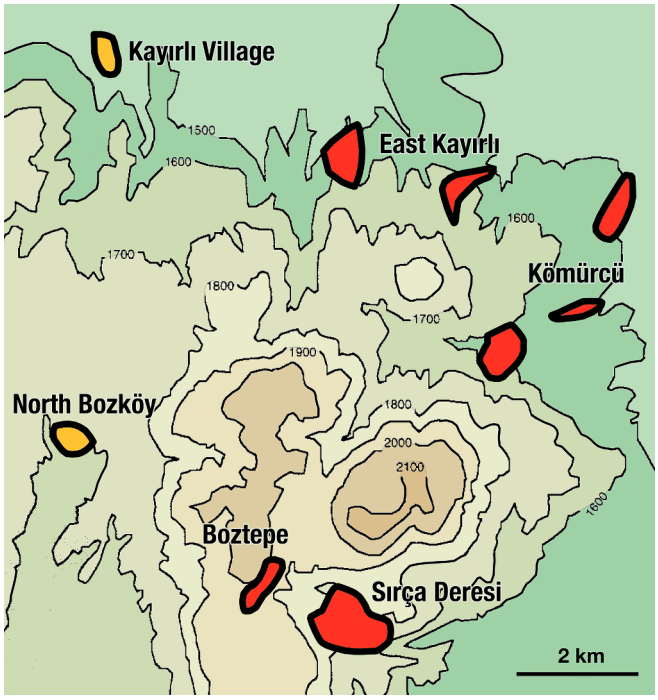

Fig. 18. Interpretation of the Göllü Dağ complex redrawn from Poidevin (1998: Fig. 9) and Varoutsikos and Chataigner (2012).

Certain aspects of the LA-ICP-MS data analysis in Binder et al. (2011) also lead to, from my view, more chemical groups than might be warranted. This, however, is difficult to fully assess as their article included only summary statistics, and individual measurements can only be extracted through digitizing their scatterplots. Consider, for example, that their Göllü Dağ 4a and 4b chemical groups are based on a small, but seemingly statistically significant, difference in Ba: 77 ± 4 vs. 98 ± 9 ppm, respectively, based on the summary statistics (Binder et al., 2011: Table 2). Fig. 21 (data digitized from Binder et al. 2011: Fig. 5) shows, though, the extent to which Göllü Dağ 4a and 4b overlap. Consequently, even Khalidi et al. (2013), whose LA-ICP-MS measurements were conducted in the very same analytical laboratory as Binder et al. (2011), chose to combine Göllü Dağ 4a and 4b in their sourcing analyses. In addition, Binder et al. (2011) used principal component analysis (PCA) to separate chemical groups among their geological specimens, but the resulting PCA functions more strongly weighed volatile, light elements, specifically Li and B (with weights of 6), than key trace elements such as Zr and Nb (with weights of 3 or 4). That is, volatile gases dissolved in the obsidian had outsized influences on defining the groups.

The identification by Binder et al. (2011) of three distinct chemical groups (Göllü Dağ 3, 6, and 7) in the southern portion of the complex is also somewhat problematic. One issue is that their Göllü Dağ 3 is defined by "a single big block of a light grey and metalescent obsidian," making it impossible to assess any elemental variability at this locus and suggesting that the obsidian had a sheen due to the presence of water/gas bubbles (Binder et al., 2011: 3183). Another issue is that Göllü Dağ 3, 6, and 7 are separated in the PCA plots; however, their PCA analysis unfortunately includes more variables (8 elements; Zr, Nb, Y, Ba, Sr, Li, B, Ti) than observations for Göllü Dağ 3 (n = 1), 6 (n = 5) and 7 (n = 5).

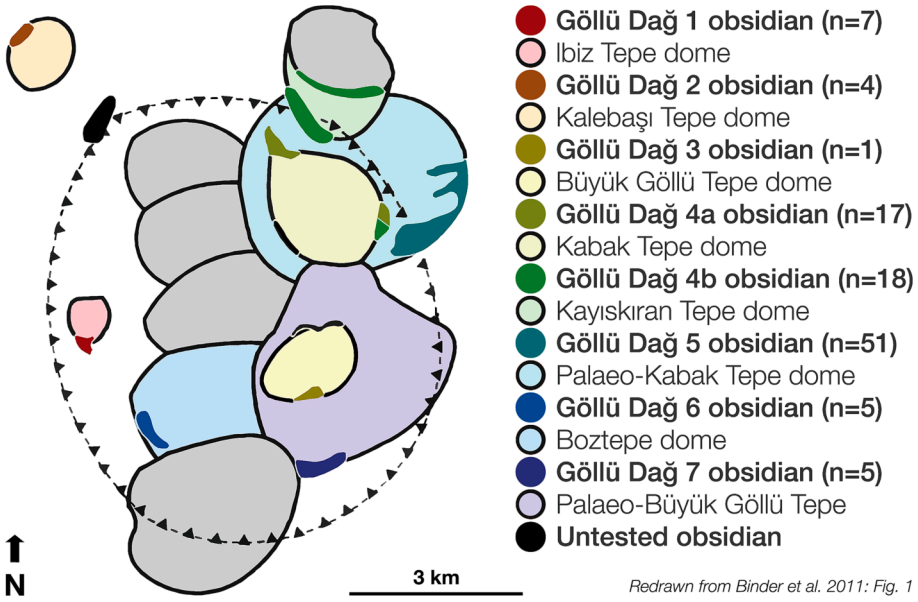

Fig. 19. Binder et al. (2011), following Mouralis et al. (2002), interpreted obsidian outcrops at the Göllü Dağ complex as ring-dike intrusions associated with the formation of specific rhyolitic lava domes in association with an ancient caldera (dashed line with triangles). This interpretation of the Göllü Dağ complex has been redrawn from Binder et al. (2011: Fig. 1) with their proposed associations between obsidian outcrops and lava domes based on their Table 3 and Appendix 1.

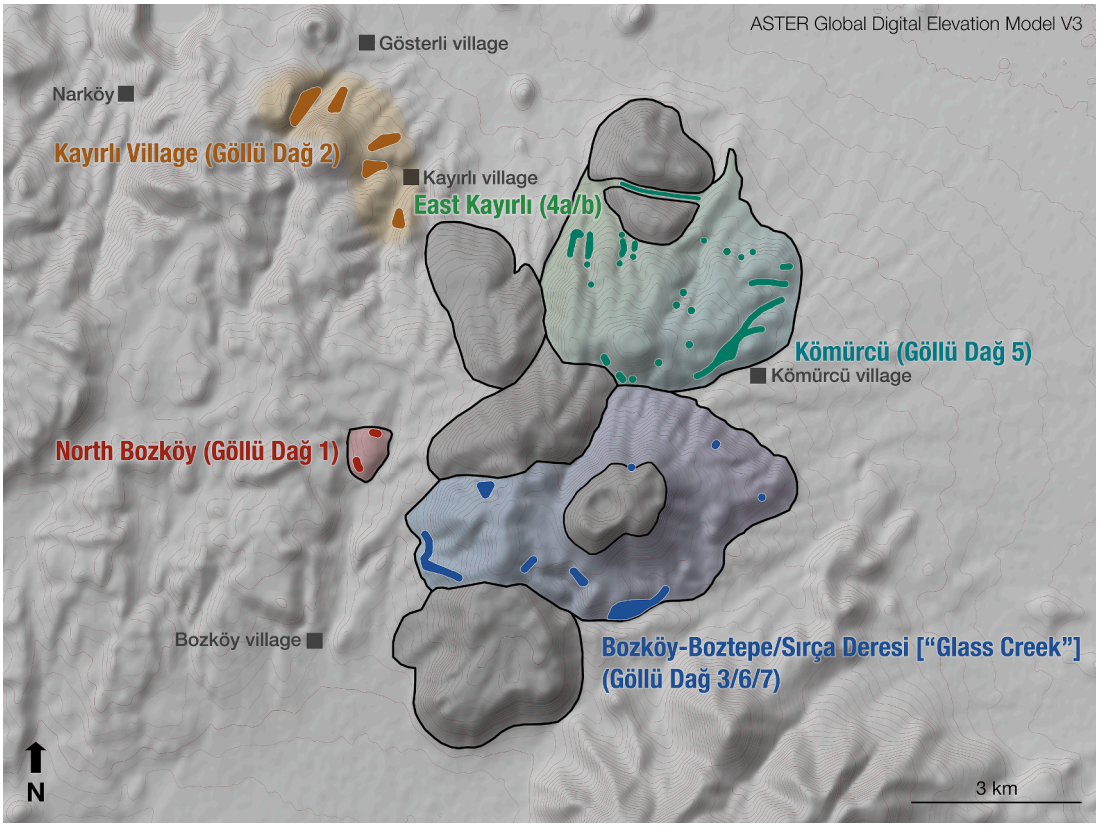

Fig. 20. Proposed obsidian sources at the Göllü Dağ complex based on my own data and other obsidian compositional datasets. This proposal interprets the Göllü Dağ complex as a series of conventional obsidian-bearing rhyolitic lava domes (e.g., Fink and Manley, 1987; Hughes and Smith, 1993) rather than ring-dike intrusions (Binder et al., 2011). Background map based on the ASTER Global Digital Elevation Map Version 3 (GDEM V3), NASA (USA) and METI (Japan). The outcrop locations were identified using high-resolution satellite photography from CNES / Airbus (dated 4 August 2021, 2 September 2019, and 9 September 2013) and Maxar Technologies (dated 4 November 2016 and 5 September 2011).

The opposite scenario, in which there are more observations than variables (even two or three times more), is highly preferred in multivariate statistics. Like Göllü Dağ 4a and 4b, the distinction between Göllü Dağ 6 (n = 5) and 7 (n = 5) obsidian appears based on a minor Ba disparity (90 ± 9 vs. 55 ± 6 ppm, respectively). More meaningful from an igneous petrology perspective, I would argue, the Total Alkali Silica (TAS)

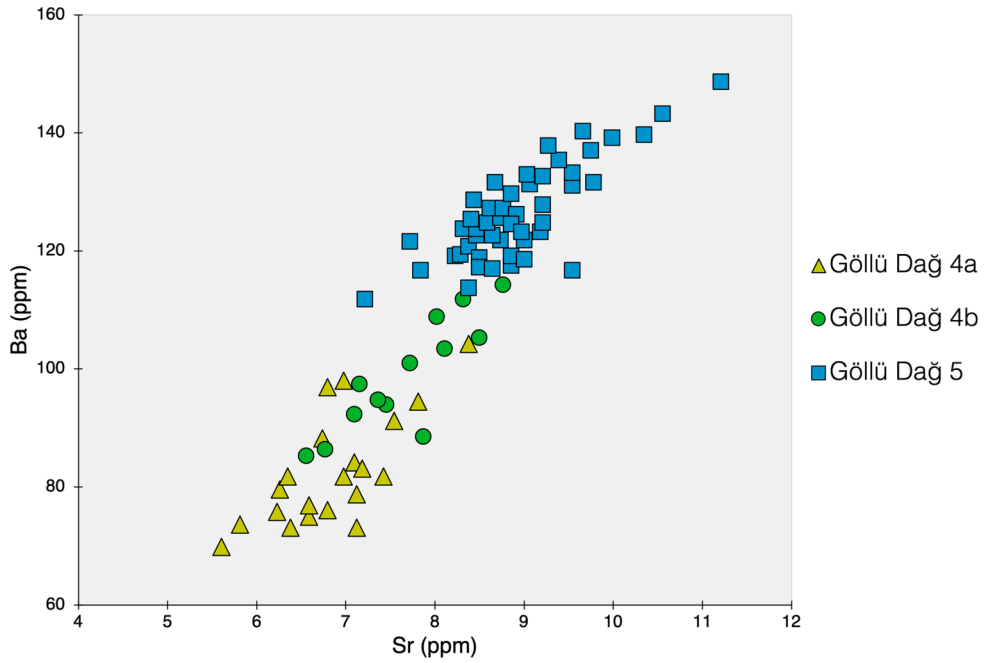

Fig. 21. Sr and Ba values extracted from Binder et al. (2011: Fig. 5) using WebPlotDigitizer v4.6 for their Göllü Dağ 4a, 4b, and 5 obsidian types, illustrating the practical overlap between their 4a and 4b types. The summary statistics of Binder et al. (2011) in their Table 2 suggest that the Ba contents of 4a and 4b obsidian are statistically significant (77 ± 4 vs 98 ± 9 ppm, respectively; Student's *t* test, $p < 0.0001$), but this plot illustrates that the two types overlap between ca. 85 and 105 ppm of Ba. Note that Khalidi et al. (2013), working in the same analytical laboratory as Binder et al. (2011), combined the Göllü Dağ 4a and 4b obsidian types in their study of obsidian artifacts from a Neolithic archaeological site in Lebanon.

diagram, which is the standard plot utilized by geochemists to classify volcanic rocks on the basis of silica (SiO_2) and combined alkali ($Na_2O + K_2O$) contents (Le Maitre, 2002). The TAS diagram in Fig. 22 shows, using the values from Binder et al. (2011), the strong geochemical affinity of Göllü Dağ 3, 6, and 7, which indicates that these three chemical groups are very closely volcanically related to one another. Furthermore, I observed the presence of spherulites in obsidian from the Sırça Deresi outcrops (Fig. 3), and Binder et al. (2011) noted spherulites in their Göllü Dağ 6 obsidian, which was "poor quality" as a result (3183). Consequently, the issues raised in Section 2 about spherulites (i.e., Ba- and Sr-depleted concentrations in the glassy matrix of obsidian) should be kept in mind as a potential complicating factor.

Fig. 20 is my reinterpretation of the Göllü Dağ complex, including equivalencies to the chemical groups proposed by Binder et al. (2011). The two West Göllü Dağ obsidian sources are consistent under our respective schemes: North Bozköy (Supplementary Table S15) is Göllü

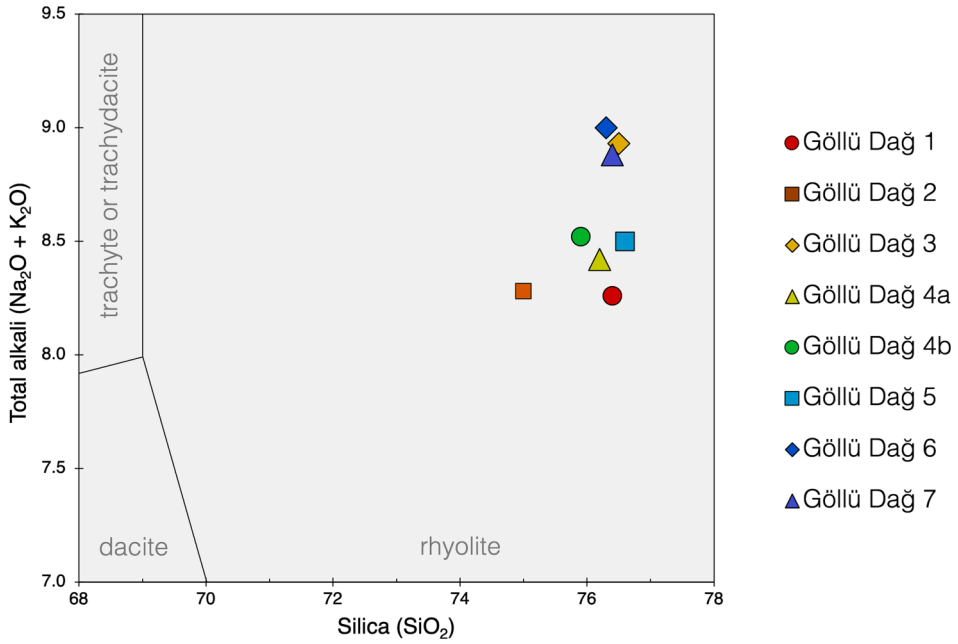

Fig. 22. This Total Alkali Silica (TAS) diagram is a standard plot for geochemists to classify volcanic rocks based on their silica (SiO_2) and combined alkali ($Na_2O + K_2O$) contents (Le Maitre, 2002). The plot shows the strong geochemical affinity of the Göllü Dağ 3, 6, and 7 obsidian types of Binder et al. (2011), which suggests that these three obsidian types are closely volcanically related to each other (even more so, it appears, than their Göllü Dağ 4a and 4b obsidian types).

Dağ 1 of Binder et al. (2011), while Kayırlı Village (Supplementary Table S16) is their Göllü Dağ 2. Our interpretations only differ for the East Göllü Dağ sources, among which many authors do not distinguish due to their chemical similarities (Supplementary Table S17). Notice that, like Yellen (1995), I define three East Göllü Dağ obsidian sources: one to the north, one to the south, and one in-between. In my interpretation, Kömürcü obsidian (Göllü Dağ 5 of Binder et al., 2011; Supplementary Table S18) grades into East Kayırlı obsidian (Göllü Dağ 4a/4b of Binder et al., 2011; Supplementary Table S19) in the northern part of the complex. In the south part, I propose, as noted above, that Göllü Dağ 3, 6, and 7 of Binder et al. (2011) can be combined into a single obsidian source, somewhat awkwardly called here "Bozköy-Boztepe/Sırça Deresi" (Supplementary Table S20), reflecting the variety of names that its outcrops have been given.

3.4.4. Acıgöl complex

The Acıgöl volcanic complex (38.5° N, 34.6° E, ca. 1300–1400 m asl) is somewhat paradoxical in the considerable amount of attention that it has received for its obsidian versus how infrequently it was actually exploited in antiquity. As noted by Chataigner et al. (1998), only two obsidian artifacts, up until that point, had been chemically matched to the Acıgöl complex (i.e., one from Aşıklı Höyük, one from El Kowm). Early obsidian sourcing studies frequently regarded Acıgöl as a single source (e.g., Group 1e-f in Renfrew et al., 1966). Wright (1969), though, noted at least five localities for collecting obsidian at this complex of lava domes and craters, and he matched "Group 1e-f" obsidian of Renfrew and colleagues to two of those five localities, meaning that the other localities had chemically different obsidian. In 1973, Payne set out to conduct a thorough survey and collection of Acıgöl (and, as noted in Section 3.4.3, Göllü Dağ) obsidian. Fig. 23 is a topographic map that shows where he had collected obsidian specimens from a range of contexts (i.e., on the surface, in streambeds, from pyroclastic deposits, from outcrops). Like the Göllü Dağ specimens, these specimens sat unanalyzed until Yellen (1995) tested about half of them with NAA. Consequently, when Rapp started his obsidian sourcing research in Turkey in 1990, he found that "not all potential source deposits have been sampled, and many deposits were not sampled systematically – with full knowledge and coverage of the geology of the site" (Rapp and Hill, 2006: 255). Fig. 24 shows the ten locations at the Acıgöl volcanic complex sampled by Rapp and Ercan during their 1991 visit to the area, specimens from which became part of my reference collection.

Fig. 25 shows one common interpretation of the Acıgöl complex found in the obsidian literature (Poidevin, 1998; Varoutsikos and Chataigner, 2012). A "pre-caldera" vs. "post-caldera" framework lies at the

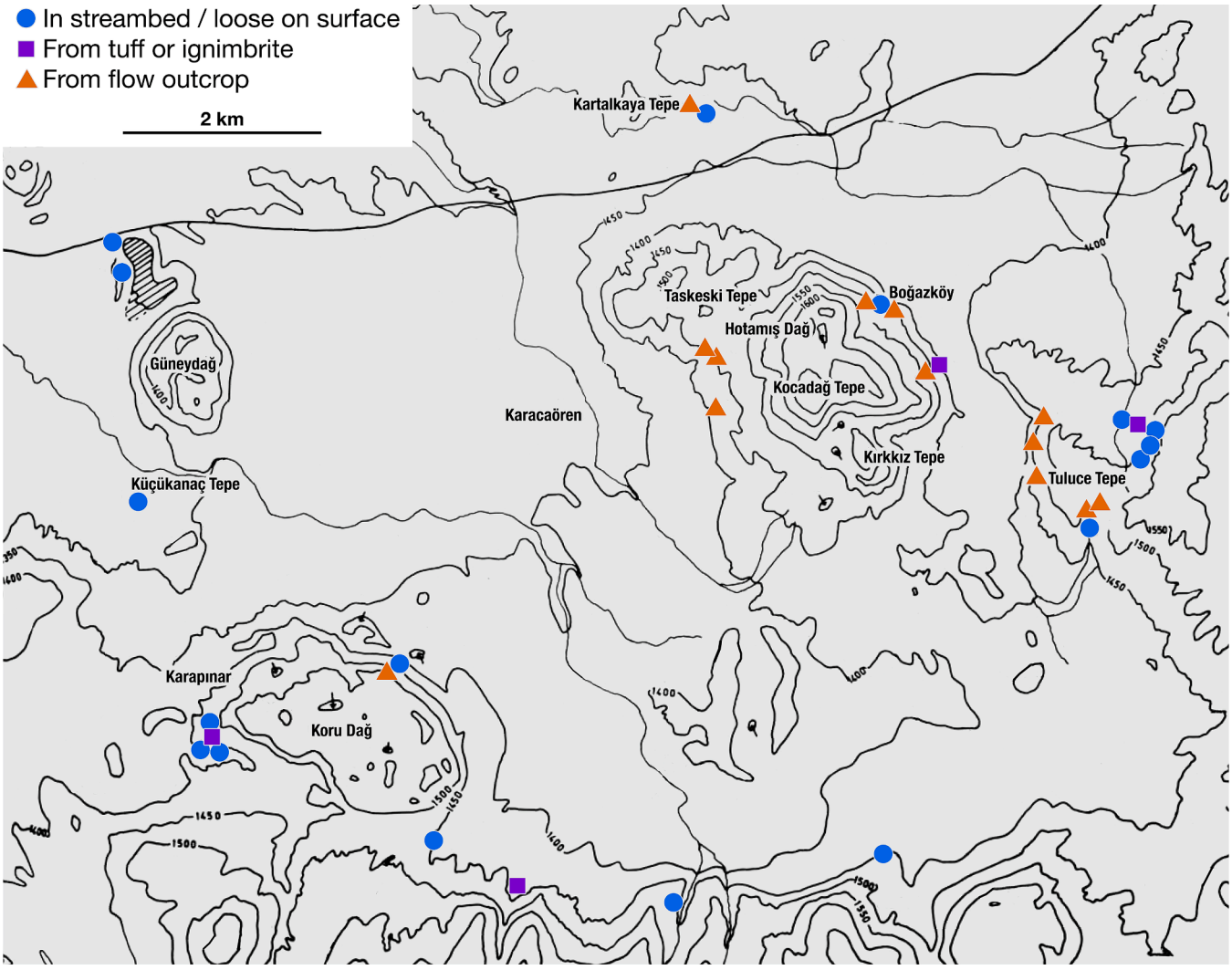

Fig. 23. Topographic map of the Acıgöl complex with Payne's 1973 collection locations, redrawn from Todd (1980: Fig. 7), which was, in turn, modified from Payne's original map. The symbols denote if the specimens were collected loose on the surface or in streambeds (blue circles), from pyroclastic deposits (purple squares), or from the outcrops of an obsidian flow (orange triangles). (For interpretation of the references to color in this figure legend, the reader is referred to the web version of this article.)

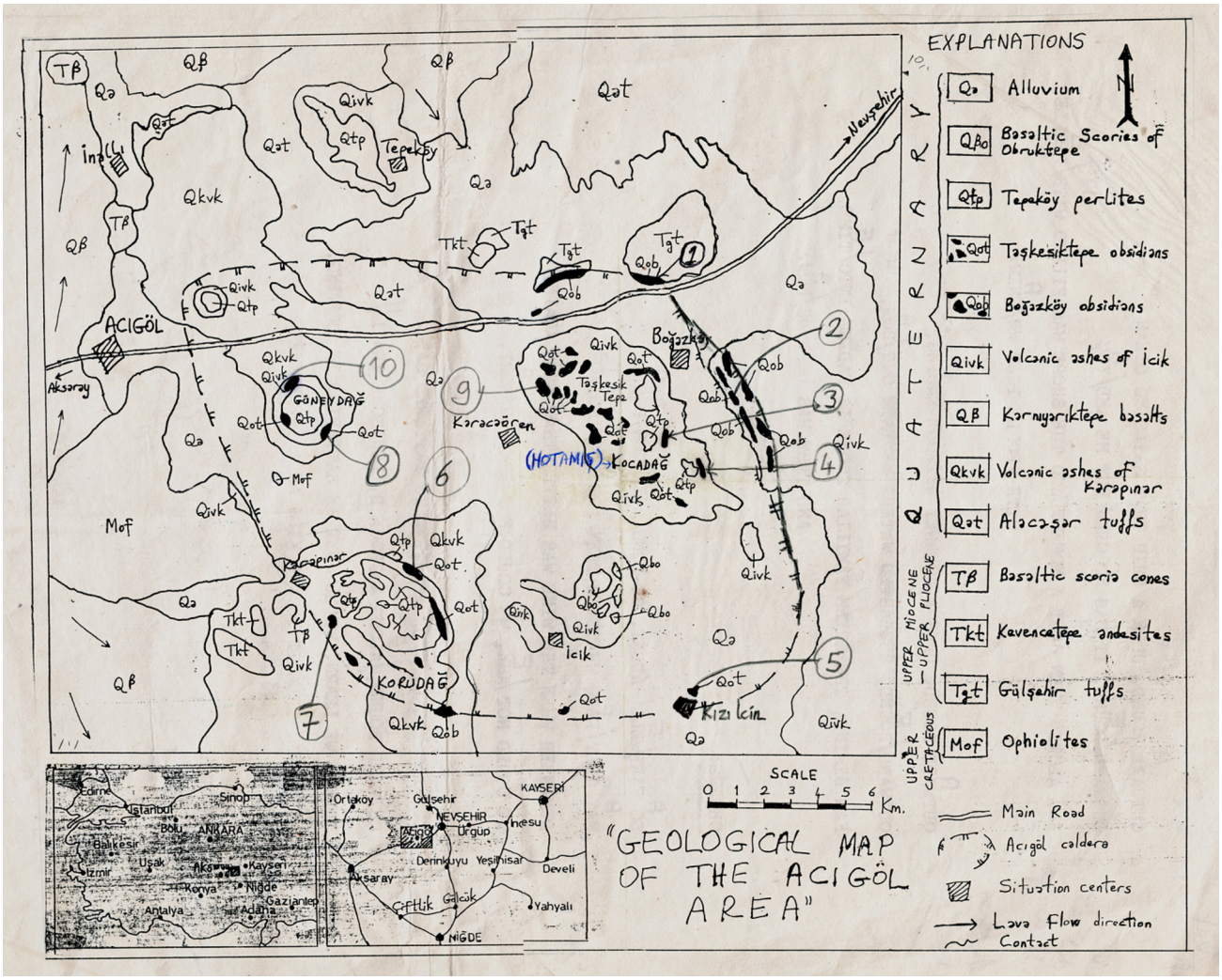

Fig. 24. A scan of the 1991 obsidian sampling map for the Acıgöl complex from Rapp and Ercan (author's personal collection). Their annotations in pencil denote their ten sampling loci through the complex.

core of this interpretation, largely informed by fission-track dates and *minimum* ages from Bigazzi et al. (1993). It is important to recognize the relevance (or lack thereof) of minimum ages to actual ages. In the United States and Canada, for example, the minimum driving age is 16 years old, but one should not assume that, simply because drivers must be at least 16, any given driver probably is that age. As shown in Figs. 24 and 25, tectonic faults have been interpreted as part of a caldera ring (Druitt et al., 1995; Mouralis et al., 2002); however, such an interpretation has been challenged by Schmitt and colleagues (e.g., Schmitt et al., 2011; Siebel et al., 2011; Atici et al., 2019) on the basis of new geochronological and stratigraphic evidence. As shown in Fig. 25, the obsidian outcrops stretching from White Tuffs Hotamış Dağ and Bogazköy to Kartalkepe and Tulucetepe have commonly been interpreted as pre-caldera flows exposed during caldera formation, whereas Kocadağ obsidian was argued to have erupted later (on the basis of a minimum fission-track age). Schmitt et al. (2011), in contrast, interpret the Acıgöl complex as a faulted, young rhyolite field without a contemporaneous caldera. Acıgöl complex, in their view, consists of two clusters of rhyolitic lava domes: "an older, morphologically subdued dome complex in the east" and an "array of younger domes with well-preserved tuff rings in the west" (Schmitt et al., 2011: 1218). In their scenario, the Bogazköy to Tulucetepe obsidian outcrops are not exposed in a caldera wall but a north–south-oriented escarpment produced by down-faulting during the Upper Acıgöl Tuff eruption. The northern and western portions of the complex, they contend, exhibit no caldera morphological margins, whereas a possible caldera margin in the southern portion predates formation of the Upper Acıgöl Tuff. Therefore, Schmitt et al. (2011: 1217) argue that outlining a caldera on the Acıgöl complex is "tenuous" at best. Furthermore, their more precise (U–Th)/He zircon ages, as included in Fig. 26, largely upset the common pre-caldera vs. post-caldera framework, as illustrated in Fig. 25.

Fig. 26 shows my interpretation of the Acıgöl complex based largely on (1) the geochronology of Schmitt et al. (2011) and (2) elemental analyses of the geo-referenced obsidian specimens collected by Rapp and Ercan as well as other authors over the last three decades (Supplementary Tables S21-25). In this interpretation, the Güneydağ and Korudağ outcrops constitute a single West Acıgöl obsidian source that dates to ca. 23.3–24.9 ka, and the compiled elemental data and consensus ranges for West Acıgöl obsidian are available in Supplementary Table S21. East Acıgöl, in contrast, has four elementally distinct sources: (1) White Tuffs Hotamış Dağ (WTHD), without a precise date but at least 112 ka, to the north (Supplementary Table S22); (2) Boğazköy, ca. 190 ka, to the east (Supplementary Table S23); (3) Hotamış Dağ / Kocadağ, also ca. 190 ka, to the south (Supplementary Table S24); and (4) Taşkesiktepe, ca. 147 ka, to the west (Supplementary Table S25). Note that, in this interpretation, there are no "pre-caldera" and "post-caldera" obsidian sources, given that framework has not held up well.

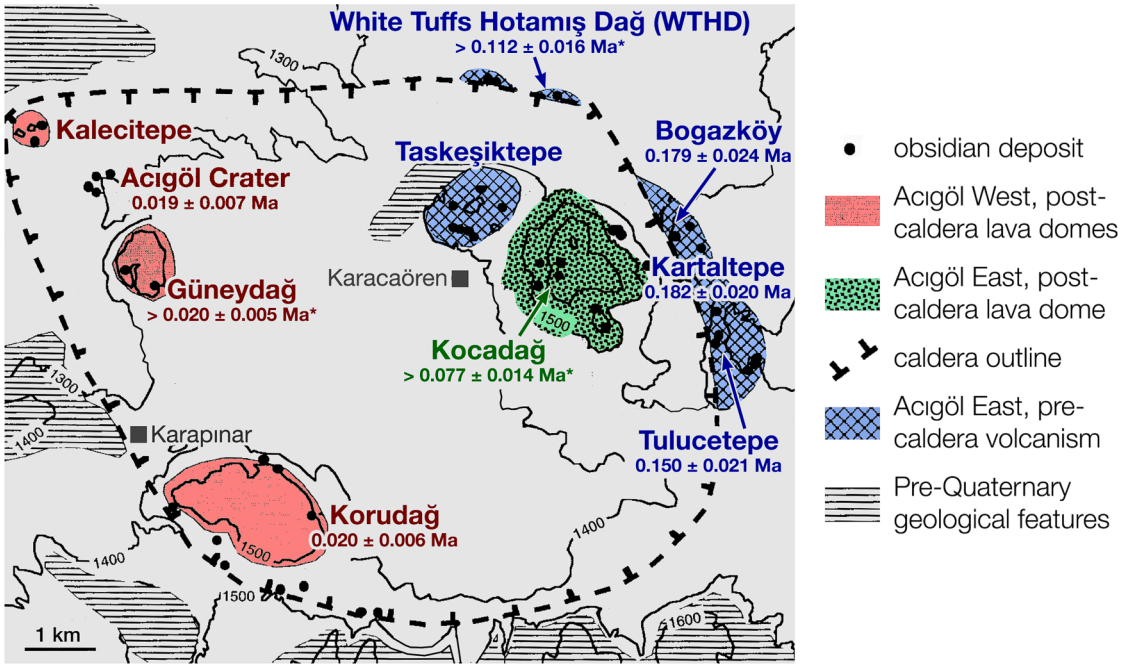

Fig. 25. Interpretation of the Acıgöl complex redrawn from Poidevin (1998: Fig. 6) and Varoutsikos and Chataigner (2012). This model was largely informed by fission-track dates from Bigazzi et al. (1993). Note that the asterisk (included in the original figure) denotes minimum fission-track ages.

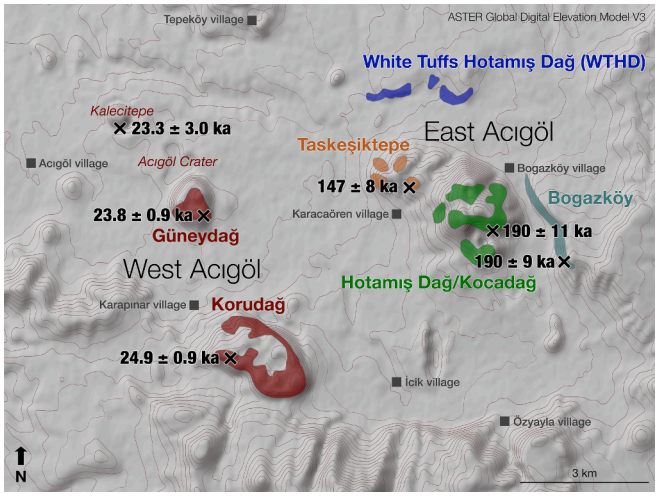

Fig. 26. Proposed obsidian sources at the Acıgöl complex based on my pXRF and EMPA data as well as updated geochronological data [i.e., (U–Th)/He zircon ages] from Schmitt et al. (2011). Background map based on the ASTER Global Digital Elevation Map Version 3 (GDEM V3), NASA (USA) and METI (Japan).

3.4.5. *Erciyes Dağ*

Poidevin (1998: Fig. 1) lists Erciyes Dağ, near the town of Kayseri, as an obsidian source, which is included here for the sake of completeness. The uncertainty around Erciyes Dağ as a potential source is evident in the literature (e.g., Varoutsikos and Chataigner, 2012 report Erciyes Dağ as an obsidian source while Chataigner et al. 1998 do not). Todd and Pasquarè (1965: 97) mention that obsidian can be found on the south face of Erciyes Dağ, without elucidation, but they conclude that their "preliminary survey of Erciyag Dağ seems to indicate that this mountain cannot be considered as a major source of obsidian" in archaeological contexts. This Quaternary stratovolcano (38.53°N, 35.45°E) has been geologically likened to Hasan Dağ (Pasquarè et al., 1988), and due to wide geological interest, Erciyes Dağ has been discussed and described in various papers (e.g., Notsu et al., 1995; Kürkcüoğlu et al., 1998; Toprak, 1998; Şen et al., 2002, 2003; Hamann et al., 2010). Beginning ca. 900 ka, the volcano formed through subsequent eruptions of andesitic and dacitic lavas, and rhyodacitic lava domes erupted on the slopes of the volcano later, ca. 110–140 ka (Şen et al. 2002, 2003). Two of the rhyodacitic eruptions reportedly created obsidian, at least in the geological sense of the term: the Perikartın/Karagüllü eruption occurred on the northern flank of Erciyes Dağ, whereas the Dikkartın eruption occurred on the volcano's southern flank.

Şen et al. (2003) describes the Dikkartın deposits as a combination of pumice and block-and-ash flows, including large dome blocks (ca. 1.5–2 m across). The pumiceous units contain obsidian fragments, as much as 25% by volume, and the blocks occasionally exhibit bands of obsidian. These Dikkartın facies likely corresponded to the obsidian mentioned by Todd and Pasquarè (1965) on the southern face of the volcano. Todd (1980) later described it, based on field observations by Pasquarè, as "smooth and shiny" only on one face but otherwise "gritty," not "true obsidian" of archaeological interest. Şen et al. (2003) implies that these textures are the result of vesiculation. About the Perikartın/Karagüllü eruption on the northern flank of Erciyes Dağ, Şen et al. (2003) explain that the pyroclastic flow contains jointed pumice, breadcrust bombs, and obsidian pieces (of unknown suitability for knapping).

In short, Erciyes Dağ has, by all accounts, obsidian in a geological sense (i.e., glassy rhyolitic lava) on its northern and southern slopes but not in the archaeological sense (i.e., homogenous glass suitable for knapping). No obsidian, to my knowledge, has been analyzed from either of the two flows; however, Supplementary Table S26 provides data for rhyolitic tephra that have been analyzed from the Dikkartın and Perikartın/Karagüllü eruptions in hopes that the values would be similar.

4. Concluding remarks

It seems somewhat odd to focus on bringing greater order to obsidian compositional data in the region where obsidian artifact sourcing was first developed and implemented (e.g., Cann and Renfrew, 1964; Renfrew et al., 1965, 1966, 1968; Dixon et al., 1968; Cann et al., 1968, 1969; Wright, 1969; Wright and Gordus, 1969). In fact, it feels downright

incongruous. The key to this apparent contradiction is that simply having more data does not yield more clarity. If anything, just having more data can create greater uncertainty, at least until one takes those data and works to assemble, reduce, process, summarize, and interpret them. Furthermore, these steps are best accomplished with insights and knowledge about the region in question. That is why here (and in my prior article) I focus on those obsidian sources that I began studying 20 years ago, during my first year as a doctoral student. The application of obsidian specialists' knowledge to organize the source data for their parts of the world is maybe even more important given the inevitable use of artificial intelligence (AI) tools. For years I have advocated in favor of automation in our field (e.g., Frahm et al., 2014c; Frahm, 2019b), from an instrument monitoring and adjusting its own settings to source identifications made via automated statistical tests and machine learning. An impetus for a project such as this, therefore, is evident from the old adage "Garbage in, garbage out." Indeed this is hardly a new issue. Consider a relevant quotation from Charles Babbage, who invented and built the Difference Engine, considered to be the first mechanical computer, during the 1820s to solve polynomial functions. Babbage (1864: 67) wrote: "On two occasions I have been asked, 'Pray, Mr. Babbage, if you put into the machine wrong figures, will the right answers come out?'… I am not able rightly to apprehend the kind of confusion of ideas that could provoke such a question." Even if researchers have the tools to measure the elemental compositions of obsidian artifacts with astounding accuracy and reliability, their identifications could be compromised by flawed elemental data for sources. While routine data collection and analysis are likely to become more automated, the application of expert knowledge is still necessary, and understanding the nature of obsidian sources remains one of those realms of knowledge. Poidevin (1998) had the foresight to accumulate obsidian source data for the Near East, and such endeavors have renewed importance as access sophisticated analytical instruments continues to expand and as AI tools inevitably become a standard means for making artifacts' source identifications.

Declaration of Competing Interest

The author is an editor-in-chief for the journal. He was not, though, involved in decisions regarding its publication, and he was blinded to the review process since the manuscript was handed by a different editor. There are no other known competing interests or relationships that could have appeared to influence the work reported in this paper.

Data availability

All data are included in the Supplementary Materials.

Acknowledgements

I am indebted to many friends and colleagues who have made this project possible – my sincere apologies if I have overlooked anyone here. Geological obsidian specimens were provided by (in alphabetical order): Tuncay Ercan (Directorate of Mineral Research and Exploration, Turkey), Adem Kahraman (Ipekyolu Mining Industry and Foreign Trade Ltd, Turkey), Vassilis Kilikoglou (National Center for Scientific Research "Demokritos," Greece), George "Rip" Rapp (University of Minnesota-Duluth, USA), John Whittaker (Grinnell College, USA), and Zehra Yeğingil (Cukurova University, Turkey). Additional research assistance was provided by (in alphabetical order): Dario Bilardello (Institute for Rock Magnetism), Julie Bowles (Institute for Rock Magnetism), Magen Coleman (MURR), Giselle Conde (University of Wisconsin-Eau Claire), Roger Doonan (University of Sheffield), Josh Feinberg (Institute for Rock Magnetism), Jeff Ferguson (MURR), Jill Ferguson (University of Wisconsin-Eau Claire), Liev Frahm, Sylvie Frahm, Michael Glascock (MURR), Kat Hayes (University of Minnesota), Amy Hillis (Macalester College), Phil Ihinger (University of Wisconsin-Eau Claire), Mike Jackson (Institute for Rock Magnetism), Charissa Johnson (University of Minnesota), Peter McSwiggen (University of Minnesota), Steve Newman (University of Minnesota), and Peter Sølheid (Institute for Rock Magnetism). I also wish to acknowledge the following organizations and institutions for their support: the Department of Earth and Environmental Sciences, University of Minnesota; Department of Anthropology, University of Minnesota; Institute for Rock Magnetism, University of Minnesota; the University of Minnesota's Undergraduate Research Opportunity Program (UROP); the University of Minnesota's Grant-in-Aid of Research, Artistry, and Scholarship Program; the New Archaeological Research Network for Integrating Approaches to Ancient Material Studies (NARNIA) Project; Department of Archaeology, University of Sheffield; Yale University's Council on Archaeological Studies and Department of Anthropology; and Yale University's Offices of the Vice Provost for Research, Dean of Science, and Dean of Social Science. Two anonymous reviewers improved and enhanced this work through their careful reading, critical eye, and encyclopedic knowledge. Any errors or (mis)interpretations should be considered my own and not those of my colleagues and collaborations over the years.

Appendix A. Supplementary data

Supplementary data to this article can be found online at https://doi.org/10.1016/j.jasrep.2023.104224.

References

Acquafredda, P., Micheletti, F., Muntoni, I.M., Pallara, M., Tykot, R.H., 2019. Petroarchaeometric data on antiparos obsidian (Greece) for provenance study by SEM-EDS and XRF. Open Archaeology 5, 18–30. https://doi.org/10.1515/opar-2019-0003.

Acquafredda, P., Paglionico, A., 2004. SEM–EDS microanalysis of microphenocrysts of Mediterranean obsidians: a preliminary approach to source discrimination. Eur. J. Mineral. 16, 419–429.

Akay, E., 2000. Magmatic and Tectonic Evolution of the Yuntdağ Volcanic Complex (Western Anatolia). Doctoral Thesis in Geology, Graduate School of Natural and Applied Science. Dokuz Eylal University.

Akay, E., Erdogan, B., 2001. Formation of Subaqueous Felsic Domes and Accompanying Pyroclastic Deposits on the Foça Peninsula (Izmir, Turkey). Int. Geol. Rev. 43, 661–674. https://doi.org/10.1080/00206810109465039.

Akkuş, M.F., 1962. The geology of the area between Kütahya and Gediz. Bull. Min. Explor. Inst. Turkey 88, 21–30.

Alan, İ., Elibol, H., Balcı, V., Böke, N., Arman, S., Soyakil, M., Demirbağ, H. 2018. Maden Tetkik ve arama Genel Müdürlüğü 1/100000 Ölçekli Türkiye Jeoloji Haritaları Serisi Eskişehir- J24 Paftası, Maden Tetkik ve Arama Genel Müdürlüğü (MTA), Ankara, No: 251.

Arias, C., Bernardes, C., Bigazzi, G., Bonadonna, F.P., Cesar, M.F., Hadler Neto, J.C., Lattes, C.M.G., Oliveira, J.X., Osorio Araya, A.M., Radi, G., 1986. Identificação da proveniência de manufaturados de obsidiana através da datação com o método do traço de fissão. Ciencia e Cultura 38 (2), 285–308.

Arias, A., Oddone, M., Oddone, M., Bigazzi, G., Bigazzi, G., Di Muro, A., Di Muro, A., Principe, C., Principe, C., Norelli, P., Norelli, P., 2006. New data for the characterization of Milos obsidians. J. Radioanal. Nucl. Chem. 268, 371–386. https://doi.org/10.1007/s10967-006-0183-9.

Arslan, M., Kurt, H., Kadioglu, Y.K., 1998. Glassy textures and emplacement characteristics of the Tahtayayla rhyolite-obsidian flow, Hasandag (Aksaray) volcanites, central Turkey. Mineral. Mag. 62A Part 1, 77–78.

Arzilli, F., Mancini, L., Voltolini, M., Cicconi, M.R., Mohammadi, S., Giuli, G., Mainprice, D., Paris, E., Barou, F., Carroll, M.R., 2015. Near-liquidus growth of feldspar spherulites in trachytic melts: 3D morphologies and implications in crystallization mechanisms. Lithos 216–217, 93–105. https://doi.org/10.1016/j.lithos.2014.12.003.

Aspinall, A., Feather, S., Renfrew, C., 1972. Neutron Activation Analysis of Aegean Obsidians. Nature 237 (5354), 333–334.

Atici, G., Schmitt, A.K., Friedrichs, B., Sparks, S., Danišík, M., Yurteri, E., Gündoğdu, E. A., Schindlbeck-Belo, J., Çobankaya, M., Wang, K.-L., Lee, H.-Y., 2019. Ages and glass compositions for paired large-volume eruptions from the Acigöl volcanic complex, Cappadocia (Turkey). Med. Geosc. Rev. 1, 167–178. https://doi.org/10.1007/s42990-019-00013-5.

Aydar, E., Gourgaud, A., 1998. The geology of Mount Hasan stratovolcano, central Anatolia, Turkey. J. Volcanol. Geoth. Res. 85 (1), 129–152. https://doi.org/10.1016/S0377-0273(98)00053-5.

Babbage, C., 1864. Passages from the Life of a Philosopher. Longman, Green, Longman, Roberts & Green.

Balkan-Atlı, N., 1994. The Typological characteristics of the Aşıklı Höyük chipped stone industry. In: Gebel, H.G., Kozlowski, S. (Eds.), Neolithic Chipped Stone Industries of the Fertile Crescent. Proceedings in Early Near Eastern Production, Subsistence and Environment. pp. 209–221.

Befus, K.S., Watkins, J., Gardner, J.E., Richard, D., Befus, K.M., Miller, N.R., Dingwell, D. B., 2015. Spherulites as in-situ recorders of thermal history in lava flows. Geology 43, 647–650. https://doi.org/10.1130/G36639.1.
Bellot-Gurlet, L., Bigazzi, G., Dorighel, O., Oddone, M., Poupeau, G., Yegingil, Z., 1999. The fission-track analysis: an alternative technique for provenance studies of prehistoric obsidian artefacts. Radiat. Meas. 31, 639–644. https://doi.org/10.1016/S1350-4487(99)00157-2.
Bent, J.T., 1884. Researches among the Cyclades. J. Hellenic Stud. 5, 42–59.
Berlin, R., Henderson, C.M.B., 1969. The distribution of Sr and Ba between the alkali feldspar, plagioclase and groundmass phases of porphyritic trachytes and phonolites. Geochim. Cosmochim. Acta 33, 247–255. https://doi.org/10.1016/0016-7037(69)90141-0.
Bigazzi, G., Radi, G., 1981. Datazione coissiraccissionsione per l'identificazione della provenienza dei manufatti di ossidiana. Rivista di Scienze Preistoriche Firenze 36, 223–250.
Bigazzi, G., Meloni, S., Oddone, M., Radi, G., 1986. Provenance studies of obsidian artifacts: Trace elements analysis and data reduction. J. Radioanal. Nucl. Chem. Art. 98, 353–363. https://doi.org/10.1007/BF02037098.
Bigazzi, G., Ercan, T., Oddone, M., Özdoğan, M., Yeğingil, Z., 1993. Application of fission track dating to archaeometry: provenance studies of prehistoric obsidian artifacts. Nucl. Tracks Radiat. Meas. 22, 757–762. https://doi.org/10.1016/0969-8078(93)90172-Z.
Bigazzi, G., Yegingil, Z., Ercan, T., Oddone, M., Özdogan, M., 1997. Age determination of obsidian bearing volcanics in eastern anatolia using the fission track dating method. Geol. Bull. Turkey 40 (2), 57–73.
Bigazzi, G., Poupeau, G., Yegingil, Z., Bellot-Gurlet, L., 1998. Provenance studies of obsidian artifacts in Anatolia using the fission-track dating method: an overview. L'obsidienne Au Proche et Moyen Orient: Du Volcan à l'outil, BAR International Series. 70–89.
Binder, D., Gratuze, B., Mouralis, D., Balkan-Atlı, N., 2011. New investigations of the Göllüdağ obsidian lava flows system: a multi-disciplinary approach. J. Archaeol. Sci. 38, 3174–3184. https://doi.org/10.1016/j.jas.2011.05.014.
Blackman, M.J., 1984. Provenance studies of middle eastern obsidian from sites in Highland Iran. Archaeol. Chem. III, 19–50.
Breitkreuz, C., Götze, J., Weißmantel, A., 2021. Mineralogical and geochemical investigation of megaspherulites from Argentina, Germany, and the USA. Bull. Volcanol. 83, 14. https://doi.org/10.1007/s00445-021-01434-7.
Bustos, E., Báez, W.A., Bardelli, L., McPhie, J., Sola, A., Chiodi, A., Simón, V., Arnosio, M., 2020. Genesis of megaspherulites in El Viejo Rhyolitic Coulee (Pleistocene), Southern Puna. Argentina. Bull Volcanol 82, 43. https://doi.org/10.1007/s00445-020-01382-8.
Cann, J.R., Renfrew, C., 1964. The characterization of obsidian and its application to the Mediterranean Region. Proc. Prehist. Soc 30, 111–133. https://doi.org/10.1017/S0079497X00015097.
Cann, J.R., Dixon, J.E., Renfrew, C., 1968. The Sources of Saliagos Obsidian. In: Evans, J. D., Renfrew, C. (Eds.), Excavations at Saliagos Near Antiparos, vol. 5. British School at Athens, pp. 105–107.
Cann, J.R., Dixon, J.E., Renfrew, C., 1969. Obsidian Analysis and the Obsidian Trade. In: Brothwell, D.R., Higgs, E. (Eds.), Science in ArchAeology: A Survey of Progress and ReseArch, Revised and Expanded Edition. Praeger Publishers, New York, pp. 578–591.
Carter, T., 2011. A true gift of mother earth: the use and significance of obsidian at Çatalhöyük. Anatol. Stud. 61, 1–19.
Carter, T., 2016. Obsidian consumption in the Late Pleistocene – Early Holocene Aegean: contextualising new data From Mesolithic Crete. Annu. Br. Sch. Athens 111, 13–34. https://doi.org/10.1017/S006824541600006X.
Carter, T., Milić, M. 2013. The consumption of obsidian at Neolithic Çatalhöyük: a long-term perspective. Stone tools in transition: From hunter-gatherers to farming societies in the Near East, pp. 495-508.
Carter, T., Contreras, D.A., 2012. The character and use of the Soros Hill Obsidian source, Antiparos (Greece). C.R. Palevol 11, 595–602. https://doi.org/10.1016/j.crpv.2012.06.005.
Carter, T., Kilikoglou, V., 2007. From reactor to royalty? Aegean and Anatolian Obsidians from Quartier Mu, Malia (Crete). J. Mediterr. Archaeol. 20, 3760. https://doi.org/10.1558//jmea.2007.v20i1.115.
Carter, T., Kilikoglou, V., 2022. Raw material choices and technical practices as indices of cultural change: characterizing obsidian consumption at 'Mycenaean' Quartier Nu, Malia (Crete). PLoS One 17, e0273093.
Carter, T., Poupeau, G., Bressy, C., Pearce, N.J.G., 2006. A new programme of obsidian characterization at Çatalhöyük, Turkey. J. Archaeol. Sci. 33, 893–909. https://doi.org/10.1016/j.jas.2005.10.023.
Carter, T., Moir, R., Marthari, M., 2023. Defining cultural traditions in the Early Bronze Age Aegean: characterizing obsidian consumption at Early Cycladic Kastri (Syros, Greece). J. Archaeol. Sci. Rep. 49, 103987 https://doi.org/10.1016/j.jasrep.2023.103987.
Carter, T., Shackley, M.S., 2007. Sourcing obsidian from Neolithic Çatalhöyük (Turkey) using energy dispersive X-ray fluorescence. Archaeometry 49, 437–454. https://doi.org/10.1111/j.1475-4754.2007.00313.x.
Carter, T., Le Bourdonnec, F.-X., Poupeau, G., Kartal, M., Calligaro, T., Moretto, P., 2011. Marginal perspectives: sourcing epi-palaeolithic to chalcolithic obsidian from the Öküzini Cave (SW Turkey). Paléorient 37, 123–149.
Carter, T., Contreras, D.A., Campeau, K., Freund, K., 2016. Spherulites and aspiring elites: the identification, distribution, and consumption of Giali Obsidian (Dodecanese, Greece). JMA 29, 3–36. https://doi.org/10.1558/jmea.v29i1.31011.
Carter, T., Strasser, T.F., Panagopoulou, E., Campeau, K., Mihailović, D.D., 2018. Obsidian circulation in the early Holocene Aegean: a case study from Mesolithic Damnoni (SW Crete). J. Archaeol. Sci. Rep. 17, 173–183. https://doi.org/10.1016/j.jasrep.2017.11.012.
Carter, T., Campeau, K., Streit, K., 2020. Transregional perspectives: characterizing obsidian consumption at early chalcolithic Ein el-Jarba (N. Israel). J. Field Archaeol. 45, 249–269. https://doi.org/10.1080/00934690.2020.1717857.
Cauvin, M.-C., Balkan-Atlı, N., 1996. Rapport sur les recherches sur l'obsidienne en Cappadoce, 1993–1995. Anatolia Antiqua 4, 249–271.
Cauvin, M.-C., Balkan, N., Besnus, Y., Şaroglu, F., 1986. Origine de l'obsidienne de Cafer Höyük (Turquie): Premiers résultats. Paléorient 12, 89–97.
Cauvin, M.-C., Gourgaud, A., Gratuze, B., Arnaud, N.O., Poupeau, G., Poidevin, J.-L., Chataigner, C. (Eds.), 1998. L'obsidienne au Proche et Moyen Orient: du volcan à l'outil, BAR international series. Archaeopress, Oxford.
Chataigner, C., Poidevin, J.L., Arnaud, N.O., 1998. Turkish occurrences of obsidian and use by prehistoric peoples in the Near East from 14,000 to 6000 BP. J. Volcanol. Geoth. Res. 85, 517–537. https://doi.org/10.1016/S0377-0273(98)00069-9.
Clay, P.L., O'Driscoll, B., Gertisser, R., Busemann, H., Sherlock, S.C., Kelley, S.P., 2013. Textural characterization, major and volatile element quantification and Ar–Ar systematics of spherulites in the Rocche Rosse obsidian flow, Lipari, Aeolian Islands: a temperature continuum growth model. Contrib. Miner. Petrol. 165, 373–395. https://doi.org/10.1007/s00410-012-0813-x.
Conde, G., Ihinger, P.D., Frahm, E. 2009a. Water in Anatolian obsidian: factors influencing hydrous species concentrations with implications for sourcing and dating artifacts, Geological Society of America Annual Conference, Portland, OR.
Conde, G., Ihinger, P.D., Frahm, E. 2009b. Water speciation in Anatolian obsidian: quenched magmatic water vs. low temperature hydration, Goldschmidt Conference, Switzerland.
Conde, G., Frahm, E., Ihinger, P.D., 2010. Effects of Low-temperature Hydrous Alteration on the Chemistry of Natural Obsidian from the Near East. Geological Society of America, Denver CO.
Conde, G., Ihinger, P.D., Frahm, E., 2011. Chemical exchange accompanying obsidian-perlite transition in the natural environment. Geological Society of America, Minneapolis, MN.
Cornaggia-Castiglioni, O., Fussi, F., D'Agnolo, G., 1962. Indagini Sulla Provenienza dell'Ossidiana in uso Nelle Industrie Preistoriche Italiane. Parte Prima: Problematica e Techniche di Indagine. Atti della Societa Italiana di Scienze Naturali e del Museo Civico di Storia Naturale di Milano 101, 12–19.
Deniel, C., Aydar, E., Gourgaud, A., 1998. The Hasan Dagi stratovolcano (Central Anatolia, Turkey): evolution from calc-alkaline to alkaline magmatism in a collision zone. J. Volcanol. Geoth. Res. 87 (1), 275–302. https://doi.org/10.1016/S0377-0273(98)00097-3.
Dixon, J., Cann, J., Renfrew, C., 1968. Obsidian and the Origins of Trade. Sci. Am. 218 (3), 38–46.
Dogan, A.U., Dogan, M., Kilinc, A., Locke, D., 2008. An isobaric–isenthalpic magma mixing model for the Hasan Dagi volcano, Central Anatolia, Turkey. Bull. Volcanol. 70, 797–804. https://doi.org/10.1007/s00445-007-0167-9.
Druitt, T.H., Brenchley, P.J., Gökten, Y.E., Francaviglia, V., 1995. Late Quaternary rhyolitic eruptions from the Acigöl Complex, central Turkey. JGS 152, 655–667. https://doi.org/10.1144/gsjgs.152.4.0655.
Duranni, S., Khan, M.T., Renfrew, C., 1971. Obsidian Source Identification by Fission Track Analysis. Nature 233, 242–252.
Ercan, T., Saroglu, F., Kuscu, I., 1996. Features of obsidian beds formed by the activity of the volcanoes in Anatolia since 25 million years B.P. The Proceedings of the 29th International Symposium on Archaeometry, 1994 May 9-14, Ankara, Turkey. pp. 505–513.
Ercan, T., Yegingil, Z., Bigazzi, G., 1989. Obsidian, definition, characteristics and distribution in anatolia: geochemical features of central anatolian Obsidians. Bull. Geomorphol. (Jeomorfoloji Bergisi) 17, 71–83.
Fink, J.H., Manley, C.R., 1987. Origin of pumiceous and glassy textures in rhyolite flows and domes, in: Geological Society of America Special Papers. Geological Society of America, pp. 77–88. 10.1130/SPE212-p77.
Fink, J., 1987. The Emplacement of Silicic Domes and Lava Flows, Geological Society of America Special Papers. Geological Society of America. 10.1130/SPE212.
Fornaseri, M., Malpieri, L., Palmieri, A.M., Taddeucci, A., 1975. Analyses of Obsidians from the Late Chalcolithic Levels of Arslantepe (Malatya). Palé orient 3 (1), 231–246.
Frahm, E., 2012. Non-destructive sourcing of Bronze-Age Near Eastern obsidian artefacts: redeveloping and reassessing electron microprobe analysis for obsidian sourcing. Archaeometry 54 (4), 623–642.
Frahm, E., 2019a. Introducing the Peabody-Yale Reference Obsidians (PYRO) sets: open-source calibration and evaluation standards for quantitative X-ray fluorescence analysis. J. Archaeol. Sci. Rep. 27, 101957 https://doi.org/10.1016/j.jasrep.2019.101957.
Frahm, E., 2020. Variation in Nemrut Dağ obsidian at Pre-Pottery Neolithic to Late Bronze Age sites (or: all that's Nemrut Dağ obsidian isn't the Sıcaksu source). J. Archaeol. Sci. Rep. 32, 102438 https://doi.org/10.1016/j.jasrep.2020.102438.
Frahm, E., 2023. The obsidian sources of eastern Turkey and the Caucasus: geochemistry, geology, and geochronology. J. Archaeol. Sci. Rep. 49, 104011 https://doi.org/10.1016/j.jasrep.2023.104011.
Frahm, E., Brody, L.R., 2019. Origins of obsidian at the "Pompeii of the Syrian Desert:" sourcing lithic artifacts from the Yale-French excavations at Dura-Europos. J. Archaeol. Sci. Rep. 24, 608–622. https://doi.org/10.1016/j.jasrep.2019.02.024.
Frahm, E., Doonan, R.C.P., Kilikoglou, V., 2014a. Handheld portable X-ray fluorescence of Aegean obsidians. Archaeometry 56, 228–260. https://doi.org/10.1111/arcm.12012.

Frahm, E., Feinberg, J.M., 2013. From flow to quarry: magnetic properties of obsidian and changing the scale of archaeological sourcing. J. Archaeol. Sci. 40, 3706–3721. https://doi.org/10.1016/j.jas.2013.04.029.
Frahm, E., Feinberg, J.M., Schmidt-Magee, B.A., Wilkinson, K.N., Gasparyan, B., Yeritsyan, B., Adler, D.S., 2016. Middle Palaeolithic toolstone procurement behaviors at Lusakert Cave 1, Hrazdan valley, Armenia. J. Hum. Evol. 91, 73–92. https://doi.org/10.1016/j.jhevol.2015.10.008.
Frahm, E., Lassen, A.W., Wagensonner, K., 2019. Gods and demons, Anatolia and Egypt: Obsidian sourcing of Mesopotamian amulets and cylinder seals using portable XRF. J. Archaeol. Sci. Rep. 24, 978–992. https://doi.org/10.1016/j.jasrep.2019.03.025.
Frahm, E., Tryon, C.A., 2019. Origin of an Early Upper Palaeolithic obsidian burin at Ksar Akil (Lebanon): Evidence of increased connectivity ahead of the Levantine Aurignacian? J. Archaeol. Sci. Rep. 28, 102060 https://doi.org/10.1016/j.jasrep.2019.102060.
Frahm, E., Feinberg, J.M., Schmidt-Magee, B.A., Wilkinson, K., Gasparyan, B., Yeritsyan, B., Karapetian, S., Meliksetian, K., Muth, M.J., Adler, D.S., 2014b. Sourcing geochemically identical obsidian: multiscalar magnetic variations in the Gutansar volcanic complex and implications for Palaeolithic research in Armenia. J. Archaeol. Sci. 47, 164–178. https://doi.org/10.1016/j.jas.2014.04.015.
Frahm, E., Schmidt, B.A., Gasparyan, B., Yeritsyan, B., Karapetian, S., Meliksetian, K.h., Adler, D.S., 2014c. Ten seconds in the field: rapid Armenian obsidian sourcing with portable XRF to inform excavations and surveys. J. Archaeol. Sci. 41, 333–348. https://doi.org/10.1016/j.jas.2013.08.012.
Frahm, E., 2010. The Bronze-Age Obsidian Industry at Tell Mozan (Ancient Urkesh), Syria. Doctoral dissertation, University of Minnesota. https://hdl.handle.net/11299/99753.
Frahm, E., 2019b. Beyond the Technical Revolution: Epistemological Shifts in Archaeological XRF (Or: "The World of XRF Will Never Be the Same Again"). Society for American Archaeology Annual Meeting, Albuquerque, New Mexico, April 10th–14th.
Francaviglia, V., 1984. Characterization of mediterranean obsidian sources by classical petrochemical methods. Preistoria Alpina 20, 311–332.
Friedrichs, B., Atıcı, G., Danišík, M., Atakay, E., Çobankaya, M., Harvey, J.C., Yurteri, E., Schmitt, A.K., 2020. Late Pleistocene eruptive recurrence in the post-collisional Mt. Hasan stratovolcanic complex (Central Anatolia) revealed by zircon double-dating. J. Volcanol. Geoth. Res. 404, 107007 https://doi.org/10.1016/j.jvolgeores.2020.107007.
Fytikas, M., Giuliani, O., Innocenti, F., Marinelli, G., Mazzuoli, R., 1976. Geochronological data on recent magmatism of the Aegean Sea. Tectonophysics 31, T29–T34. https://doi.org/10.1016/0040-1951(76)90161-X.
Fytikas, M., Innocenti, F., Kolios, N., Manetti, P., Mazzuoli, R., Poli, G., Rita, F., Villari, L., 1986. Volcanology and petrology of volcanic products from the island of Milos and neighbouring islets. J. Volcanol. Geoth. Res. 28, 297–317. https://doi.org/10.1016/0377-0273(86)90028-4.
Gale, N.H., 1981. Mediterranean obsidian source characterization by strontium isotope analysis. Archaeometry 23, 41–51.
Gall, H., Kürkçüoğlu, B., Cipar, J., Crispin, K., Furman, T., 2022. Recycling and recharge at Hasandağ stratovolcano, Central Anatolia: insights from plagioclase textures and zoning patterns. Contrib. Miner. Petrol. 177, 84. https://doi.org/10.1007/s00410-022-01949-y.
Gardner, J.E., Befus, K.S., Watkins, J., Hesse, M., Miller, N., 2012. Compositional gradients surrounding spherulites in obsidian and their relationship to spherulite growth and lava cooling. Bull. Volcanol. 74, 1865–1879. https://doi.org/10.1007/s00445-012-0642-9.
Gemici, H.C., Dirican, M., Atakuman, Ç., 2022. New insights into the Mesolithic use of Melos obsidian in Anatolia: a pXRF analysis from the Bozburun Peninsula (southwest Turkey). J. Archaeol. Sci. Rep. 41, 103296 https://doi.org/10.1016/j.jasrep.2021.103296.
Georgiades, A., 1956. Research on Greek obsidians. Praktika tis Akademias Athinon 31, 150–163.
Gratuze, B., Barrandon, J.N., Isa, K.A., Cauvin, M.C., 1993. Non-destructive analysis of obsidian artefacts using nuclear techniques: investigation of provenance of Near Eastern artefacts. Archaeometry 35, 11–21. https://doi.org/10.1111/j.1475-4754.1993.tb01020.x.
Hamann, Y., Wulf, S., Ersoy, O., Ehrmann, W., Aydar, E., Schmiedl, G., 2010. First evidence of a distal early Holocene ash layer in Eastern Mediterranean deep-sea sediments derived from the anatolian volcanic province. Quat. Res. 73, 497–506. https://doi.org/10.1016/j.yqres.2009.12.004.
Hancock, R.G.V., Carter, T., 2010. How reliable are our published archaeometric analyses? Effects of analytical techniques through time on the elemental analysis of obsidians. J. Archaeol. Sci. 37, 243–250. https://doi.org/10.1016/j.jas.2009.10.004.
Harbottle, G., 1982. Chemical Characterization in Archaeology. In: Contexts for Prehistoric Exchange. Academic Press, New York, pp. 13–51.
Harrison, R.J., Feinberg, J.M., 2009. Mineral magnetism: providing new insights into geoscience processes. Elements 5, 209–215.
Healey, E., 2000. The Role of Obsidian in the Late Halaf. The University of Manchester.
Hughes, R.E., 1998. On Reliability, Validity, and Scale in Obsidian Sourcing Research. In: Unit Issues in Archaeology: Measuring Time, Space, and Material. University of Utah Press, pp. 103–114.
Hughes, R.E., Smith, R.L., 1993. Archaeology, geology, and geochemistry in obsidian provenance studies, in: Geological Society of America Special Papers. Geological Society of America, pp. 79–91. 10.1130/SPE283-p79.
Innocenti, F., Mazzuoli, R., Pasquarè, G., Radicati Di Brozolo, F., Villari, L., 1982. Tertiary and quaternary volcanism of the Erzurumkars area (Eastern Turkey): geochronological data and geodynamic evolution. J. Volcanol. Geoth. Res. 13, 223–240. https://doi.org/10.1016/0377-0273(82)90052-X.
Kayani, P.I., McDonnell, G., 1996. An assessment of back-scattered electron petrography as a method for distinguishing Mediterranean obsidians. Archaeometry 38, 43–58. https://doi.org/10.1111/j.1475-4754.1996.tb00759.x.
Keller, J., Seifried, C., 1990. The Present Status of Obsidian Source Identification in Anatolia and the Near East, in: PACT 25: Volcanology and Archaeology, Proceedings of the European Workshops of Ravello. pp. 57–87.
Keller, J., Bigazzi, G., Pernicka, E., 1996. The Galatia-X source: A combined major-element, trace-element and fission track characterization of. an unknown obsidian source in northwestern Anatolia. Archaeometry 94. In: Proc. of the 29th Int. Symp. on Archaeometry, 9-14 May 1994, Ankara. pp. 543-551.
Keller, J., Jung, D., Eckart, F.J., Kreuzer, H., 1992. Radiometric ages and chemical characterization of the Galatean andesite massif, Pontus, Turkey. Acta Vulcanol. 2, 267–276.
Khalidi, L., Gratuze, B., Haidar-Boustani, M., Ibáñez, J.J., Teira, L., 2013. Results of geochemical analyses of obsidian artifacts from the Neolithic site of Tell Labwe South, Lebanon., in: Stone Tools in Transition: From Hunter- Gatherers to Farming Societies in the Near East. Universitat Autònoma de Barcelona, pp. 475–494.
Kilikoglou, V., Bassiakos, Y., Doonan, R.C., Stratis, J., 1997. NAA and ICP analysis of obsidian from Central Europe and the Aegean: source characterisation and provenance determination. J. Radioanal. Nucl. Chem. 216, 87–93. https://doi.org/10.1007/BF02034501.
Kolia, E., Spiroulias, A. 2017. Keryneia, Achaea. A recently excavated Bronze Age site in the northern Peloponnese. Aspects of cultural Connections with the West. In: Vlachopoulos A., Lolos Y., Laffineur R., Fotiadis M. (eds.), Hesperos. The Aegean Seen from the West, Proceedings of the 16th International Aegean Conference, University of Ioannina, Department of History and Archaeology, Unit of Archaeology and Art History, 18-21 May 2016 (Aegaeum 41).
Kolia, E., 2012. Aigialeia. In: Vlachopoulos, A. (Ed.), Αρχαιολογία Πελοπόννησος (Archaeology Peloponnese). Melissa Publications, Athens, pp. 324–331.
Kolia, E., 2013. Archaeological Research in Eastern Achaea Within the Framework of Large-Scale Technical Works. Αρχαιολογία Online. Online at http://www.archaeology.wiki/blog/2013/12/16/archaeological-research-in-eastern-achaea.
Köprübaşi, N., Güçtekin, A., Çelebi, D., Kirmaci, M.Z., 2014. Mineral chemical constraints on the petrogenesis of mafic and intermediate volcanic rocks from the Erciyes and Hasandağ volcanoes, Central Turkey. Geochemistry 74 (4), 585–600. https://doi.org/10.1016/j.chemer.2013.11.003.
Kotsakis, G., 1982. On the electrical conductivity of the obsidian from Milos (Greece) in the temperature range 250°C–600°C. Neues Jahrbuch fur Mineralogie-Monatshefte 10, 471–480.
Kürkcüoğlu, B., Şen, E., Aydar, E., Gourgaud, A., Gundogdu, N., 1998. Geochemical approach to magmatic evolution of Mt. Erciyes stratovolcano, central Anatolia, Turkey. J. Volcanol. Geotherm. Res. 85, 473–494.
Kuzucuoğlu, C., Gündoğdu Atakay, E., Mouralis, D., Atıcı, G., Guillou, H., Türkecan, A., Pastre, J.-F., 2020. Geomorphology and tephrochronology review of the Hasandağ volcano (southern Cappadocia, Turkey). Mediterranean Geoscience Reviews 2 (2), 185–215. https://doi.org/10.1007/s42990-019-00017-1.
Landsberger, S., 1986. Spectral interferences from uranium fission in neutron activation analysis. Chem. Geol. 57, 415–421. https://doi.org/10.1016/0009-2541(86)90061-6.
Latour, B., Woolgar, S., 1986. Laboratory Life: The Construction of Scientific Facts. Princeton University Press, Princeton, N.J.
Le Maitre, R.W., 2002. Igneous Rocks: A Classification and Glossary of Terms Recommendations of the International Union of Geological Sciences, Subcommission on the Systematics of Igneous Rocks, 2nd ed. Cambridge University Press.
Liritzis, I., 2008. Assessment of Aegean obsidian sources by a portable ED-XRF analyser: Grouping, provenance and accuracy. In: Proceedings of the 4th Symposium of the Hellenic Society for Archaeometry, National Hellenic Research Foundation, Athens, 28–31 May 2003 (eds. Y. Facorellis, N. Zacharias and K. Polikreti), 399–406, BAR International Series 1746, Tempus Reparatum, Oxford.
Liritzis, I., Zacharias, N., 2011. Portable XRF of archaeological artifacts: current research, potentials and limitations. In: Shackley, M.S. (Ed.), X-ray Fluorescence Spectrometry (XRF) in Geoarchaeology. Springer, pp. 109–142.
McDougall, J.M., Tarling, D.H., Warren, S.E., 1983. The magnetic sourcing of obsidian samples from Mediterranean and Near Eastern sources. J. Archaeol. Sci. 10, 441–452. https://doi.org/10.1016/0305-4403(83)90059-6.
Meece, S., 2006. A Bird's Eye View – of a Leopard's Spots: the Çatalhöyük "Map" and the development of cartographic representation in prehistory. Anatol. Stud. 56, 1–16.
Mellaart, J., 1964. Earliest of Neolithic cities: delving deep into the Neolithic religion of Anatolian Chatal Huyuk, Part 2 – Shrines of the vultures and the veiled goddess. The Illustrated London News, 8 February. Archaeol. Sec. 2170, 194–197.
Milić, M., 2014. PXRF characterisation of obsidian from central Anatolia, the Aegean and central Europe. J. Archaeol. Sci. 41, 285–296. https://doi.org/10.1016/j.jas.2013.08.002.
Mouralis, D., Pastre, J.-F., Kuzucuoğlu, T.A., Atıcı, Y., Slimak, L., Guillou, H., Kunesch, S., 2002. Les complexes volcaniques Rhyolithiques quaternaires d'Anatolie centrale (Gölludağ et Acıgöl, Turquie): Genèse, instabilité, contraintes environnementales. Quaternaire 13, 219–228.
Moutsiou, T., 2019. A Compositional Study (pXRF) of Early Holocene Obsidian Assemblages from Cyprus, Eastern Mediterranean. Open Archaeology 5, 155–166. https://doi.org/10.1515/opar-2019-0011.
Neff, H., 1998. Units in Chemistry-Based Ceramic Provenance Investigations. In: Unit Issues in Archaeology: Measuring Time, Space, and Material. University of Utah Press, pp. 115–127.
Nikolakopoulos, K., Lampropoulou, P., Papoulis, D., Rogkala, A., Giannakopoulou, P., Petrounias, P., 2018. Combined use of remote sensing data, mineralogical analyses, microstructure studies and geographic information system for geological mapping of

Antiparos Island (Greece). Geosciences 8, 96. https://doi.org/10.3390/geosciences8030096.
Notsu, K., Fujitani, T., Ui, T., Matsuda, J., Ercan, T., 1995. Geochemical features of collision-related volcanic rocks in central and eastern Anatolia, Turkey. J. Volcanol. Geoth. Res. 64, 171–191. https://doi.org/10.1016/0377-0273(94)00077-T.
Olanca, K., 1994. Géochimie des Laves Quaternaires de Cappadoce (Turquie): Les Appareils Monogeniques. Blaise Pascal.
Orange, M., Le Bourdonnec, F.-X., Scheffers, A., Joannes-Boyau, R., 2016. Sourcing obsidian: a new optimized LA-ICP-MS protocol. STAR: Sci. Technol. Archaeol. Res. 2, 192–202. https://doi.org/10.1080/20548923.2016.1236516.
Özdoğan, M. 1994. Obsidian in Anatolia: An Archaeological Perspective on the Status of the Research. In: Archaeometry 94: The Proceedings of the 29th International Symposium on Archaeometry; Ankara, 9-14 May 1994, pp. 423-431.
Pappalardo, G., Karydas, A., La Rosa, V., Militello, P.M., Pappalardo, L., Rizzo, F., Romano, F.P., 2003. Provenance of obsidian artefacts from different archaeological layers of Phaistos and Haghia Triada. Creta Antica 4, 287–300.
Pasquarè, G., Poli, S., Vezzoli, L., Zanchi, A., 1988. Continental arc volcanism and tectonic setting in Central Anatolia, Turkey. Tectonophysics 146, 217–230. https://doi.org/10.1016/0040-1951(88)90092-3.
Perlès, C., Takaoğlu, T., Gratuze, B., 2011. Melian obsidian in NW Turkey: evidence for early Neolithic trade. J. Field Archaeol. 36, 42–49. https://doi.org/10.1179/009346910X12707321242313.
Pernicka, E., Keller, J., Rapp, G., Ercan, T. 1996. Provenance of Late Neolithic and Early Bronze Age Obsidian Artifacts from the Troad. In: Archaeometry 94: The Proceedings of the 29th International Symposium on Archaeometry; Ankara, 9-14 May 1994, pp. 515-519.
Pernicka, E., Keller, J., Cauvin, M.-C., 1997. Obsidian from Anatolian Sources in the Neolithic of the Middle Euphrates Region (Syria). Paléorient 23, 113–122.
Poidevin, J.-L., 1998. Les Gisements d'Obsidienne de Turquie et de Transcaucasie: Géologie, Géochimie et Chronométrie. In: L'obsidienne Au Proche et Moyen-Orient: Du vVolcan à l'Outil. British Archaeological Reports, pp. 105–167.
Polymeris, G.S., Gogou, D., Afouxenidis, D., Rapti, S., Tsirliganis, N.C., Kitis, G., 2010. Prelim- inary TL and OSL investigations of obsidian samples. Mediter. Archaeol. Archaeom. 10 (4), 83–91.
Poupeau, G., Le Bourdonnec, F.-X., Carter, T., Delerue, S., Shackley, M.S., Barrat, J.-A., Dubernet, S., Moretto, P., Calligaro, T., Milić, M., Kobayashi, K., 2010. The use of SEM-EDS, PIXE and EDXRF for obsidian provenance studies in the Near East: a case study from Neolithic Çatalhöyük (central Anatolia). J. Archaeol. Sci. 37, 2705–2720. https://doi.org/10.1016/j.jas.2010.06.007.
Rapp, G.R., Hill, C.L., 2006. Geoarchaeology: The Earth-Science Approach to Archaeological Interpretation, 2nd ed. Yale University Press, New Haven.
Renfrew, C., Cann, J.R., Dixon, J.E., 1965. Obsidian in the Aegean. Annu. Br. Sch. Athens 60, 225–247. https://doi.org/10.1017/S0068245400013976.
Renfrew, C., Dixon, J.E., Cann, J.R., 1966. Obsidian and Early Cultural Contact in the Near East. Proc. Prehist. Soc 32, 30–72. https://doi.org/10.1017/S0079497X0001433X.
Renfrew, C., Dixon, J.E., Cann, J.R., 1968. Further analysis of near eastern obsidians. Proc. Prehist. Soc 34, 319–331.
Rinaldi, M., Campos Venuti, M., 2003. The submarine eruption of the Bombarda volcano, Milos Island, Cyclades, Greece. Bull. Volcanol. 65, 282–293. https://doi.org/10.1007/s00445-002-0260-z.
Schmitt, A.K., Danišík, M., Evans, N.J., Siebel, W., Kiemele, E., Aydin, F., Harvey, J.C., 2011. Acigöl rhyolite field, Central Anatolia (Part 1): high-resolution dating of eruption episodes and zircon growth rates. Contrib. Miner. Petrol. 162, 1215–1231. https://doi.org/10.1007/s00410-011-0648-x.
Schmitt, A.K., Danišík, M., Aydar, E., Şen, E., Ulusoy, İ., Lovera, O.M., 2014. Identifying the volcanic eruption depicted in a neolithic painting at Çatalhöyük, Central Anatolia. Turkey. PloS ONE 9 (1), e84711.
Şen, E., Aydar, E., Gourgaud, A., Kurkcuoglu, B., 2002. La phase explosive précédant l'extrusion des dômes volcaniques : exemple du dôme rhyodacitique de Dikkartin Dag, Erciyes, Anatolie centrale, Turquie. C. R. Geosci. 334, 27–33.
Şen, E., Kurkcuoglu, B., Aydar, E., Gourgaud, A., Vincent, P.M., 2003. Volcanological evolution of Mount Erciyes stratovolcao and origin of the Valibaba Tepe ignimbrite (Central Anatolia, Turkey). J. Volcanol. Geoth. Res. 125, 225–246.
Shackley, M.S., 1988. Sources of Archaeological Obsidian in the Southwest: An Archaeological, Petrological, andGeochemical Study. Am. Antiq. 53 (4), 752–772.
Shackley, M.S. (ed.), 2011. X-Ray Fluorescence Spectrometry (XRF) in Geoarchaeology. Springer Science+Business Media, DOI 10.1007/978-1-4419-6886-9_6.
Shelford, P., Hodson, F., Cosgrove, M.E., Warren, S.E., Renfrew, C., 1982. In: The Obsidian Trade. In: An Island Polity: The Archaeology of Exploitation in Melos. Cambridge University Press, pp. 182–221.
Siebel, W., Schmitt, A.K., Kiemele, E., Danišík, M., Aydin, F., 2011. Acigöl rhyolite field, central Anatolia (part II): geochemical and isotopic (Sr–Nd–Pb, δ18O) constraints on volcanism involving two high-silica rhyolite suites. Contrib. Miner. Petrol. 162, 1233–1247. https://doi.org/10.1007/s00410-011-0651-2.
Sterba, J.H., Eder, F., Bichler, M., 2018. Identification of Obsidian Sources on Milos, Greece. Bulletin Geological Society of Greece 53, 125. 10.12681/bgsg.18559.
Storzer, D., Wagner, G.A., 1969. Correction of thermally lowered fission track ages of tektites. Earth Planet. Sci. Lett. 5 https://doi.org/10.1016/S0012-821X(68)80080-9.
Tank, S.B., Karaş, M., 2020. Unraveling the electrical conductivity structure to decipher the hydrothermal system beneath the Mt. Hasan composite volcano and its vicinity, SW Cappadocia, Turkey. J. Volcanol. Geoth. Res. 405, 107048 https://doi.org/10.1016/j.jvolgeores.2020.107048.
Tankut, A., Wilson, M., Yihunie, T., 1998. Geochemistry and tectonic setting of Tertiary volcanism in the Güvem area, Anatolia, Turkey. J. Volcanol. Geoth. Res. 85, 285–301. https://doi.org/10.1016/S0377-0273(98)00060-2.
Tauxe, L., 2010. Essentials of Paleomagnetism. University of California Press.
Todd, I.A., 1980. The Prehistory of Central Anatolia I: The Neolithic Period. Coronet Books.
Todd, I.A., Pasquarè, G., 1965. The Chipped Stone Industry of Avla Dağ. Anatol. Stud. 15, 95–112. https://doi.org/10.2307/3642504.
Toprak, V., 1998. Vent distribution and its relation to regional tectonics, Cappadocian Volcanics. Turkey. J. Volcanol. Geotherm. Res. 85, 55–67.
Toprak, V., Göncöoğlu, M.C., 1993. Tectonic control on the development of the Neogene-Quaternary Central Anatolian Volcanic Province. Turkey. Geological Journal 28 (3–4), 357–369. https://doi.org/10.1002/gj.3350280314.
Torrence, R., 1986. Production and Exchange of Stone Tools: Prehistoric Obsidian in the Aegean. New Studies in Archaeology. Cambridge University Press, Cambridge.
Tuffen, H., Castro, J.M., 2009. The emplacement of an obsidian dyke through thin ice: Hrafntinnuhryggur, Krafla Iceland. J. Volcanol. Geoth. Res. 185, 352–366. https://doi.org/10.1016/j.jvolgeores.2008.10.021.
Türkecan, A., Kuzucuoğlu, C., Mouralis, D., Pastre, J.-F., Atıcı, Y., Guillou, H., Fontugne, M. 2004 Upper Pleistocene volcanism and palaeogeog- raphy in Cappadocia (Turkey). MTA-CNRS-TÜBİTAK 2001–2003 research programme. Tübitak Project No. 101Y109. M.T.A., Ankara, pp 180.
Varoutsikos, B., Chataigner, C., 2012. Obsidatabase: Collecter et organiser les données relatives à l'obsidienne préhistorique au Proche-Orient et en Transcaucasie. Archéologies et espaces parcourus. Istanbul: Institut français d'études anatoliennes. https://doi.org/10.4000/books.ifeagd.987.
Wagner, G.A., Weiner, K.L.. 1987. Spaltspurenanalyse an obsidianproben. [Fission track analysis on obsidian samples.] In: Korfmann M (ed) Demircihüyük: Die Ergebnisse der Ausgrabungen 1975–1978, Band II: Naturwissenschaftliche Untersuchungen [Demircihüyük: the results of the excavations, Vol 2, Scientific Investigations]. Philipp von Zabern, Mainz am Rhein, pp 24–29.
Watkins, J., Manga, M., Huber, C., Martin, M., 2009. Diffusion-controlled spherulite growth in obsidian inferred from H2O concentration profiles. Contrib. Miner. Petrol. 157, 281. https://doi.org/10.1007/s00410-008-0340-y.
Wilson, L., Pollard, A.M., 2001. The Provenance Hypothesis. In: Handbook of Archaeological Sciences. John Wiley and Sons, pp. 507–517.
Wright, G.A., 1969. Obsidian Analyses and Prehistoric Near Eastern Trade: 7500 to 3500 B.C. Anthropological Papers, Museum of Anthropology, University of Michigan 37.
Wright, G., Gordus, A., 1969. Distribution and Utilization of Obsidian from Lake Van Sources Between 7500 and 3500 BC. Am. J. Archaeol. 73 (1), 75–77.
Yeğingil, Z., Oddone, M., Bigazzi, G., Erkanal, H., Kolankaya Bostanci, N., Şahoğlu, V., 2020. Chronological and chemical approaches to obsidians from Bakla Tepe and Liman Tepe, Western Anatolia. J. Archaeol. Sci. Rep. 32, 102458 https://doi.org/10.1016/j.jasrep.2020.102458.
Yellen, J., 1995. Trace Element Characteristics of Central Anatolian Obsidian Flows and their Relevance to Pre-History. Isr. J. Chem. 35 (2), 175–190.
Zapheiropoulou, P., 2008. Early Bronze Age cemeteries of the Kampos Group on Ano Kouphonisi. In: Brodie, N., Doole, J., Gavalas, G., Renfrew, C. (Eds.), Horizons: A Colloquium on the Prehistory of the Cyclades. McDonald Institute Monographs, pp. 183-194.
Zielinski, R.A., Lipman, P.W., Millard, H.T., 1977. Minor-element abundances in obsidian, perlite, and felsite of calc-alkalic rhyolites. Am. Mineral. 62 (5–6), 426–437.